Stress Resistance and Ageing in *Saccharomyces cerevisiae*

Nicholas Harris

Thesis submitted to University College London for the degree of Doctor of Philosophy

Department of Biochemistry and Molecular Biology
UCL
Gower Street
London WC1E 6BT

September 2002

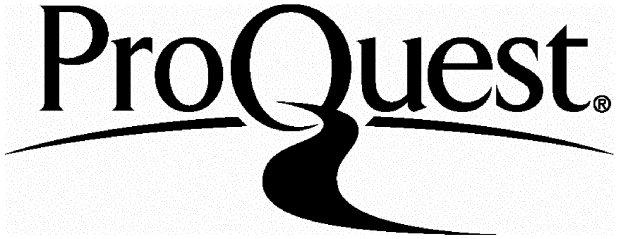

ABSTRACT

The budding yeast, *Saccharomyces cerevisiae*, can be used as a model in which the processes behind ageing can be investigated. Yeast life span can be determined in two ways, i) the number of buds produced by an actively dividing mother cell can be counted as a measure of a yeast's budding life span, ii) the viability over time of cells arrested in G0 can be recorded as a measure of yeast's chronological life span.

As is the case for *Drosophila* and *C. elegans* increasing the cellular stress resistance and antioxidant scavenging capabilities of yeast extends the chronological life span. By increasing the stress resistance of *S. cerevisiae* through the overactivation of the heat shock response resulting
from defects in the Hsp90 chaperone the chronological ageing of G0 arrested cells was extended. The budding potential of these cells however was not increased. Extensions to the chronological lifespan of yeast adapted torespiratory growth was achieved with the overexpression of the superoxide dismutase enzymes, Cu,Zn-Sod and Mn-Sod, as well as catalase. A two-fold extension to chronological lifespan extension was observed in cells with increased Cu,Zn-Sod activity. In this strain levels of free radicals are low and the onset of total cellular protein oxidation, which coincides with a dramatic reduction in cellular viability, is delayed. The generation of free radicals during respiration is therefore a limiting factor for longevity. Over expressions of the free radical scavenging enzymes did not increase the budding potential of yeast cells. Despite the benefits for chronological survival gained from the overexpression of Mn-Sod, a disruption in mitochondrial morphology and inheritance in this strain leads to a reduced number of buds a mother cell could produce.

A future goal for yeast ageing research is the identification of novel pathways involved in the determination of lifespan. The final part of this study included the development of a system by which the Euroscarf collection of deleted yeast strains can be screened for long lived mutants.

ACKNOWLEDGEMENTS

I am grateful to my supervisor Prof. Peter Piper, for his guidance throughout this research and completion of this thesis. His extensive background in yeast research and wealth of knowledge in the subject has led to some exciting and novel approaches to yeast ageing research, which I have been lucky to be part of.

I am grateful to those collaborators who have provided us with strains, and must thank Vitor Costa who performed some of the analyses of the SODs! Thanks are also due to the members of the lab, past and present, who have helped me with my research and made working in the "Piper" lab fun and entertaining. I would like to acknowledge BBSRC for funding this project.

Finally thanks must also go to my family and friends for their support and encouragement.

ABBREVIATIONS

ATP	adenosine triphosphate
bp	base pair
cAMP	cyclic adenosine monophosphate
CR	Calorie restriction
d	day
dATP	adenosine deoxyribonucleoside triphosphate
dCTP	cytidine deoxyribonucleoside triphosphate
dGTP	guanosine deoxyribonucleoside triphosphate
dH_20	distilled water
DHR	di-hydrorhodamine
dNTP	equimolar mixture of dATP, dCTP, dGTP dTTP
DTT	dithiothreitol
ERC	extrachromosomal rDNA circle
GDP	guanosine diphosphate
GFP	green fluorescent protein
GTP	guanosine triphosphate
HSF	heat shock factor
Hsp	heat shock protein
NAD+	nicotinamide adenine dinucleotide (oxidised form)
NADH	nicotinamide adenine dinucleotide (reduced form)
NBT	nitrotetrazolium blue chloride
OD	optical density
ORF	open reading frame
PDS	post diauxic shift
PKA	protein kinase A
PKB	protein kinase B
rDNA	ribosomal DNA
SDS	sodium dodecyl sulphate
SOD	superoxide dismutase

TABLE OF CONTENTS

TABLE OF FIGURES

CHAPTER 5: A screen for prosenescence genes in the yeast genome

1 Introduction

Beyond a certain point in the life span of metazoan organisms the genetically regulated phenotypic changes occurring that constitute development stop and the subsequent phenotypic changes which occur are more readily associated with a deterioration in the fitness of the organism. This decline is referred to as ageing and genetically predetermined although it is unlikely that there are specific genes that direct ageing (Kirkwood, 2002). In the last decade ageing has been the focus of much research. The hope is that an understanding of how and why it occurs will give a greater insight into the many diseases whose incidence increases with a human's age. Ageing is an important social and economic issue that affects an increasing number of elderly people in industrialised countries. It is however unlikely that it exerts much impact on the survival of species in the wild (Kirkwood, 2002).

Many different approaches to understanding ageing have been undertaken but some of the most informative research has been carried out using model organisms. These have been chosen partly for their very short life spans, an essential consideration when researching ageing. *Caenorhabtidis elegans*, a nematode worm with a life span of 2-3 weeks at 20-21°C; *Drosophila melanogaster*, a fruit fly with a life span of 20-30 days at 25°C; and *Saccharomyces cerevisiae*, a budding yeast with a life span of 20-40 buds or 4-6 weeks at 30°C have been widely used. In addition the mouse and rat with lifespans up to three years are proving useful as models of mammalian ageing.

In these model organisms, one is generally seeking to identify factors that can effect on the natural events of ageing. A general theme identified as an important longevity determinant is stress resistance. Many life span extensions in the above model systems appear to be the direct result of, or are at least associated with, increases in cellular stress resistance. Long-lived *Drosophila* can be obtained by the selective breeding of

individuals with long life span. Remarkably these lines have a greater resistance to environmental stress (Service et al., 1985). It has also been shown that elevating oxidative stress resistance in *Drosophila* by increasing the Cu/Zn-Sod levels in adult flies (Parkes et al., 1998; Sun and Tower, 1999) extends life span. Also in *C. elegans* (Melov et al., 2000; Taub et al., 1999) increases in ROS scavenging appear to elevate resistance to oxidative stress and increase longevity. Other mutations lengthening life in *C. elegans*, either affect general metabolic rates (e.g. *clk1*) or are in the dauer/insulin receptor signalling pathway (Ewbank et al., 1997; Lithgow, 1996; Martin et al., 1996; Wood, 1998). Initial experiments identified mutants with an up to two-fold increase in life span. Of these *daf-2* (Kenyon et al., 1993) and *age-1* (Larson et al., 1995) affect the starvation signalling that regulates dauer formation (Riddle et al., 1981). daf2 reduces the activity of the insulin-like receptor, (Kimura et al., 1997) and age1 is a phosphatidylinositol-3-OH kinase (PI3K), (Morris et al., 1996). Down regulation of this insulin-like pathway activates the forkhead transcription factor daf16 (Lin et al., 1997; Ogg et al., 1997), which may regulate stress resistance and longevity in adults (Fig. 1.1). Dietary restriction, the only protocol consistently shown to extend life span in mammals, increases stress tolerance in rodents and leads to an increased capacity for expression of molecular chaperone genes in response to acute stress (Heydari et al., 1996). Also Ames dwarf mice, which have a pituitary deficiency, exhibit an extended life span and increased stress resistance (Brown-Borg et al., 1996). All of these extensions to life span probably involve primarily chronological ageing of postmitotic tissues.

These findings are consistent with the notion that, for most organisms, stress protection and repair systems are not optimised for a maximisation of life span. They raise the important issue of why natural selection prevents the higher constitutive expression of antioxidant defences and perhaps heat shock proteins, whereby life spans would be maximal (Lithgow, 1996). This probably relates to natural selection exerting negligible impact on the survival to old age in the wild (Kirkwood, 2002).

Figure 1.1)

Life span control mechanism of *C. elegans*. The nuclear localization of the DAF-16 forkhead transcription factor is regulated by *daf-2*. (a) An insulin-like hormone and its receptor (DAF-2) initiate a signaling cascade that impinges on the activity of the protein-Ser/Thr kinases (AKT-1, AKT-2). When the forkhead transcription factor DAF-16 is phosphorylated by the AKT kinases, it is localized in the cytoplasm. Under these conditions, the organism follows a developmental program that favors reproductive growth. (b) When signaling through the *daf-2* pathway is inhibited, for example through mutational inactivation of DAF-2, AGE-1 the AKT kinases are not activated, leading to hypophosphorylation of DAF-16. The DAF-16 protein can then enter the nucleus. Here it is thought to have a role in regulating the expression of genes that influence resistance to environmental stresses (ultraviolet light, heat, radiation, H_2O_2, etc.) such as *sod-3*, the gene encoding mitochondrial superoxide dismutase (Honda, *et al.*, 1999). This general increase in stress resistance is essential for the lifespan extension observed in *daf-2* mutants (Lin, *et al.*, 2001).

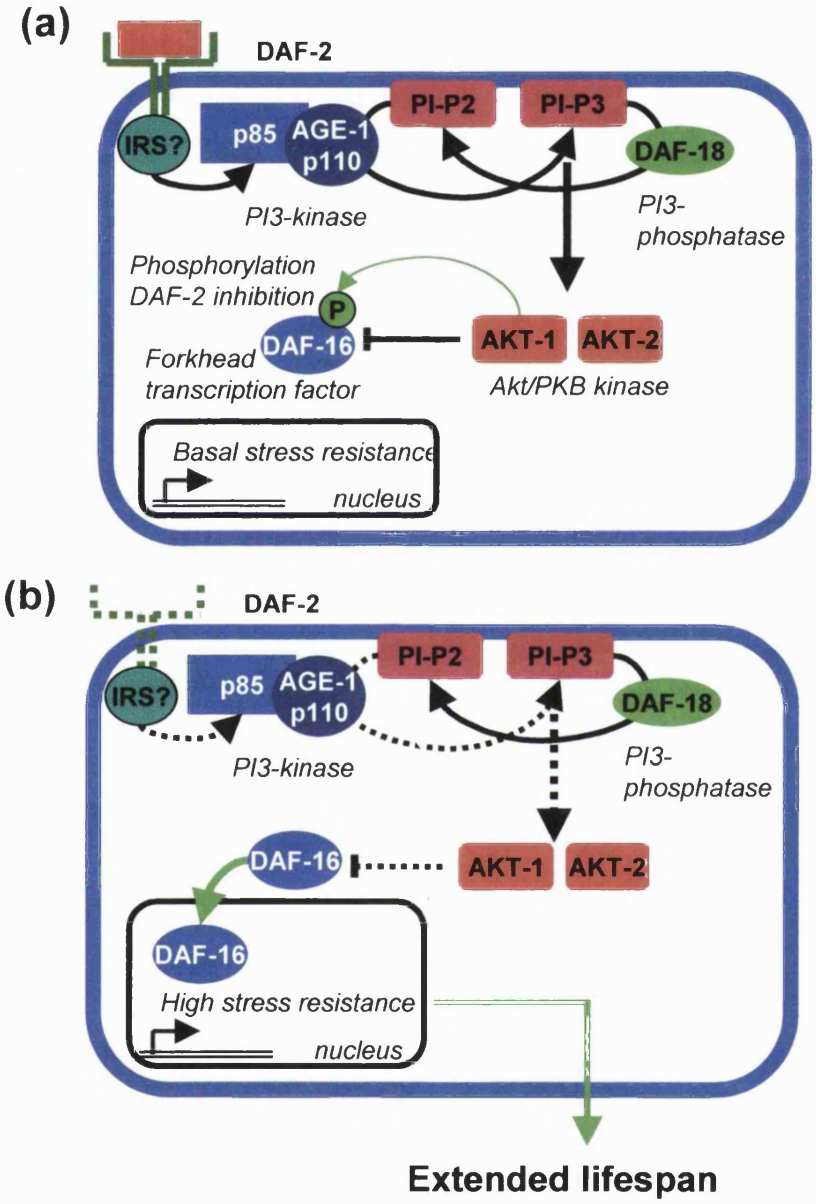
(a)
DAF-2
IRS?
p85
AGE-1
p110
PI-P2
PI-P3
DAF-18
PI3-kinase
PI3-
phosphatase
Phosphorylation
DAF-2 inhibition
P
DAF-16
AKT-1
AKT-2
Forkhead
transcription factor
Akt/PKB kinase
Basal stress resistance
nucleus
(b)
DAF-2
IRS?
p85
AGE-1
p110
PI-P2
PI-P3
DAF-18
PI3-kinase
PI3-
phosphatase
DAF-16
AKT-1
AKT-2
DAF-16
High stress resistance
nucleus
Extended lifespan

1.1 Yeast Ageing

Yeast provides one of the simplest models of ageing. Budding yeast can be considered to have two life spans: (i) a *replicative (budding, nonchronological) life span*, measured as the number of daughters produced by each actively-dividing mother cell (Mortimer and Johnston, 1959); and (ii) a *chronological life span*, measured as the ability of stationary cultures to maintain viability over time (Muller et al., 1980).

Traditionally, ageing in *S. cerevisiae* has been viewed as the events that limit the number of daughters that an individual mother cell can produce. In 1950 Barton was the first to demonstrate that *S. cerevisiae* becomes senescent after a finite number of divisions and could hence be used as a model to study ageing. Mother cells divide a relatively fixed number of times and undergo characteristic changes as they age. As they progress through the replicative life span the cells become swollen and sterile (Fig. 1.2) It is therefore possible to visually distinguish the daughter cell from the mother and hence the daughter cell can be microscopically dissected away from the mother cell and a division can be recorded (Fig 1.3). Although yeast seem to violate the rule of demarcation of soma and germ line, closer inspection reveals a renewal process in the budding of daughter cells, from an ageing soma-like lineage of mother cells (Guarente and Kenyon, 2000). Chronological life span is more akin to the situation experienced by most microbial cells in nature, where survival as nondividing populations exposed to scarce nutrients is the norm (Fabrizio et al., 2001). This system also models ageing of post mitotic cells in the tissues of adult metazoan organisms, where most cells have ceased dividing and have undergone terminal differentiation.

The determinants of both of these life spans of yeast are most probably different. Both lifespans are probably genetically regulated and pre-determined, as there is little variation between their average and maximum values within strains (Mortimer and

Figure 1.2)

(a) As *S. cerevisiae* progresses through its replicative life span the mother cell increases in size and becomes sterile before division eventually ceases and the cell becomes senescent (adapted from Guarente and Kenyon, 2000) (b) A cell array constructed by micromanipulation showing the increase in cell size with successive cell divisions. All are images of the same mother and are arranged in order of age. Numbers represent the generation from which the cell was derived (adapted from Powell, *et al.*, 2000)

(a)

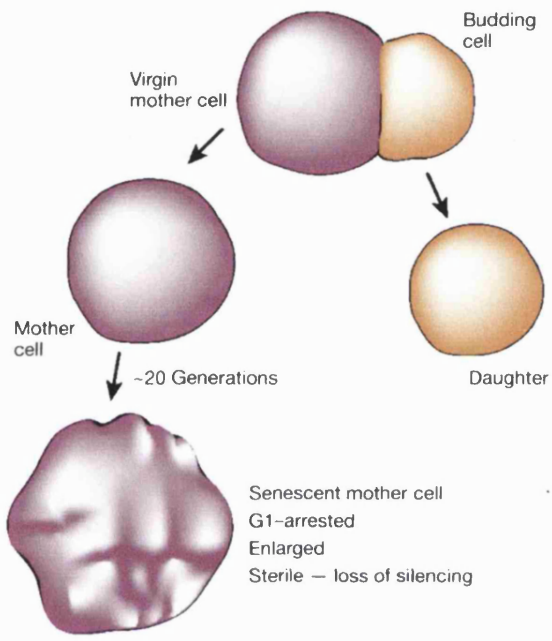
Budding
cell
Virgin
mother cell
Mother
cell
~20 Generations
Daughter
Senescent mother cell
G1-arrested
Enlarged
Sterile — loss of silencing

(b)

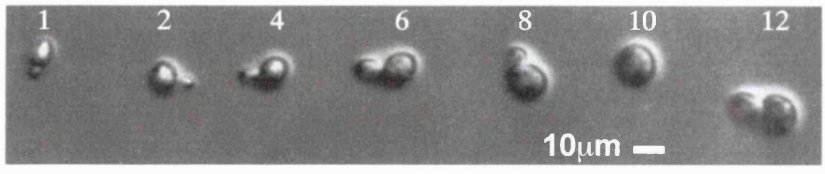
1
2
4
6
8
10
12
10μm

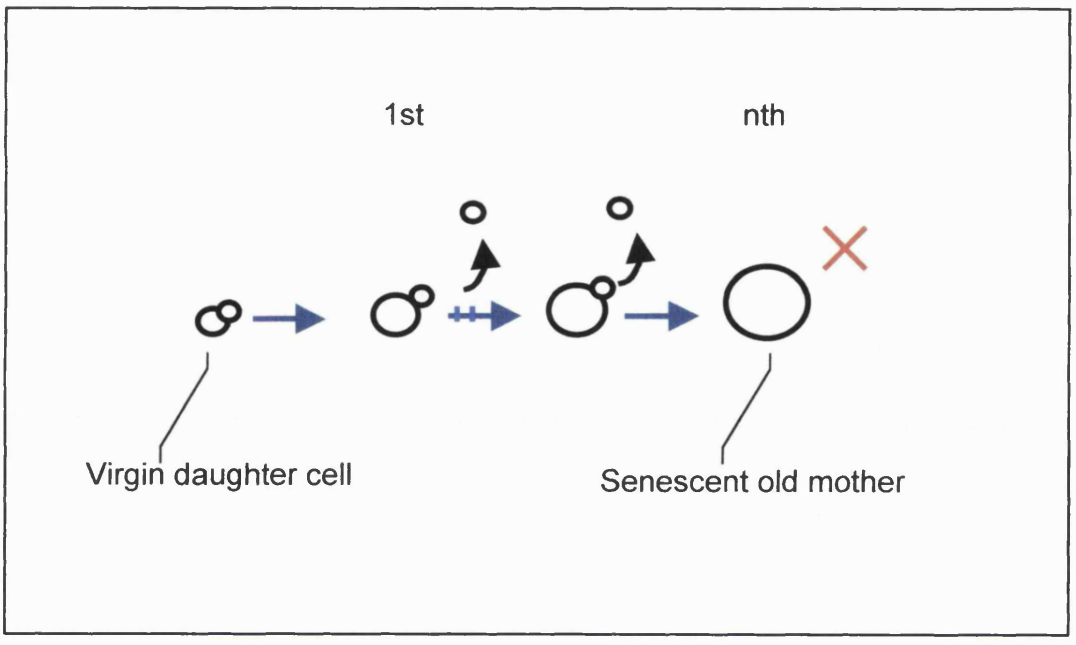

Figure 1.3)

Replicative life span of the budding yeast *S. cerevisiae*. The number of divisions a cell undergoes is known as its replicative potential and is a measure of its replicative life span. Cells are grown on agar plates and the replicative life span is recorded by the microscopic dissection of the smaller daughter cells away from the larger mother cell using the Singer MSM micromanipulator (Singer Instruments, UK), see methods.

Johnston 1959). In addition studies on both replicative life span and chronological life span have identified molecular mechanisms responsible for yeast ageing. These mechanisms will be discussed below.

1.2 Molecular mechanisms of replicative ageing

1.2.1 Sterility is a marker for old generation cells.

Towards the end of their replicative life span yeast cells have a characteristic phenotype. They increase in size (Fig. 1.2), have a slower cell cycle (Mortimer and Johnston, 1959) become sterile with a fragmented nucleolus (Smeal et al., 1996). Cell type specific gene expression in yeast is governed by the control of gene expression at the MAT expression locus on chromosome III, a chromosome which also contains two repositories of silent mating-type information, *HMLa* and *HMRα* (Rine and Herskowitz, 1987). As cells age the silencing control over *HML a* and *HMRα* is lost. The resultant simultaneous expression of both *HMLa* and *HMRα* information leads to sterility. *MATα* information do not become sterile in old age (Smeal et al., 1996). Silencing at the *HM* loci is regulated by silent information regulator (*SIR*) genes *SIR2*, *SIR3* and *SIR4* (Gottschling et al., 1990; Rine and Herskowitz, 1987). These encode the Sir2/3/4p complex which is responsible for silencing not just at *HMLa* and *HMRα*, but also at telomeres and ribosomal DNA (rDNA) (Gottlieb and Esposito, 1989).

1.2.2 Silencing at the nucleolus: the ERC model of senescence

The causal link between silencing and ageing was first made by the identification of the *sir4-42* longevity mutation (Kennedy et al., 1995). This mutation redirected silencing from the telomeres and *HM* loci to the region of the genome encoding the rDNA. The deletion of either *SIR2*, *SIR3* or *SIR4* shortens life span, whereas life span is increased when the Sir complex is prematurely redirected to the rDNA as in *sir4-42* alleles. The importance of silencing at this location became clear when the accumulation of extrachromosomal rDNA circles (ERCs) throughout the replicative life span was

observed (Sinclair and Guarente, 1997). Silencing in rDNA chromatin serves to repress the formation of these DNA circles (Gottlieb and Esposito, 1989), a greater level of silencing slowing the accumulation of ERCs. ERC accumulation appears to be a very important factor limiting in the yeast replicative life span (Sinclair and Guarente, 1997), although other models of replicative senescence are promoted by the Jazwinski (Kirchman et al., 1999; Shama et al., 1998) and Breitenbach (Nestelbacher et al., 2000) laboratories.

The rDNA comprises 100-200 tandem repeats of the 9.1kb rDNA repeat on chromosome XII. This region organises itself into a nuclear structure known as the nucleolus, the site of ribosome synthesis. Each repeat encodes one 35S pre-rRNA transcribed by RNA polymerase I and a small 5S RNA gene transcribed by RNA polymerase III. The repeats are separated by an untranslated region which contains an autonomous replication sequence (ARS) for initiation of DNA synthesis (Fig. 1.4).

As mother cells divide there is a high probability that homologous recombination will occur between rDNA repeats resulting in the generation of an ERC (Fig. 1.5). During each S-phase this excised rDNA self replicates due to the ARS sequence. Although this ARS is relatively weak (Larionov et al., 1984) larger multimeric ERC species will have multiple ARSs increasing their replication potential. Larger multimeric ERC molecules were observed in cells which had been through many divisions (Sinclair and Guarente, 1997). The ERCs lack a centromeric region and are therefore maintained almost exclusively in the mother cell, and not segregated to the daughter. This explains why the accumulation of ERCs is so rapid. Segregation bias also assures that the daughter cells are born ERC free and enjoy a full life span.

ERC accumulation results in fragmented nucleoli, cessation of cell division, and cellular senescence. It is likely that this senescence is brought about by the sheer volume of ERC DNA, which can be equal to the other DNA of the yeast after 15 divisions (Sinclair et al., 1998). It is proposed that the mother cell loses its ability to replicate or transcribe its

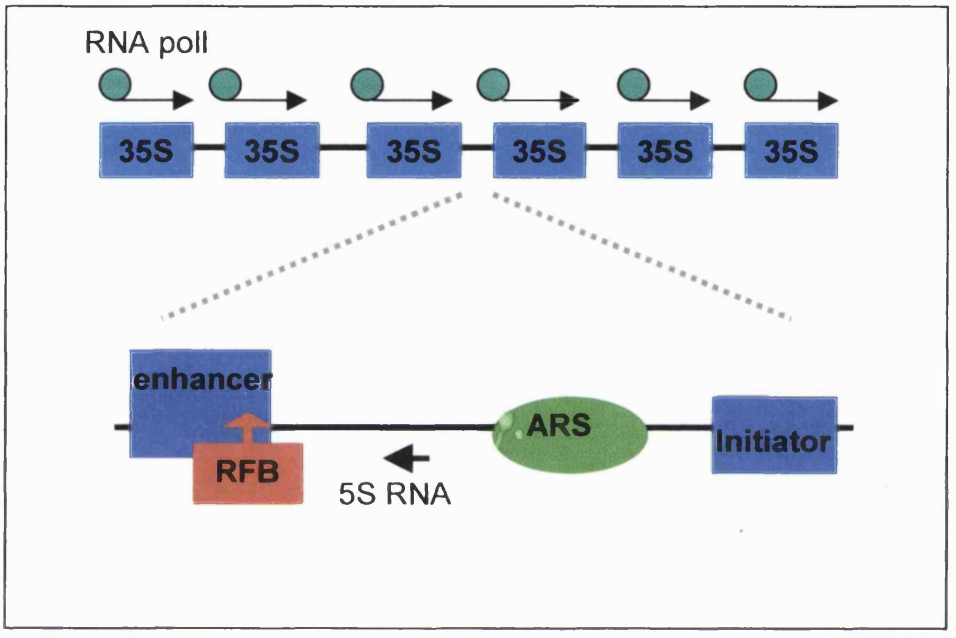

Figure 1.4)

The rDNA repeats, present in 100-200 copies on yeast chromosomeXII, are indicated. Each repeat contains the coding sequence for the 35S rRNA, transcribed in the direction of the arrows, and the spacer which is enlarged. The spacer region contains the enhancer and initiator for 35S transcription, the ARS for initiation of DNA replication, the 5S RNA-coding sequence, and the replication fork block site (RFB).

Figure 1.5)

The ERC model for yeast ageing. The rDNA locus comprises of 100-200 tandem copies of a 9.1kb repeat (blue rectangles) and is located within a compact nucleolus. Homologous recombination between rDNA repeats (**a**) results in the formation of an extra-chromosomal rDNA circlular molecule, or ERC (blue circle). ERCs can self replicate via an ARS element contained within the rDNA repeat (green circle) (**b**) Assymetrical segregation of ERCs, ERCs have no centromeric region and are retained by the mother cell during cell division, reulting in their exponential accumulation in mother cells. ERC accumulation causes nucleolar fragmentation, relocalisation of silencing proteins to the rDNA and eventually the cessation of cell division. (Adapted from Sinclair *et al,* 1998)

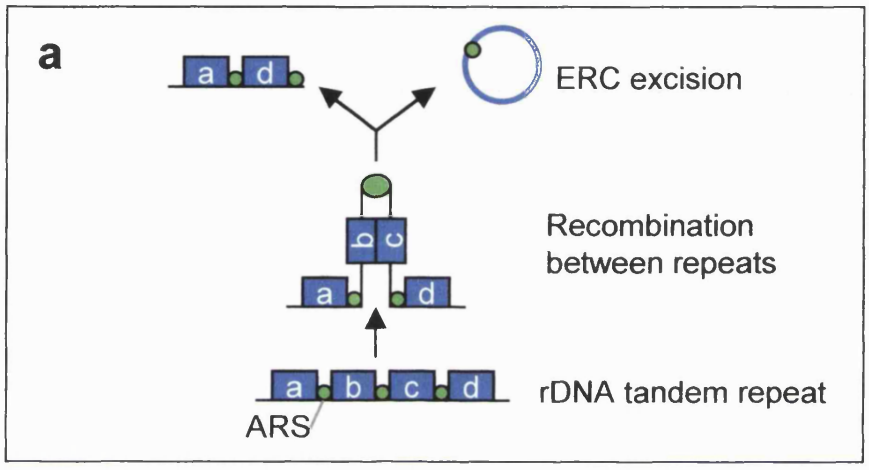
a
a
d
ERC excision
b
c
a
d
Recombination
between repeats
a
b
c
d
rDNA tandem repeat
ARS

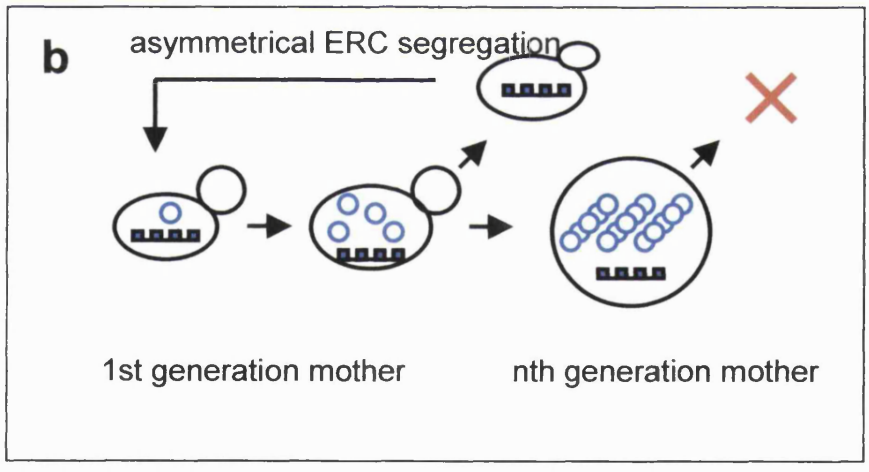
b
asymmetrical ERC segregation
1st generation mother
nth generation mother

genomic DNA by a titration of important components of the replication and transcription machinery by the ERC DNA (Sinclair and Guarente, 1997).

Such genetic instability imposing a limit to replicative life span is not unique to *S.cerevisiae*. In certain isolates of filamentous fungi (*Neurospora crassa* and *Podospora anserina*) linear mitochondrial DNA plasmids accumulate and regulate senescence (Hermanns et al., 1994; Jamet-Vierny et al., 1980). However genetic instabilities have yet to be identified as the cause of normal ageing in nonfungal systems. However a premature ageing disease in humans, Werner's syndrome, appears to be associated with altered DNA metabolism. This rapid ageing phenotype is due to a defective Rec-Q like helicase (Yu et al., 1996). Loss of the yeast homologue Sgs1p is associated accelerated ERC accumulation(Sinclair et al., 1997).

1.2.3 Life span extension in a mutant that has reduced ERC production.

Further support for the ERC model of yeast replicative ageing can be found in mutants with reduced ERC production. The replication of rDNA which proceeds in the same direction as the 35S rRNA transcription is unique in yeast because it is uni-directional (Brewer and Fangman, 1988). It is proposed that replication is halted at a replication fork block (RFB) (Fig. 1.4). The RFB is dependent on *FOB1* (Kobayashi and Horiuchi, 1996) a gene whose product has been localised by immunofluorescence to the nucleolus (Defossez et al., 1999), and whose loss dramatically extends life span by 30-60%(Defossez et al., 1999). The deletion of *FOB1* also suppresses the initial ERC excision event and therefore the onset of senescence (Defossez et al., 1999). This is because double strand breaks within the rDNA, normally repaired by homologous recombination, are enhanced by the block to replication which can lead to an excision of an ERC (Defossez et al., 1999; Gangloff et al., 1996; Johnson et al., 1999).

1.2.4 SIR2 regulates silencing at the rDNA locus and promotes long lifespan

The Sir2/3/4p protein complex is a critical component of silenced chromatin in yeast. This complex blankets the underlying nucleosome by interacting with the histones H3 and H4, thus impeding the access to DNA by transcription, replication and

recombination machinery (reviewed by (Gottschling, 2000)). The function of Sir2p does not, however appear to be the same stabilisation of silenced chromatin as Sir3p and Sir4p. There is no compelling evidence that demonstrates Sir2p is bound to DNA or histones. Sir2p is the only Sir protein which is highly conserved, the four *S. cerevisiae* Sir2p homologues being encoded by the *HST1-4* genes (Brachmann et al., 1995). A core domain of Sir2p has been widely conserved from bacteria to humans (Frye, 1999). This conservation indicates a further function of Sir2p quite separate from silencing of chromatin. Also one of the homologues resides in the cytoplasm and eubacteria have no histones nor are they known to silence chromatin (Afshar and Murnane, 1999).

Deletion of *FOB1* suppresses the shortened life span of the *sir2* mutant implying that accelerated generation of ERCs is the mechanism of the premature senescence in the *sir2* mutant. Furthermore the integration of a second copy of *SIR2* into the genome results in a 30% increase in budding potential over wild-type mother cells (Kaeberlein et al., 1999). *SIR2* expression is therefore limiting yeast replicative life span.

1.2.5 Enzymatic activity of SIR2

The amino termini of the histones in chromatin are lysine rich tails which protrude outside the periphery of the nucleosome unit (Luger and Richmond, 1998). Acetylation of these lysine tails serves to regulate silencing. In yeast the amino-terminal tails of histones H3 and H4 are hypoacetylated in silent DNA, relative to the rest of the genome (Braunstein et al., 1996). Sir2p functions as a histone deacetylase which requires NAD+(Imai et al., 2000). Cells in which *SIR2* is highly overexpressed have hypoacetylated histones (Braunstein et al., 1993).

This NAD-dependent deacetylase activity seems to be a universal property of Sir2 proteins from bacteria to mammals. Mutational studies indicate that the histone deacetylase activity is specific for lysines 9 and 14 of histone H3 and lysine 16 of H4 (Imai et al., 2000). The NAD requirement of Sir2p sets it aside from other known histone deacetylases. It also suggests a link between metabolism, the control of silencing

and replicative life span. NAD+ is an electron donor (NADH) or as an electron acceptor (NAD) in many metabolic reactions. It is proposed by Imai *et. al* therefore proposed that NAD+ couples the Sir2p deacetylase activity to the energy state of the cell (Imai et al., 2000). The increase in NAD+ levels as cells become pro-oxidant in normal ageing (Ashrafi et al., 2000) would therefore act to oppose any parallel reduction in genomic silencing (Imai et al., 2000).

1.2.6 Metabolism and replicative life span

A direct correlation between life span and nutrient deprivation (calorie restriction) is observed in both model organisms (*C.elegans* and *Drosophila)* and mammals. Mice fed on a calorie restricted diet have extended maximal life spans and exhibit a delay in ageing-associated physiological and pathological changes (Arking, 1998).

The link between NAD+ and the deacetylase activity of Sir2p suggests a plausible link between cellular energy levels and the control of life span. The influences of calorie restriction (CR) on yeast replicative life span have been investigated (Lin et al., 2000). Either growth on media with limiting glucose or a mutation in *HXK2* significantly extends the budding potential of the cell (Lin et al., 2000). Glucose enters yeast cells by highly regulated glucose-sensing transporters (Hxtp) (Ozcan and Johnston, 1999) and is then phosphorylated to glucose-6-phosphate (G-6-P) by hexokinases (Hxk1p, Hxk2p, and Glk1p) (Walsh et al., 1983). The *hxk2* mutation may therefore mimic caloric restriction.

The process by which CR extends life span in yeast has also been dissected by looking at the cAMP-Protein kinase A pathway (cAMP-PKA). This pathway is activated by glucose (Fig. 1.6). Low PKA causes derepression of genes involved in stress resistance and the metabolism of carbon sources other than glucose. The Msn2p, Msn4p transcription factors which mediate stress-induced gene expression are repressed by the cAMP-PKA signalling pathway (Smith et al., 1998). Major components of this pathway include guanosine triphosphate/guanosine diphosphate (GTP/GDP)-binding proteins

(Ras1p and Ras2p), a GTP-GDP exchange factor (Cdc25p), GTP hydrolysis factors (Ira1p and Ira2p), the adenylate cyclase (Cdc35p/Cyr1p), phosphodiesterases (Pde1p and Pde2p), a PKA regulatory subunit (Bcy1p), and a PKA catalytic subunit (encoded by three functionally redundant genes, *TPK1*, *TPK2*, and *TPK3*) (Fig. 1.6) (Thevelein and de Winde, 1999).

Mutations which reduce the activity of PKA extend replicative life span, whilst the deletion of *PDE2* responsible for cAMP hydrolysis and reduction of PKA activity decreased replicative life span. Furthermore, life spans of these mutants were not enhanced by limiting glucose levels suggesting that they were working as part of CR (Fig. 1.6) (Lin et al., 2000).

Interestingly the life span increase with these mutations in the PKA pathway was not because of derepression of Msn2p/Msn4p and the resulting general increase in stress resistance. Msn2p/Msn4p activity induces several stress genes including heat shock proteins, catalase (*CTT1*), and the DNA damage inducible gene *DDR2* (Thevelein and de Winde, 1999). Mutants in both these transcription factors did not inhibit the life span extension of the *cdc25-10* mutation. The shortened life span of a *sir2* mutant, however could not be extended by the *cdc25-10* mutation. Elimination of ERC hyper accumulation, by the deletion of *FOB1* in this doubledeletantonly rescued life span to wild type *sir2 fob1* mutant levels, thus indicating that Sir2p must play a role in this CR-mediated replicative life span extension (Lin et al., 2000). A further gene *NPT1* was found to be essential for CR-mediated life span extension by *cdc25-10*. *NPT1* encodes a nicotinic acid phosphoribosyl transferase (NPRTase) (Rajavel et al., 1998) which functions to synthesise NAD by recycling nicotinic acid (Grubmeyer et al., 1999; Lin et al., 2000). In addition ERC accumulation in the *cdc25-10* mutant was reduced compared to that of wild type cells (Lin et al., 2000). These findings suggest that the increased longevity with CR requires the activation of Sir2p by NAD+. It is therefore proposed that CR extends life span in yeast by regulating rDNA recombination via NAD+ control over Sir2p-mediated silencing at the rDNA array (Fig. 1.6) (Lin et al., 2000).

Figure 1.6)

Caloric restriction in yeast. Glucose stimulates a signal transduction pathway including a Ras GTP-binding protein, a GTP/GDP exchange factor (*Cdc25*), an adenylate cyclase, and cAMP-dependent protein kinase A (PKA). Without cyclic AMP, the PKA catalytic subunit (*Tpk*) is in a complex with the inhibitor protein Bcy1. Signalling is attenuated either by lowering the glucose levels in the media (caloric restriction) or by mutating genes that encode components of the pathway (for example, *Cdc25*, *Cdc35* or tyrosine protein kinase (*Trk*), shown in red). Surprisingly this lifespan extension is not as a result of an increase in stress resistance by the derepression of the Msn2/4 transcription factors but rather the reduction in signalling leads to an increase in silencing by Sir2 and its NAD cofactor and an extended life span.

Chronological lifespan extension is however extended through the disruption of an adenylate cyclase and the reduced repression of the Msn2/4 transcription factors (Longo, *et al.*, 2000)

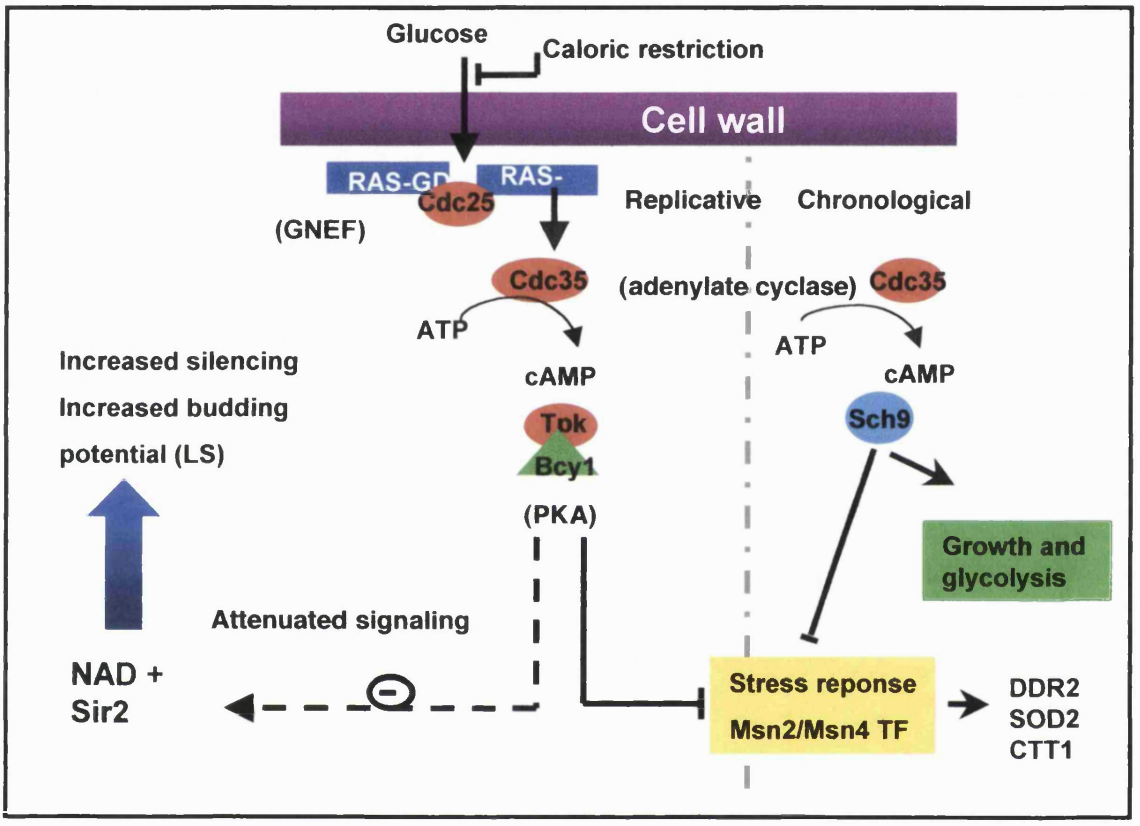
Glucose
Caloric restriction
Cell wall
RAS-GD
RAS-
Cdc25
(GNEF)
Replicative
Chronological
Cdc35
(adenylate cyclase)
Cdc35
ATP
ATP
Increased silencing
Increased budding
potential (LS)
cAMP
cAMP
Tok
Sch9
Bcy1
(PKA)
Growth and
glycolysis
Attenuated signaling
NAD +
Sir2
Stress reponse
Msn2/Msn4 TF
DDR2
SOD2
CTT1

1.3 SIR2 involvement in other ageing models

1.3.1 C. elegans

As a result of this work in yeast, the role of *SIR2* in other systems was investigated. A life span extension of up to 50% was observed in a *C.elegans* with a genomic duplication of the DNA region containing the *C.elegans SIR2* homologue *sir-2.1* (Tissenbaum and Guarente, 2001). The insulin signalling like pathway has a major influence on life span in *C. elegans*. Mutations reducing the activity of the *daf2* (Kimura et al., 1997) insulin receptor or the age1 PI3K (Morris et al., 1996) extend life span in adults (Lin et al., 1997; Ogg et al., 1997) by activating the *daf16* transcriptional regulator of stress resistance genes (Fig. 1.1). Mutations in *daf16* reduce the life span of adult worms and consequently the life span of these mutants is unaltered by mutations in signalling molecules which lie upstream of this transcription factor. The life span extension by *sir2.1* was dependent upon the activity of *daf16,* indicating that the *sir2.1* influence on life span acts similarly to the insulin-like signalling pathway. This provides evidence that the Sir2 protein may couple longevity to nutrient availability, not just in yeast but also in many eukaryotic organisms (Tissenbaum and Guarente, 2001)

1.3.2 Mammalian systems.

Among its other functions in *S. cerevisiae*, Sir2p is involved in DNA damage responses (Martin et al., 1999; McAinsh et al., 1999; Mills et al., 1999). By looking at the well characterised mammalian DNA damage response pathway regulated by the p53 tumour suppressor, an involvement for the mammalian homologue of Sir2 was found (Luo et al., 2001; Vaziri et al., 2001).

p53 exerts antiproliferative effects, including growth arrest, apoptosis, and cell senescence, in response to various types of stress (Levine, 1997; Prives and Hall, 1999; Vogelstein et al., 2000). For this reason p53 is a short-lived protein, its activity being

maintained at low levels in normal cells. Following DNA damage, p53 is protected from rapid degradation and acquires transcription-activation functions, largely as a result of posttranslational modifications (Canman et al., 1998; Shieh et al., 2000; Siliciano et al., 1997). p53 transcription factor activity leads to upregulation of genes for cell cycle exit (such as the $p21^{WAF1}$ gene (el-Deiry et al., 1993)) or apoptosis (Lin et al., 2000).

Though the activation of p53 is not completely understood (reviewed in (Appella and Anderson, 2000)), there is growing evidence for the importance of acetylation in p53 activation. In response to DNA damage p53 is phosphorylated by the ATM protein kinase (Appella and Anderson, 2000) this increasing the p53 affinity for the p300 (Lambert et al., 1998) acetylase, which leads to acetylation of p53 at four residues (Guarente, 2001). Two of these residues are acetylated in response to DNA damage (Abraham et al., 2000). Furthermore MDM2 involved in the negative regulation of p53, is able to block this acetylation of p53 (Oren, 1999)

As in yeast the mouse homologue of Sir2, Sir2α, and its human orthologue hSIRT1 have NAD-dependent deacetylase activity. The deacetylation activity of these mammalian Sir2 homologues has been implicated in the negative regulation of p53 (Luo et al., 2001; Vaziri et al., 2001). These recent studies showed; (1) a direct interaction of p53 with Sir2α and SIRT1 (Luo et al., 2001; Vaziri et al., 2001); (2) that p53 is a substrate for the NAD-dependent deacetylase of mammalian Sir2α (Luo et al., 2001; Vaziri et al., 2001) (3) that the sir2α-mediated deacetylation antagonizes p53 dependent transcription and apoptosis (Luo et al., 2001); (4) that Sir2α specifically inhibits p53-dependent apoptosis in response to DNA-damage as well as oxidative stress, but not p53-independent, Fas-mediated cell death (Luo et al., 2001). It was also demonstrated that a point mutation Sir2α increased the sensitivity of cells to stress (Luo et al., 2001). Therefore mammalian cells can control proliferation and post-mitotic survival through the activity of Sir2α.

1.3.3 SIR2 could regulate life span .

Why are the replicative ageing in yeast and post-mitotic ageing in worms both regulated by Sir2? One proposed explanation for this could be the requirement of NAD by Sir2p for its deacetylation activity. As such, Sir2 proteins might have the ability to monitor metabolic rate, reflected by the amount of available NAD, and couple this status to regulatory events. *SIR2* controls life span in yeast by regulating the silencing of chromatin and in worms *sir-2.1* regulates life span by the inhibition of insulin like signalling. In this way Sir2 genes may regulate life span in many organisms. Although Sir2α and the regulatory control of p53 is not a known regulator of life span in mammals, mammalian studies highlight the importance of Sir2 function in higher systems (Luo et al., 2001; Vaziri et al., 2001).

In evolutionary terms any mechanism that could slow ageing and postpone reproduction when growth conditions were poor would be selectively adaptive. Sir2 genes could provide the basis for this control because of their link to metabolism. Further support for such a theory is found in *C.elegans* where insulin like signalling pathway responsible for long life also regulates entry into a dormant larval stage termed "*dauer*" when growth conditions are poor.

1.4 Molecular mechanisms of chronological life span

Less is known about the processes involved in the chronological ageing of *S. cerevisiae*. The full growth cycle of a yeast batch culture begins with log phase and progresses through the diauxic shift to true stationary phase. In log phase, the cells use glucose to make energy via glycolysis. The diauxic shift occurs when glucose becomes limited and energy metabolism shifts to respiration, at which point mitochondrial proteins are synthesised at a higher level, growth rate slows, and cells utilise ethanol and other two and three carbon chain compounds for energy. During this phase, glycogen and trehalose

are synthesised and stored, and the cells become much more resistant to stress. Many of these events are due, in part, to the fall of PKA activity (Thevelein and de Winde, 1999). In the total absence of any nutrients, yeast cells enter true stationary phase. No cell division occurs, the metabolic rate slows, and the cells can survive for weeks to months. Many markers, such as increased heat shock resistance and glycogen accumulation, have been utilised to define stationary yeast, although it appears that the best definition of stationary phase is the ability to survive for long periods without added nutrients (Werner-Washburne et al., 1993).

Stationary phase yeast resembles most of the cells of multicellular organisms, in that the cells receive most of their energy through mitochondrial respiration and have exited from the cell cycle and entered G_0 phase. Non-dividing cells have to protect essential cellular components from damage accumulation. Components that do become damaged must, of necessity, be repaired or turned over and renewed. The chronological life span of stationary phase yeast cells therefore provides a model system for ageing research which more closely mimics the ageing of non-dividing cells and tissues in higher eukaryotes than the yeast replicative life span.

The chronological life span of stationary phase yeast is therefore not limited by an accumulation of ERCs. These cells require a functional antioxidant defence system, since cells lacking copper-zinc superoxide dismutase (Cu,Zn-SOD) and manganese superoxide dismutase (Mn-SOD) have a reduced viability over time when maintained in stationary phase (Longo et al., 1996; Longo et al., 1999). The severity of this life span defect is reduced when these mutants are maintained in low oxygen conditions. Furthermore, the short life spans of these mutants can be extended upon the introduction of the human anti-apoptotic protein Bcl-2 (Longo et al., 1997). In humans Bcl-2 inhibits cell death by blocking the generation of oxygen radical species (Hockenbery et al., 1993). Bcl-2 therefore appears to have similar activities in yeast as in mammalian cells. These results indicate the chronological life span of stationary phase yeast is limited by oxidative damage processes.

Oxidative stress has not, to date, been identified as a limiting factor in yeast replicative life span. This could be because ERC accumulation causes its life span limiting affects before the onset of oxidative damage. Another reason could be that the experiments were carried out on actively growing cultures with ample nutrients and a fermentable carbon source. They may not have provided conditions of high endogenous oxidative stress. In fermentative growth, the cells depend more heavily on glycolysis than respiration for energy and growth, and cell division allows for dilution of any accumulated damage.

1.4.1 Stress resistance identified as an important chronological life span determinant.

As for replicative life span, cellular processes involved in nutrient sensing and metabolic control have recently been linked to the control of the survival of yeast over time. Mutations in two genes, *SCH9* and *CYR1/CDC35,* were shown to increase longevity over time of cells grown to stationary phase on glucose (Fig. 1.5) (Fabrizio et al., 2001). These mutations reduced the activity of both genes, and on addition of a wild type copy the life span extensions disappeared. Hence the activities of these genes accelerate mortality over time.

The COOH-terminal of Sch9 is highly homologous to the ACG family of protein serine/threonine kinases which includes Akt/PKB. PKB acts in the pathway of insulin signalling in mammals and the pathway that regulates longevity in *C.elegans*. *C.elegans* AKT-1 and AKT-2 function downstream of the insulin receptor homologue DAF-2 in a longevity/diapause pathway (Fig. 1.1) (Guarente and Kenyon, 2000; Paradis et al., 1999). The *CYR1* gene encodes adenylate cyclase, which stimulates cAMP-dependent PKA in the Ras/cAMP/PKA pathway required for cell cycle progression and growth. Disruption of this pathway in *S.cerevisiae* increases stress resistance by activating Msn2/4p (Fig. 1.6). Both Sch9p and Cdc35p function in pathways that mediate glucose dependent signalling, stimulate growth and glycolysis, and decrease stress resistance, glycogen accumulation and gluconeogenesis (Thevelein and de Winde, 1999). These

effects of *SCH9* and *CDC35* therefore demonstrate a link between stress resistance and yeast chronological survival.

The extension of chronological life span by *SCH9* removal, though independent of *MSN2/MSN4* is dependent upon *RIM15* (Fabrizio et al., 2001). Rim15p is a kinase which regulates genes containing a PDS (postdiauxic shift) element involved in the induction of thermotolerance and starvation resistance by Msn2p/Msn4p-independent mechanisms (Fig. 1.6) (Pedruzzi et al., 2000).

1.5 Outline of this research project.

At the start of this research much was already known about the causes of replicative senescence in yeast. The ERC model had been described as a rate limiting mechanism for the replicative age. However as this is exclusive to fungal systems, it was not considered to be very informative when considering mammalian ageing processes. The importance of free radical scavenging for a full chronological lifespan had been shown with demonstrations of the reduced viability over time of sod mutants (Longo et al., 1996; Longo et al., 1999), To be certain that processes involved in ageing have been identified, however, life span has to be extended.

The aim of this research project was to identify the role of stress resistance in both the replicative and chronological life spans of yeast. Both the general stress response pathway and the cellular antioxidant defence were investigated. The role of the general stress response on yeast life span was investigated by its elevation as a result of a reduced level of negative regulation by the Hsp90 chaperone. The life span effects of increased levels of oxidant scavenging enzymes was investigated, as had been done with *Drosophila* (Parkes et al., 1998; Sun and Tower, 1999) and *C. elegans* (Melov et al., 2000; Taub et al., 1999). Life span extensions as a result of these modifications would

bring yeast ageing research in line with other model systems, and demonstrate relevance of yeast ageing research to processes of ageing in other systems.

The final aim of this project was to identify new determinants of yeast life span, by isolating mutants of *S. cerevisiae* with lengthened chronological life span directly. Such a mutant screen can be expected to identify genes whose loss is somewhat detrimental for propagation of the species, yet beneficial for long-term maintenance of nondividing cells. It might identify mutations that lead to overactivation of the regulons of oxidative stress protection or strains with reductions in levels of endogenous ROS production. Alternatively it might provide indications of the existence of prosenescence functions, comparable to *age1* of *C.elegans* (Morris et al., 1996) in a simple eukaryote

2 Materials and methods.

2.1 Growth media and culture conditions

Yeast culture were grown in rich media (YPD) or synthetic defined minimal media (SD). The recipes for all yeast media are given below (all % values are w/v):

YPD: 2% D-glucose, 2% Bacto-peptone, 1% Bacto-yeast extract.
YPG: 3% glycerol, 2% Bacto-peptone, 1% Bacto-yeast extract.
SD: 2% D-glucose, 0.67% yeast nitrogen base (without amino acids) plus one or more of the following auxotrophic amino acids where required; adenine (20mg/l), L-histidine (20mg/l), L-leucine (30mg/l), L-lysine (30mg/l), L-tryptophan (20mg/l), uracil (20mg/l).
PCA (plate count agar): 0.25% D-glucose, 0.5% Bacto-tryptone, 0.25% Bacto-yeast extract, 1.5% Bacto-agar.
Sporulation media: 0.05% D-glucose, 0.8% Bacto-yeast extract, 0.3% Bacto-peptone.
Pre-sporulation: 10% D-glucose, 0.3% Bacto-peptone, 0.8% Bacto-yeast extract.

2% bacto agar was used for the preparation of solid media. Plates were left on the bench for 1-2 days after pouring to dry. Liquid media cultures were grown at the appropriate temperature with rapid agitation in a media/volume ratio of 1/5 of the flask volume. Yeast strains were maintained in frozen stocks in 2X YPD + 15% glycerol at –70°C. All solutions and glassware were sterilised by autoclaving at 15psi for 20min.

2.1.1 Monitoring of cell growth

Yeast cell growth in liquid media was monitored by taking OD_{600} readings at appropriate time intervals . Alternatively an improved Neunauer haemocytometer (Hawksley) was used.

2.2 Genetic techniques.

2.2.1 Yeast transformation

Transformation of *S. cerevisiae* strains with DNA was performed chemically as described by Gietz et al.,(1995) or by electroporation as described by Thompson et al., (1998)

2.2.2 Yeast mating

Diploids were created by mating haploid strains of opposing mating types (a and α Strains were mixed on YPD plates and left for 4-hours at 30°C, or until "shmooing" cells could be observed. Diploid strains were plated on sporulation medium (1% potassium acetate, 0.1% yeast extract, 0.05% dextrose) and incubated at 25°C, formed spore tetrads after 5+ days. These spores were collected and incubated in a $5mgml^{-1}$ lyticase (Sigma) solution at 37°C for 15 minutes, to allow sufficient enzymic digestion of the ascus surrounding the spores. Spore tetrads were thinly spread on a YPD agar plates. Dissection of tetrads was performed on a micromanipulator (Singer Instruments, Somerset). Individual spores were allowed to germinate into haploid colonies at 30°C for 3 days. Spores were transferred to SD minimal plates, plus amino acids required for selection, by replica plating.

2.3 Molecular techniques.

2.3.1 Restriction enzyme digest

0.1 to 4 μg DNA (in dH_2O or TE buffer) was digested with restriction endonuclease (1 to 5U/μg DNA) and with 1/10 volume 10x restriction buffer for 1 hour at specific temperature recommended by NEB.

2.3.2 Polymerase chain reaction (PCR)

The PCR was used for DNA amplification and site-directed mutagenesis (Chapter 3). A 50 μl preparative PCR reaction contained 5 μl of 10X Expand™ high fidelity (HF) buffer with 15 mM $MgCl_2$ {20 mM Tris-HCL, pH 7.5, 100 mM KCl, 1 mM dithiothreitol(DTT), 0.1 mM EDTA, 0.5% Tween® 20(v/v), 0.5% Nonidet® p40 (v/v), 50% glycerol (v/v)}, 100 μM dNTP mix (100 μM of each of dATP, dCTP, dTTP, dGTP (PE Applied Biosystems)), 100 pmol of each primer, and 1.14 unit Expand™ HF polymerase (Boehringer Mannheim, Germany).

PCR conditions (Boehringer Mannheim, Germany).

Number of cycles	Conditions
1x	Denature template 2 min. at 94°C
35-40x	Denaturation at 94°C for 30 sec Annealing usually at 45-65°C* for 30 sec Elongation at 72 or 68°C** for 45sec-8min Table 2.6.
1x	Final elongation at 72°C for min

* Annealing temperature depends on the melting temperature of the primers used.

** Elongation temperature depends on the length of amplification product: 72°C was used for amplification up to 3.0 kb; 68°C was used for amplification >3.0 kb.

PCR elongation times

Elongation time	45 sec	1 min	2 min	4 min	8 min
PCR fragment length (kb)	<0.75	1.5	3.0	6.0	10.0

2.3.3 Purification and precipitation of DNA

Plasmid DNA was purified by vortexing with an equal volume of phenol/chloroform/iso-amyl alcohol (25:24:1). The top layer was recovered after centrifugation. Routine precipitation of DNA was achieved by adding 2 volumes of 100% ethanol and 1/10 volume 6M ammonium acetate. The mixture was stored at –20°C for 20 minutes and centrifuged at 12 000g for 20 minutes. The pellet was washed twice with 70% ethanol to remove precipitated salt and resuspended in dH2O or TE buffer (10mM Tris HCl pH 7.0; 1 mM EDTA).

2.3.4 Agarose gel electrophoresis of DNA

DNA fragments between 0.5 and 25 kb were routinely separated using the following protocol. 0.8% w/v agarose gel was prepared using 0.5x TBE electrophoresis buffer (90mM Tris base, 90mM boric acid, 2mM EDTA) and appropriate weight of agarose. The mixture was melted in a microwave oven, mixed, cooled to 55°C and after adding ethidium bromide (EtBr) 0.5μg/ml, it was poured into a sealed platform with the gel combs. The DNA samples were electrophoresed (at 1 to 10 V/cm of agarose gel) with an appropriate amount of 10x DNA loading buffer (0.5xTBE, 10% glycerol (v/v), 0.1% bromophenol blue (w/v)) and appropriate DNA molecular weight markers. Gels were viewed using short wave UV transilluminator and photographed.

2.3.5 Isolation and purification of DNA fragments from agarose gels

DNA fragments of 70 bp to 10 kb were extracted and purified from agarose gel using the QIAquick™ gel extraction kit (QIAGEN Ltd.).

2.3.6 Dephosphorylation of 5' end of DNA and oligonucleotides

An appropriate amount of DNA or oligonucleotide was dephosphorylated using the Calf Intestine Alkaline Phosphatase (CIAP) kit (Promega Cor.).

2.3.7 Ligation of DNA fragments to plasmid vectors

Ligations were routinely carried out as described in Maniatis et al.,(1989).

2.3.8 Insertion of a Gly-6xHIS tag into pFA6A3xHAkanMX6

Oligos 6xHISFAvaI/AscI and 6xHISRAscI/AvaI (listed in table 4.1) were synthesised so that they could be annealed to each other creating the Gly-6xHIS epitope tag between *Ava*I and *Asc*I restriction endonuclease sites respectively. Oligos were annealed by mixing 4ng of each primer in 50μl of H_20, these were heated to 95°C for 5mins and left to cool at room temperature for 1-hour. The subsequent dsDNA fragment was digested with *Ava*I and *Asc*I, purified with a QIAquick™ PCR purification column (QIAGEN Ltd.) and then cloned into the *Ava*I and *Asc*I pre-digested pFA6A3xHAkanMX6 plasmid.

2.3.9 Handling bacteria

2.3.9.1 E. coli growth media and culture conditions

E.coli strains were grown in LB (Luria-Bertani), (1% w/v tryptone, 0.5% w/v yeast extract, 1% w/v NaCl and 1mM NaOH final concentration) at 37°C. Cultures for plasmid transformation and selection were grown in LB plus ampicillin to a final concentration of 100μg/ml.

2.3.9.2 Preparation of competent E. coli

Competent *E. coli* cells were prepared according to a calcium chloride technique as described in Maniatis et al.,(1989). The competent cells were resuspended in ice cold 0.1M $CaCl_2$ plus 15% glycerol and stored in 0.1 ml aliquots at -70°C.

2.3.9.3 E. coli transformation

Competent *E. coli* cells were thawed on ice and 100 μl pipetted into a chilled eppendorf. An appropriate amount of plasmid DNA was added and the cells were incubated on ice for 15 minutes. The cells were heat-shocked at 42°C for 90 seconds and placed on ice for 5 minutes. The cell were then resuspended in 900 μl of SOC medium (2% w/v tryptone, 0.5% w/v yeast extract, 10 mM NaCl, 2.5mM KCl, 10 mM $MgCl_2$, 20 mM $MgSO_4$, 20 mM D-glucose) and incubated at 37°C for 45 minutes. The cells were centrifuged at 6,000g for 30 seconds. The pellet was resuspended in 100 μl of the supernatant and then plated on LB plus ampicillin to a final concentration of 100μg/ml and incubated at 37°C overnight.

2.3.9.4 High efficiency transformation by electroporation

Electro-competent *E. coli* cells were prepared as described in (Zabarovsky and Winberg, 1990).50 μl aliquots of electro-competent *E. coli* cells and an appropriate amount of DNA (10 μl) were added to a Flowgen cuvette and electroporated (at 2500 V, 0.25 mF, 201 Ω, 5 msec) in an EasyjectT+ electroporator (Flowgen, Inc.). Immediately after electroporation 1 ml of LB or SOC was added to the cuvette and quickly but gently resuspended the cells. The cells suspension was then incubated at 37°C for 45 minutes. The cells were centrifuged at 6000g for 30 seconds. The pellet was resuspended in 100 μl of the supernatant and then plated on LB plus ampicillin to a final concentration of 100μg/ml and incubated at 37°C overnight.

2.3.9.5 Preparation of plasmid DNA from E.coli.

Approximately 20-100 μg of high-copy plasmid DNA was obtained from 5ml or 3ml overnight cultures of *E. coli* using QIAprep® Miniprep or Midiprep kits respectively as described in the appropriate QIAprep® handbooks (QIAGEN Ltd.).

2.3.10 Procedures for nucleic acid analysis

2.3.10.1 Isolation of yeast total genomic DNA

Yeast genomic DNA was prepared as previously described by Adams et al., (1997), except that proteinase K (200 μg/ml final concentration) was added at the point of

spheroplast lysis. The lysate was extracted by phenol:chloroform:isoamylalcohol (25:24:1) and DNA was precipitated by addition of an equal volume of isopropanol. High molecular weight DNA was recovered by spooling and washed twice in 70% ethanol. DNA was resuspended in (TE or dH2O) and treated with ribonuclease A and respooled before final resuspension in (TE or dH2O).

2.3.10.2 Quantification of DNA

DNA samples were quantified as described in Maniatis et al., (1989). An A260 of 1.0 was taken to indicate 50 μg/ml double stranded DNA, 37 μg/ml single stranded DNA. The ratio of A at 260 and 280nm was used to indicate nucleic acid purity.

2.3.10.3 Southern analysis

Following electrophoresis the DNA was denatured and agarose gels were blotted by capillary transfer of DNA as described in Maniatis et al., (1989). Blotting was carried out overnight with Hybond-N nylon transfer membrane (Amersham, Ltd.) in 20x SSC (3M NaCl, 0.3M sodium citrate; pH 7.0). Membranes were wrapped in 3MM Whatman filter paper and dried for 2 hours at 80°C.

2.3.10.4 In vitro labelling of single stranded DNA probes.

DNA probes were prepared as described by Feinberg and Vogelstein, (1983). Double stranded DNA was first denatured by boiling 100 ng of DNA in 10 μl of sterile dH_2O for 3 minutes. The DNA was cooled rapidly on ice and 12.5 μl of oligonucleotide labelling mix (25 μl nucleotide stock: 100 μM dGTP, dATP, dTTP, 250 mM Tris.Cl, pH 8.0, 25 mM $MgCl_2$; 25 μl 1M HEPES pH 6.6; 7 μl pd(N)6 sodium salt (100 ODU/ml, Pharmacia Biotech Ltd., UK), 20 μCi of (γ^{32}P)-5'-cytosine triphosphate and 5 units of Klenow were added. The probe was centrifuged at 12 000g for 10 seconds and incubated at 37°C for 1-2 hours. After annealing, the reaction was quenched by adding 50 μl of 20mM EDTA. The probe was denatured with 100 μl of 0.2M NaOH for 5 minutes at 37°C.

2.3.10.5 Hybridisation analysis of DNA probes to membrane bound nucleic acid

Hybridisation analysis was carried out by a modified method described by Meinkoth and Wahl, (1984). Dried membranes were pre-hybridised in siliconised glass bottles (Hybaid) in hybridisation solution (0.125 ml/cm^2; 5x Denhardt's solution, 0.5% (w/v) SDS, 10% dextran sulphate and 100 mg/ml single stranded salmon sperm DNA) for at least 30 minutes at the appropriate temperature with constant agitation. The denatured probe was added to the pre-hybridisation buffer and hybridisation was carried out overnight at the appropriate temperature. After hybridisation, the blot was washed at room temperature for 15 minutes in 2x SSC plus 0.1% (w/v) SDS. This was followed by a 15 minute moderate stringency wash at the appropriate temperature in 2x SSC plus 0.1% (w/v) or a minutes high stringency wash in 65°C 0.1x SSC plus 0.1% SDS (w/v). All washes were carried out in duplicate with constant agitation.

2.3.10.6 Autoradiography

Membranes were placed in direct contact with Fuji RX film in light proof autoradiographic cassettes for the appropriate length of time at –70°C with an intensifying screen. X-ray film was developed according to the manufacturers instruction.

2.3.10.7 Removal of probe from hybridised membrane

The hybridised probe was removed from membranes by boiling in 0.1% SDS for 10 minutes followed by cooling to room temperature. The membranes were wrapped in Saranwrap and stored at room temperature.

2.3.10.8 DNA sequencing analysis

Nucleotide sequences were determined using the ABI Prism® BigDye™ Terminator Cycle Sequencing Ready Reaction Kit (PE Applied Biosystems, Corp.) For each reaction the following reagents were added on ice to a PCR tube:

Terminator ready reaction mix	8 μl
Template:	
Single-stranded DNA	50-100 ng

Double-stranded DNA	200-500 ng
PCR product DNA	30-90 ng
Primer	3.2 pmol

The volume was made up to 20 μl by adding dH_2O. Reagents were mixed and spun briefly. The tube was placed in GENIUS TECHNE thermal cycler and the following cycle was repeated 25 times.

96°C for 30 sec.

50°C for 30 sec.

60°C for 4 min.

After completion of temperature cycle; 2 μl of 3 M sodium acetate pH 4.6 and 50 μl of 100% ethanol were added to each extension reaction and placed on ice for 10 minutes. The tubes were centrifuged at 12 000g for 15 minutes. The pellet was washed twice with 250 μl 70% ethanol, dried in a vacuum centrifuge for 1-3 minutes and then electrophoresed on the ABI Prism™ 377 DNA sequencer Kit (PE Applied Biosystems, Corp.). Signals were analysed using ABI Automated DNA Sequence Viewer version1.0 software (PE Applied Biosystems, Corp.).

2.4 *Biochemical techniques.*

2.4.1 Extraction of total cell protein.

Yeast cells were pelleted by centrifugation (3000 rpm, 5min) and the supernatant was discarded. Two volumes of acid washed glass beads (BDH, 40 mesh), were added to the cell pellet. Protein extraction buffer (50mM Tris-HCl[pH8.0], 1mM $MgCl_2$, 2mM EDTA, 1mM DTT, 1mM PMSF, 0.5mM TPCK and 2μg/ml Pepstatin A) was added at a volume sufficient to cover the cell/bead suspension. Cells were disrupted by vortexing for 30 second by vortexing and then chilling on ice for 30seconds, this procedure was repeated 5 times to ensure complete cell breakage. Beads and cellular debris were removed by centrifugation at (14000rpm, 5min, 4°C) and soluble protein-rich supernatant was removed.

2.4.2 Determination of protein concentration

proteins concentrations were determined using the BioRad protein determination kit and bovine serum albumin as standard. Both standard and unknown protein concentrations were assayed as by manufacturer's instructions.

2.4.3 Separation of proteins by SDS polyacrylamide gel electrophoresis (PAGE)

Proteins and their subunits can be separated by size using a discontinuous electrophoresis system (Laemmli, 1970). Slab gels were cast in the Bio-Rad Mini-Protean-1® system, gel solutions are listed below.

The Laemmli system consists of a stacking gel, containing 3% acrylamide and a resolving gel containing the appropriate percentage of acrylamide for efficient separation of proteins/fragments of interest (ranging from 7-15% acrylamide). Both gels were cast using a 40% acrylamide:bis-acrylamide stock and polymerised upon addition of 0.05%(v/v) TEMED and 0.7% (w/v) APS.

Prior to loading, protein samples were boiled for 10mins in sample buffer. These samples were loaded into wells formed within the stacking gel, and electrophoresis

proceeded at a constant current of 30mA until the appropriate level of protein separation had occurred. Molecular standard markers (Marker 12, SeeBlue2, Invitrogen®) were run beside the samples to indicate protein size. Solutions given below.

2.4.4 SDS-PAGE solutions

30%Acrylamide stock(BDH)	29.2% acrylamide and 0.8%Bis-acrylamide
APS	10% (w/v) solution stored at 4°C
Stacking Gel	125mM Tris-HCL[pH6.8]; 0.1%SDS, 4%polyacrylamide.
Resolving Gel (x%)polyacrylamide	500mM Tris-HCL[pH8.8]; 0.1%SDS,
Electrode buffer[pH 8.3]	0.025M Trizma base; 0.192M glycine and 0.1%SDS
Protein sample buffer	0.125M Tris-HCl[pH6.8]; 10% (v/v) glycerol, 5% (v/v) ßmercaptoethanol; 2%SDS and 0.015% (v/v) bromophenol blue.

2.4.5 Analysis of proteins after SDS-PAGE

After electrophoresis was completed the gel was dismantled and the proteins were visualised by one of the following methods.

2.4.5.1 Direct staining.

Staining with Coomassie blue R-250 allows detection of abundant proteins (1μg or more). Gels were incubated for 1 hour at room temperature, in 0.05% (w/v) Coomassie blue R-250, 50% methanol and 10% acetic acid. Gels were subsequently de-stained by gentle agitation at room temperature in a solution of 10% methanol and 7.5% acetic acid. Destain solutions were periodically changed.

2.4.5.2 Western blotting

SDS-PAGE separated proteins were blotted onto a nitrocellulose membranes by means of electrophoretic transfer. The electrophoresed gel, transfer membrane, 6 pieces of Whatman filter paper were pre-equilibrated in transfer buffer (25mM Tris and 150mM glycine [pH 8.3] with 29% methanol to minimise swelling of the gel during transfer). A

gel-blot sandwich was constructed of 3 pieces of filter paper, the gel, the membrane and the remaining sheets of paper. The sandwich was immersed within a buffer-filled Western blotting tank, with gel towards the cathode and membrane towards the anode. The electrophoretic transfer proceeded at 50V, 10°C, overnight. Efficiency of protein transfer was verified by staining the membrane with Ponceau-S. The transient stain was water soluble and did not affect further analysis of blotted proteins. By running pre-stained protein marker during SDS-PAGE, both the efficiency of transfer and molecular weight of sample proteins, was identified.

2.4.5.3 Immunodetection of proteins on blotted membranes

All immunodetection steps were carried out at room temperature with constant agitation. Phosphate Buffer Saline + 0.1% Tween (PBS-T) was used as both a base for blocking agent (5% non-fat dried milk powder dissolved in PBS-T), and as between-step washes. Antibodies were diluted in blocking agent and applied to the blot in a final volume of $0.1 ml cm^{-1}$ of membrane.

After Ponceau –S staining, the remaining protein-binding sites on the blot were blocked by incubation in blocking agent for 1 hour. Excess blocking agent was removed with 3 ten minutes washes in PBS-T. Primary antibody was diluted in blocking agent and used to probe the blot for 1 hour. The wash step was repeated before the secondary antibody was diluted in blocking agent and applied to the membrane for a further hour. Again surplus antibody was removed by washing the blot 3 times with PBS-T. Antibody binding was visualised by means of enhance chemiluminessence (ECL), (Amersham). Equal volume of reagents A and B were mixed and applied to the blot for 1 min. The localised fluorescence can be detected by exposure to Fuji X-ray film.

2.4.6 Analysis of protein synthesis in cells under different heat stress conditions.

Cells were pulse labelled with [35S]-methionine for 1-hour at varying temperatures. Labelled proteins were analysed by SDS-PAGE, the gel was dried and exposed X-ray film.Major Heat shock proteins were determined by their increased level of labelling and molecular weight as described (Panaretou et al., 1998).

2.4.7 Assay of β-Galactosidase in yeast.

This procedure was carried out as described in Adams et al.,(1997).

2.4.8 Superoxide activity assay.

Yeast extracts were prepared in 50mM potassium phosphate buffer (pH 7.0) containing a cocktail of protease inhibitors, and proteins concentrations were determined using the BioRad protein determination kit and bovine serum albumin as standard. Sod activity in these extracts was measured either from its ability to inhibit the xanthine oxidase , or its ability to inhibit reduction of nitro blue tetrazolium to formazan PAGE (Flohe and Otting, 1984). Distinction of Mn-Sod from Cu,Zn-Sod was based, in the former assay, on the selective capability of 2mM cyanide to inhibit Cu,Zn-Sod (Flohe and Otting, 1984) and, in the latter assay, on the different gel migrations of Mn-Sod and Cu,Zn-Sod.

2.4.9 Catalase assay.

Yeast extracts were prepared in 50mM potassium phosphate buffer (pH 7.0) containing a cocktail of protease inhibitors, and proteins concentrations were determined using the BioRad protein determination kit and bovine serum albumin as standard. Catalase activity of the protein extract was determined using the method of (Aebi, 1984). H_2O_2 solution (0.1 M), enzyme extract, and 50 mM phosphate buffer pH 7 were pipetted into a 3 ml cuvette. The reduction of H_2O_2 was followed at a wavelength of 240 nm for 1 min against a blank containing 50mM phosphate buffer and enzyme extract. Catalase activity was expressed in catalase U per g of protein.

2.4.10 To analyse oxidised proteins.

Samples of total cell protein were derivatised by mixing an aliquot with one volume of 12%(w/v) SDS and 2 volumes of 20mM 2,4-dinitrophenylhydrazine in 10% (v/v) trifluoroacetic acid (a blank control was treated with 2 volumes of 10% (v/v) trifluoroacetic acid alone) (Levine et al., 1995). The mixture was incubated 30 min at room temperature, in the dark, and subsequently neutralised with 1.5 volumes of 2M Tris 30% (v/v) glycerol 19% (v/v) 2-mercaptoethanol. Proteins (10 μg/lane) were loaded on a 12.5% SDS-PAGE. After electrophoresis, proteins were electroblotted onto a

nitrocellulose membrane, and the membrane was probed with rabbit IgG anti-DNP (Dako) at a 1:5000 dilution, and goat anti-rabbit IgG linked to horseradish peroxidase (Sigma) at a 1:5000 dilution, by standard techniques. Immunodetection was performed by chemiluminescence, using a kit from Amersham (RPN 2109).

2.5 Lifespan and physiological analysis.

2.5.1 Analysis of stationary phase survival (chronological lifespan).

Unless stated otherwise, all cultures were grown aerobically at 30°C in liquid YPDA medium (1% Difco yeast extract, 2% bactopeptone, 20mg/l adenine, 2% glucose (YPDA)(all concentrations %w/v). Flask cultures (flask volume/medium volume of 5:1) were first inoculated from an overnight stationary YPDA culture, at an initial density of $5x10^5$ cells/ml. These cultures were then grown to stationary phase, by shaking in a rotary shaker at 200rpm 30°C. They were confirmed as being in stationary phase by phase-contrast microscopy (large cells, <10% budded, with a single vacuole). They were then harvested, washed twice in sterile water, resuspended in water at t=0 at 1 x 10^8 cells/ml, and then shaken aerobically (flask volume/medium volume 5:1) at 30°C, 35°C or 37°C. At the indicated time intervals three serial dilutions of these cell suspensions were prepared, these being plated on plate count agar. After 5d growth of the plates at 30°C, cell viability was determined by colony counting. The plotted data represents the mean and SD of survival from the three viability determinations at each time point, >300 colonies being counted for each survival determination. At 30°C loss of viability was at least 2-fold slower than at 35°C or 37°C. However most survival determinations were conducted at the latter temperatures, so as to allow viability measurements to be conducted over a reasonable time scale.

2.5.2 Analysis of replicative lifespan.

Replicative life spans determinations and statistical analysis of life-span differences were essentially as described (Kennedy et al., 1995). Exponentially growing yeast were spread at low density onto a YPD plate and incubated 3h at 30°C to allow bud emergence. Typical experiments used 60 virgin buds, these being moved to fresh areas of the YPDA plate using a Singer MSM Micromanipulator (Singer Instruments, Taunton, U.K.). Life span of these virgin cells was determined by counting and removing each of the buds that they produced, until they divided no more. A cell was classed as senescent when no division occurred over a period of 48h at 30°C (Fig. 1.3).

For determining the replicative potential of stationary phase cells, these were plated at low density on YPGlycerol medium until bud emergence was observed, whereupon the newly-budded cell was micromanipulated to a designated position on the plate for measurement of replicative life span as above.

2.5.3 Measurement of tolerance to heat stress

Resistance to a heat shock of 50°C was determined over a period of 20-mins taking measurements every 2-mins. 2ml of an exponential culture of cells was exposed to the stress in glass tubes. Cell viability was determined by plating serial dilutions of the culture on plate count agar and plotting this as a percentage reduction of the viability at time point zero.

2.5.4 Measurement of mutation frequencies.

To measure mutation to canavanine resistance, appropriate dilutions were spread onto YPD plates for viability determinations, also synthetic media lacking arginine (Difco YNB without amino acids and supplemented with 150 ug of each leucine, adenine, uracil, tryptophan, and histidine per ml, 100 μg canavanine per ml and 2% glucose). After incubation at 30°C for 5 days, canavanine resistant cells were counted to determine *CAN1*^{s} to *can1*^{r} mutagenesis.

2.5.5 Measurements of free radical production .

Free radical production *in vivo* was measured from dihydrorhodamine fluorescence (Tarpey and Fridovich, 2001). After 1hour incubation with 50mM DHR-123 (SIGMA) exponential cultures were observed down a Fluoresecence was measured using an Axioplan 2 fluorescent microscope equipped with a Plan-Neofuar 100x/1,30 Ph3 oil objective and a 100W mercury lamp (Carl Ziess, Jena, GmbH, Germany). Fluorescence measurements were carried out using *ImagePro+* software. 75 individual cells were scored in three independent experiments per strain.

2.5.5.1 Analyses of "Old Mother" yeast cells.

2.5.5.2 Purification of old mother cells

High yields of old cells were obtained by a modification of a biotin-streptavidin magnetic sorting procedure (Fig. 2.1) (Sinclair and Guarente, 1997; Smeal et al., 1996). An overnight YPG (3%-Glycerol) culture was diluted in 50 ml YPG and grown for at least 12 hr to an OD_{600} = 0.7. Cells were harvested and washed twice in 1X phosphate-buffered saline (PBS tablets, Sigma) and resuspended in 1 ml of PBS. Between 8–10 mg of sulfo-NHS-LC-biotin (Pierce, IL) was added to the cells and incubated at room temperature with gentle shaking for 15 min. Sulfo-NHS-LC-biotin is sensitive to moisture and batches were found to vary. Cells were washed seven times in 1 ml PBS and resuspended in 1 ml YPG. Cell density was determined using a haemocytometer, and $1x10^8$ cells/liter were added YPG. Cells were grown at 30°C for 15-hrs (5 doubling times) with shaking (OD_{600} should not exceed 1.0), harvested by centrifugation, and resuspended in 40 ml of cold PBS. 250–300 μl of PBS-washed M-280 Dynabeads (streptavidin-coated magnetic beads; Dynal A.S., Oslo, Norway) were added to the cells and kept on ice for 2 hr with occasional swirling. Cells (10 ml) were added to test tubes and placed in a magnetic sorter (PerSeptive Biosystems, MA) for 10 min at 4°C. Free cells were gently removed with a pipette, and the remaining cells were resuspended gently in 10 ml of cold YPD, this was repeated 5 times to increase the purity of the old cell sample.

2.5.5.3 DNA purification from old mother cells

DNA was extracted from old cells within 2 hr. Freezing of cells in YPD + 15% glycerol at -80°C resulted in poor recovery of closed circular DNA. The following modifications to the spheroplast method were made to isolate total DNA (Ausubel et al., 1994). Cells were incubated in 15 μg/ml zymolyase (Sigma) in 1XTE/1 M sorbitol for 30 min at 37°C with shaking. Cells were gently lysed in 1M sorbitol/14% SDS at 65°C, and the solution was phenol extracted twice before ethanol precipitation. The pellet was resuspended in 1XTE/0.1 mg/ml RNase and incubated at room temperature for 15 min before ethanol precipitation. DNA was gently resuspended in 1XTE and stored at -80°C.

Figure 2.1)

Sorting old cells by biotinylation of the cell wall and magnetic purification with streptavidin-conjugated magnetic beads. The grey shaded ring indicates biotinylated proteins on the surface of the cell wall. The emerging daughter cell does not contain biotin because its surface is synthesised de novo at the budding site. Thus, the entire pedigree deriving from the indicated mother cell will contain only one biotinylated cell, the mother originally labeled. Avidin-magnetic beads (small black circles) will bind to these biotinylated cells, allowing them to be sorted by a magnet.

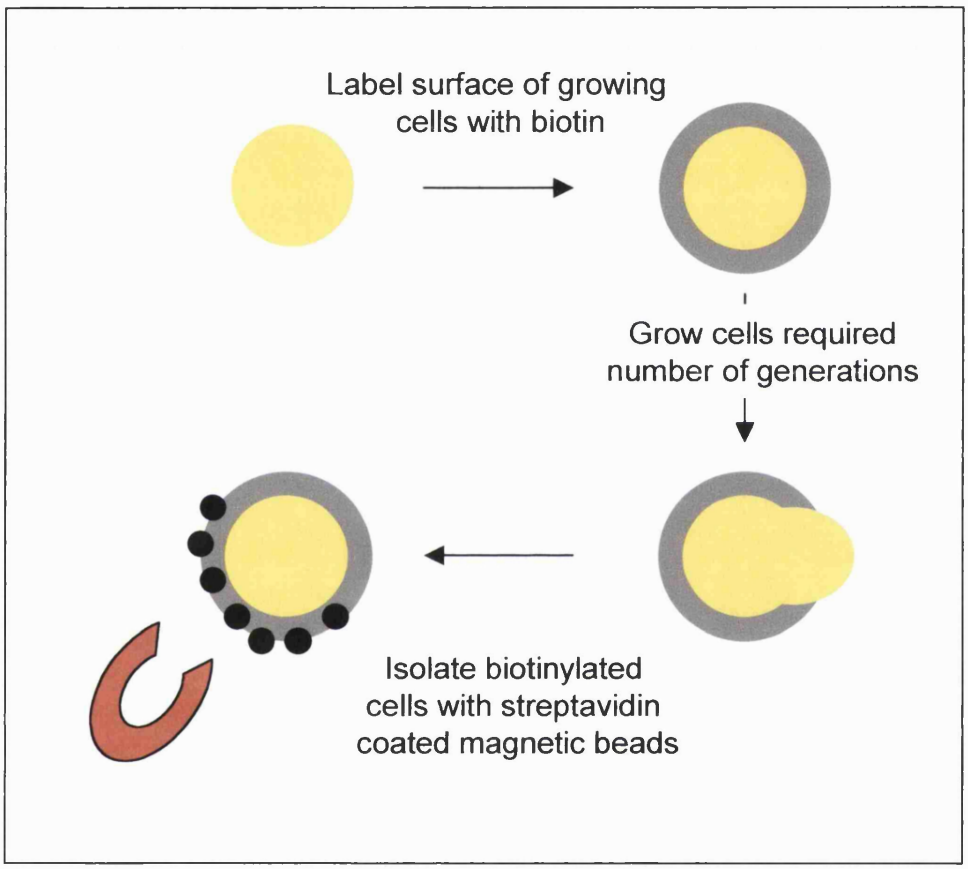
Label surface of growing
cells with biotin
Grow cells required
number of generations
Isolate biotinylated
cells with streptavidin
coated magnetic beads

2.5.5.4 ERC identification

DNA isolated from old mother cells (above) was heated with loading dye at 55°C for 10-mins prior to loading onto a horizontal 1XTAE (Tris-acetate-EDTA) 1% agarose slab gel. Electrophoresis was performed at room temperature at 1V/cm for 30hrs. The subsequent gel was blotted to HybondN-nitrocellulose membrane (Amersham). The blot was probed with a $dCTP^{32}$ labelled 2.8kb *Eco*RI fragment of the yeast rDNA derived from pNL47.

2.5.5.5 GFP-labelleing of mitochondria, and visualisation.

To visualise mitochondria, strains were transformed with a vector (pX232; (Westermann and Neupert, 2000)) for *TPI* promoter-driven expression of a mitochondrial-targetted GFP (mtGFP). These transformants were then biotinylated, grown for 5 generations on minimal glycerol medium + 0.5% casamino acids (Adams et al., 1997), and magnetically purified. Young cells were isolated from a mid-logarithmic culture for comparison. These cells were fixed and examined by fluorescence microscopy using a Zeiss Axiskop2 microscope equipped with a Plan-Neofluor 100x/1,30 Ph3 oil objective and a 100W mercury lamp (Carl Ziess, Jena, GmbH, Germany).

3 The role of the heat shock reponse pathway on yeast life span

3.1 Introduction

The precise relationship of stress resistance to replicative life span in *S. cerevisiae* is unclear. The deletion of the major Ras protein; Ras1p (Fig. 1.6)(Sun et al., 1994) or losses in transcriptional silencing as with mutation of *SIR4* (Kennedy et al., 1995) are both reported to increase lifespan and heat and starvation resistance. However whether these effects on life span and stress resistance are interrelated is unknown. They might reflect some of the genes that influence rDNA circle formation being regulated by oxidative stress (Bandara et al., 1998); or the influences of redox state on the NAD+ dependent Sir2p deacetylase (section 1.2.5). Cells that are growing on respiratory carbon sources do not consistently produce more daughters than cells that are growing mainly by fermentation of glucose (Barker et al., 1999), even though stress resistances are generally higher in respiratory cells (Martinez-Pastor et al., 1996). Yeast replicative life span may therefore, not always increase with general increases in stress resistance.

At the start of this project we reasoned that in *S.cerevisiae*, as in *Drosophila* and *C. elegans*, stress resistance might relate more to chronological life span (the ability of *nondividing* cultures to maintain viability over time) than to the replicative senescence of dividing cells. To test this theory strains with reduced Hsp90 chaperone activity were initially used. In organisms as diverse as yeast (Duina et al., 1998) and man (Zou et al., 1998), Hsp90 acts to down regulate the activity of the transcription factor (heat shock factor, HSF) that transcribes heat shock genes. Reduction in Hsp90 activity therefore activates heat shock genes. We investigated whether the Hsp90 chaperone system has an influence on yeast ageing, measured either as the replicative (nonchronological) senescence of budding cells or as the chronological ageing of nondividing (stationary) aerobic cultures. Yeast cells in which Hsp90 activity is lowered have a constitutively higher expression of heat shock genes and elevated levels of thermotolerance (Duina et al., 1998). In view of the apparent correlation between higher stress resistance and an

extended life span in other model systems of ageing (section 1), it seemed reasonable to ask whether the higher HSF activity and stress tolerance with lowered Hsp90 activity affects ageing processes. Hsp90 activity can be reduced through the *in vivo* administration of specific inhibitors of the Hsp90 chaperone, such as geldanamycin (Zou et al., 1998). For both *Drosophila* and *C. elegans* such drug inhibition of Hsp90 would probably only be a realistic strategy in the adult (geldanamycin causes developmental defects, at least in *Drosophila* (Rutherford and Lindquist, 1998)). In yeast it is necessary to use high geldanamycin levels to arrest growth, since this drug is actively effluxed from cells and a substrate of the Pdr5 drug efflux pump (our unpublished observations). We therefore resorted to the use of defined yeast mutants of W303-1a genetic background (Table 3.1) that have lowered activity of the Hsp90 chaperone system.

3.2 Results

3.2.1 Selection of yeast strains, with overactivation of the heatshock response, for use in this study.

Yeast *hsc82* and *cpr7* mutants were reported to overactivate the heat shock response as a result of defects in the Hsp90 chaperone complex (Duina et al., 1998) (Table 3.1). Yeast carries two genes for Hsp90, *HSC82* and *HSP82*. The *hsc82* mutation causes loss of the major constitutively-expressed form of Hsp90, with the result that *hsc82* cells have Hsp90 levels that are only 10-15% of normal (Borkovich et al., 1989). The *cpr7* mutation causes loss of the Cpr7p, a cyclophilin that is both a heat shock protein and Hsp90 system cochaperone (Duina et al., 1998). Loss of either *HSC82* or *CPR7* results in small or moderate overactivations respectively of yeast HSF (see Figs. 1,2 of (Duina et al., 1998)).

The essential functions of the Hsp90 chaperone cause it to be extremely conserved, with the result that only a few specific amino acid changes within this protein seem to give conditional mutant phenotypes. A collection of *hsp82* alleles that result in a temperature-sensitive growth phenotype when expressed as the sole Hsp90 in yeast, was described earlier (Nathan and Lindquist, 1995). Work carried out by other members of the laboratory on these temperature sensitive mutants identified a single *hsp82* allele which

was relevant to this study, E381K. Using a *lacZ*-based plasmid-borne reporter of HSF activity (see methods section 2.4.7) a number of these *hsp82* alleles that cause partial loss of the Hsp90 function were shown to cause appreciable overactivation of HSF at heat shock temperatures (as previously reported for the G170D mutant (Duina et al., 1998)) (Fig. 3.1a). However only *one* (E381K) displayed a strong heat shock response at 25°C (Fig. 3.1b). Nevertheless the ability of this E381K point mutation in the Hsp90 chaperone to produce such strong HSF activity at 25°C is a strong indication that the Hsp90 downregulation of HSF is still operative at normal, non-stressful temperatures. Protein pulse-labelling studies on these cells expressing the E381K mutant Hsp90 confirmed the unusually high levels of heat shock protein synthesis at 25°C and 30°C (Fig. 3.2).

Although temperature-sensitive for growth at 37°C (Nathan and Lindquist, 1995) the E381K mutant does not rapidly lose viability at high temperature. Instead its thermotolerance is elevated compared to the wild type, even in the absence of any preconditioning heat shock (Fig 3.1b; Fig. 3.2). Therefore, when expressed as the only functional Hsp90 gene in yeast, the E381K *hsp82* allele dramatically elevates the heat tolerance of cells growing at nonstressful temperatures.

Table 3.1) Strains used in this Chapter

Strain	Genotype	Source
W303-1a	MATa *ura1*-1 *trp1*-1 *leu2*-3,112 *his3*-11 *ade2*-1 *can1*-100	Duina et al. (1998)
cpr7	W303-1a *cpr7*::*TRP1*	Duina et al. (1998)
hsc82	W303-1a *hsc82*::*LEU2*	Duina et al. (1998)
cpr7 hsc82	W303-1a *hsc82*::*LEU2 cpr7*::*TRP1*	Duina et al. (1998)
P82a	W303-1a*hsc82*::*LEU2* *hsp82*::*LEU2* HIS3-GPD-HSP82[a]	Nathan and Lindquist (1995)
E381K	W303-1a *hsc82*::*LEU2 hsp82*::*LEU2* *HIS3*-GPD-*hsp82*(E381K)[a]	Nathan and Lindquist (1995)

Figure 3.1)

(a) HSF activity measurements in eight *hsp82* mutants and their p82a wild type (WT) parent , both during growth at 25°C (blue bars) and 1h after heat shock to 39°C (red) (data provided by Dr K Hatzixanthis). (b) Measurement of 50°C survival of cells of the E381K *hsp82* mutant (■) and p82a wild-type (■), initially in exponential growth at 25°C before heat challenge at high temperature for the time indicated. Cells of the E381K mutant have a high basal thermotolerance

a

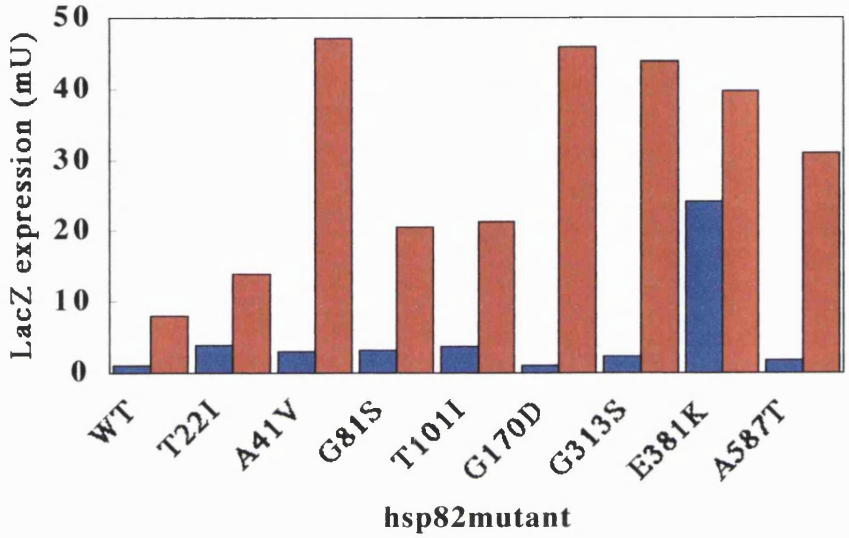
LacZ expression (mU)
50
40
30
20
10
0
WT
T22I
A41V
G81S
T101I
G170D
G313S
E381K
A587T
hsp82mutant

b

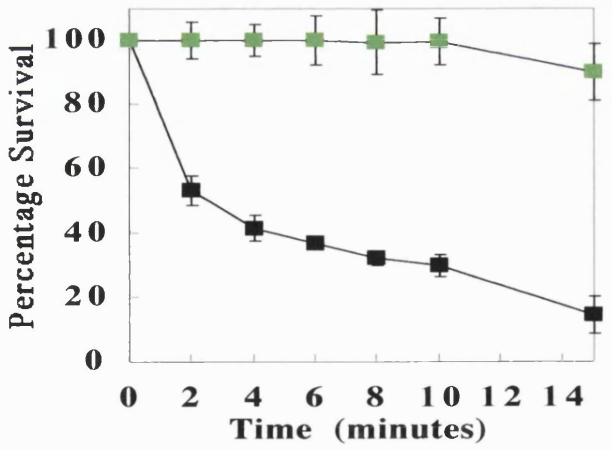
Percentage Survival
100
80
60
40
20
0
0 2 4 6 8 10 12 14
Time (minutes)

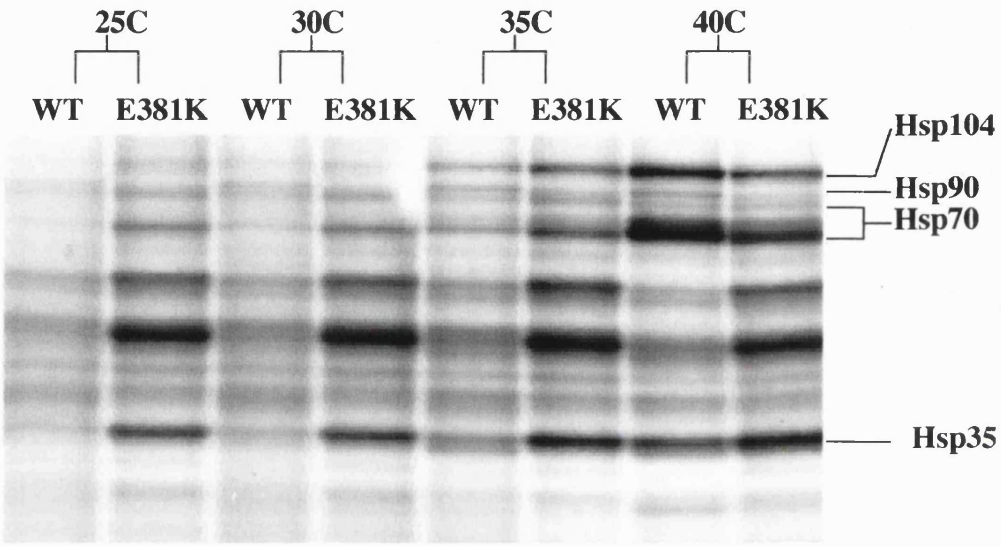

Figure 3.2)

Analysis of protein synthesis in cells expressing either wild type (WT) or the E381K mutant version of *Hsp82* as their sole Hsp90 protein (strains p82a and E381K respectively; (Table 3.1). Cells were pulse-labelled with [35S]methionine for 1h at the indicated temperature and labelled proteins were analysed by SDS-PA gel electrophoresis, as described earlier (Panaretou et al. 1998). Major heat shock proteins are indicated. Note that the Hsp90 in these strains is expressed under the control of the *GPD1* promoter, not HSF (Table 3.1) and is therefore not strongly induced in E381K. The abundant small heat shock protein Hsp26 is also not detected, since it lacks methionine residues (data provided by B. Panaretou).

3.2.2 *Over activation of the heat shock response, resulting from a defect in Hsp90, can extend chronological life span whilst reducing replicative potential of the dividing cell.*

Neither the *hsc82* or *cpr7* mutations alone had any significant effect on the mean or maximal replicative life span (Fig. 3.3a). However the presence of both together in the same strain caused replicative life span to be shortened dramatically (Fig. 3.3b), which possibly reflects the inherent lack of "fitness" of the *cpr7,hsc82* double mutant (a strain which grows extremely poorly (Duina et al., 1998)).

In contrast to these effects on replicative senescence, loss of *CPR7* lengthened the chronological life span of nondividing stationary cells (Fig. 3.4a). *CPR7* is therefore a potential prosenescence gene in yeast, a gene whose activity is clearly beneficial for vegetative growth (Duina et al., 1998) but detrimental for stationary survival (Fig. 3.4a). In contrast to this life span-extending effect of *cpr7*, chronological life span was shortened slightly by the *hsc82* mutation. Also the poorly-growing *cpr7,hsc82* double mutant did not survive well in stationary phase (Fig. 3.4b).

The E381K *hsp82* allele that caused a longevity benefit for chronological life span but not for replicative lifespan. Even though this E381K mutant Hsp90 elevates stress tolerances, it produces a statistically significant ($P=<0.01$) shortening of replicative life span (Fig. 3.3b). The presence of the same mutant Hsp90, in contrast, leads to extension to the chronological life span of stationary cells (Fig. 3.4b). It is therefore chronological ageing, not replicative senescence, which is slowed by the E381K mutation within Hsp90 protein.

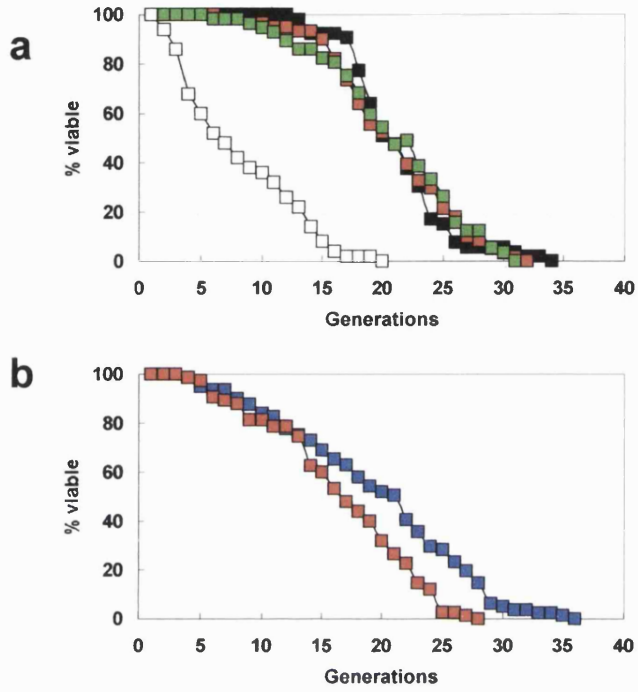

Figure 3.3

(a.) Replicative life spans of *cpr7* (■), *hsc82* (■) and *cpr7,hsc82* (□) mutants and their parental W303 wild-type strain (■). (b.) Replicative life spans of the E381K *hsp82* mutant (■) and its p82a parent (■). All life spans were analysed on YPD agar.

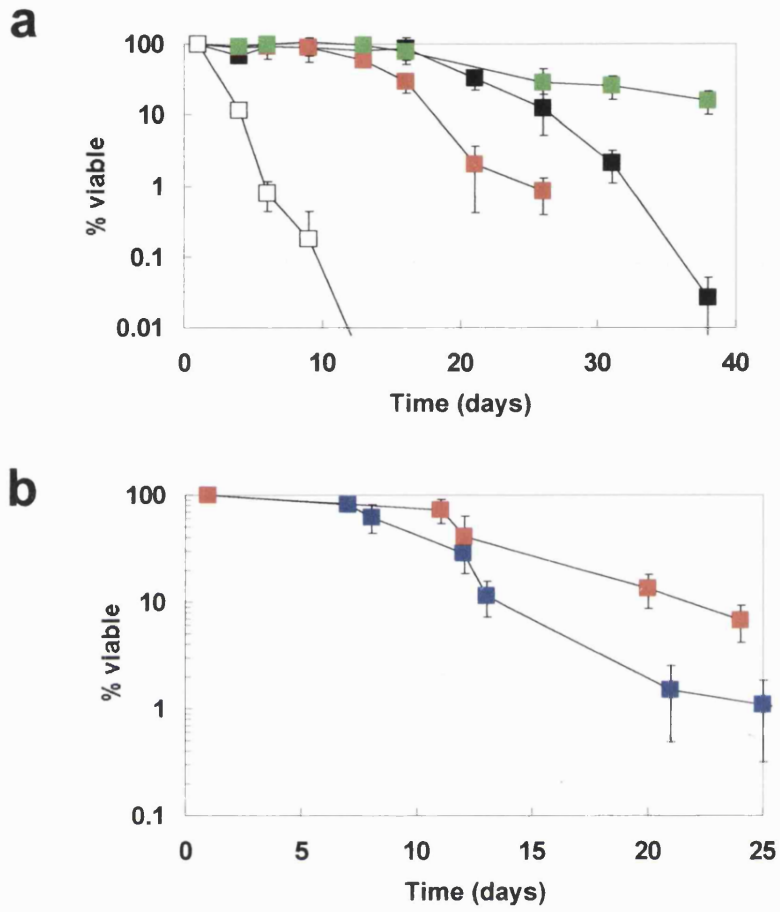

Figure 3.4)

(a) Chronological life spans of cells grown to stationary phase on YPD. *cpr7* (■), *hsc82* (■) and *cpr7,hsc82* (□) mutant cells and of the parental W303 strain (■). (b) Chronological life spans of the E381K *hsp82* mutant (■) and its p82a parent (■). Cells were grown to stationary phase on 2% glucose at 30°C, transferred to water and then maintained under normoxic conditions at either 35°C (a) or 37°C (b)

3.2.3 *The cpr7, hsc82 and E381K-hsp82 mutations do not further extend the chronological life spans of cells pre-adapted to respiratory growth*

The increases in chronological life span described above were for cells grown to stationary phase on 2% glucose. The life span benefits of defects in Hsp90 regulation seen in fermentative grown cells were not observed when these mutants were grown to stationary phase on respiratory 3% glycerol media (Fig. 3.5). The p82a wild type had a longer life span when grown by respiration than those grown on glucose (data for the W303 strain was not comparable because these experiments were carried out at different temperatures)(Fig. 3.5). In general cells grown by respiration have a higher tolerance for stress and survive longer periods of stationary phase maintenance (MacLean et al., 2001). The survival of respiratory cells must therefore be optimal, the data indicating that further increases in stress resistance due to low Hsp90 chaperone activity may not give further extension to life span in such respiration-adapted cells optimised for stationary maintenance.

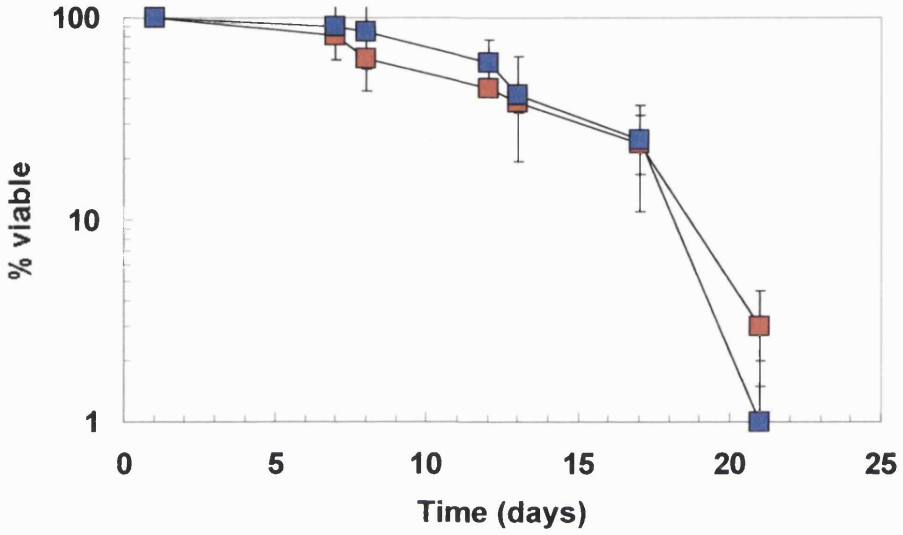

Figure 3.5)

Chronological life spans of the respiratory adapted E381K *hsp82* mutant (■) and its p82a parent (■). Cells were grown to stationary phase on 3% glycerol at 30°C, transferred to water and then maintained under normoxic conditions at 37°C

3.3 Conclusion

These results on yeast with lowered Hsp90 chaperone activity reinforce the view that higher stress resistances slow ageing, not through any major effects on the replicative senescence of dividing cells, but by effects on the chronological ageing of nondividing (postmitotic) cells. In nondividing cells, essential components that become damaged cannot be diluted out through cell division but must, of necessity, be turned over and renewed. There is increasing evidence that elevated stress resistance is associated with an increased ability to eliminate such damaged cell components. For example, many genes of aberrant protein turnover (Hershko and Ciechanover, 1998) or which confer resistance to the toxic products of lipid peroxidation (Evans et al., 1997; Turton et al., 1997) are stress-inducible. By elevating stress resistances, the gene products needed for this renewal will be elevated, presumably with a commensurate reduction in the steady-state levels of damaged cell components. A slower chronological ageing may be one manifestation of these events.

4 Life span analyses of yeast strains with increased levels of major free radical scavenging enzymes.

4.1 Introduction

Recent studies in other model organisms have shown that chronological life-spans can be increased by increasing stress resistance, especially with the increased free radical scavenging that accompanies the overexpression of antioxidant enzymes. *Drosophila* life span can be increased by increasing levels of the cytosolic Cu,Zn-superoxide dismutase (Cu,Zn-Sod) or the mitochondrial Mn-Sod in *adult* flies (Sun and Tower, 1999; Tower, 2000) or expressing human Cu/Zn-Sod in motorneurons (Parkes et al., 1998). Long-lived *Drosophila* obtained by the selective breeding of individuals with long life-span and long-lived mutants the nematode *C. elegans* obtained by direct selection also generally have a greater stress resistance (Lithgow, 1996; Service et al., 1985; Taub et al., 1999). C. *elegans* overexpressing catalase (Taub et al., 1999) or treated with Sod mimetics (Melov et al., 2000) also live longer. In this chapter we investigate whether increases in free radical scavenging enzymes extend life span in yeast.

The increases in the life spans of adult *Drosophila* and *C. elegans* with increased stress resistance, discussed above, primarily reflect the ageing of postmitotic tissues. High antioxidant defence probably counteracts ageing of post mitotic cells by providing increased long term protection to cellular macromolecules. In nondividing cells, essential components that become damaged must, of necessity, be repaired or turned over and renewed. Many activities needed for preventing such damage and possibly those needed for renewal of damaged components appear to be stress-inducible. Thus elevating stress resistances may reduce ROS-mediated damage and increase levels of repair activities, with commensurate reduction in the steady-state levels of damaged cell components.

Sods and catalases constitute the first line of defence of all aerobic cells (Fig. 4.1). The first of these enzymes catalyses the dismutation of superoxide free radicals to hydrogen peroxide and water; the second the breakdown of this hydrogen peroxide (Halliwell and Gutteridge, 1998). *S. cerevisiae* possesses an abundant Cu,Zn-Sod (Sod1) found in the cytosol and the intermembrane space of the mitochondrion, as well as a Mn-Sod (Sod2) in the lumen of the mitochondrion (Gralla and Kosman, 1992; Moradas-Ferreira and Costa, 2000; Sturtz et al., 2001; Westerbeek-Marres et al., 1988). The former enzyme constitutes at least 90% of total Sod activity in yeast growing aerobically by fermentation of glucose, since Mn-Sod is substantially glucose-repressed, in common with several other mitochondrial activities (Gralla and Kosman, 1992; Westerbeek-Marres et al., 1988). However with growth on respiratory substrates such as glycerol the gene for Mn-Sod (SOD2) is derepressed (Flattery-O'Brien et al., 1997; Galiazzo and Labbe-Bois, 1993), with the result that Mn-Sod constitutes 30-40% of the total Sod activity in respiratory cells (Westerbeek-Marres et al., 1988). This induction of the mitochondrial Mn-Sod in respiratory cells probably reflects the need to counteract higher levels of endogenous ROS production with much greater activity of the mitochondrial respiratory chain.

Figure 4.1)

Cellular defence against the free radical, toxic byproducts of mitochondrial oxidative phosphorylation. Oxidation of NADH to NAD+ by Complex I or oxidation of succinate to fumarate by Complex II releases electrons which are shuttled through the mitochondrial inner membrane by ubiquinone to Complex III. (*S. cerevisiae* does not have Complex I, instead reducing agents are delivered to the respiratory chain via independent NADH dehydrogenases). Electrons are then passed from Complex III to Complex IV by cytochrome *c*, and ultimately donated directly to 1/2 O_2 to give H_2O. The energy released is captured in a proton gradient which is used by Complex V to synthesise ATP. Electrons however from Complex I and ubiquinone can be passed directly to O_2 to give superoxide. $O_2^{-}\bullet$ is dismutated to H_2O_2 by the Mn-Sod and Cu,Zn-Sod of the mitochondria and cytoplasm respectively. H_2O_2 is detoxified by catalase and glutathione to H_2O.

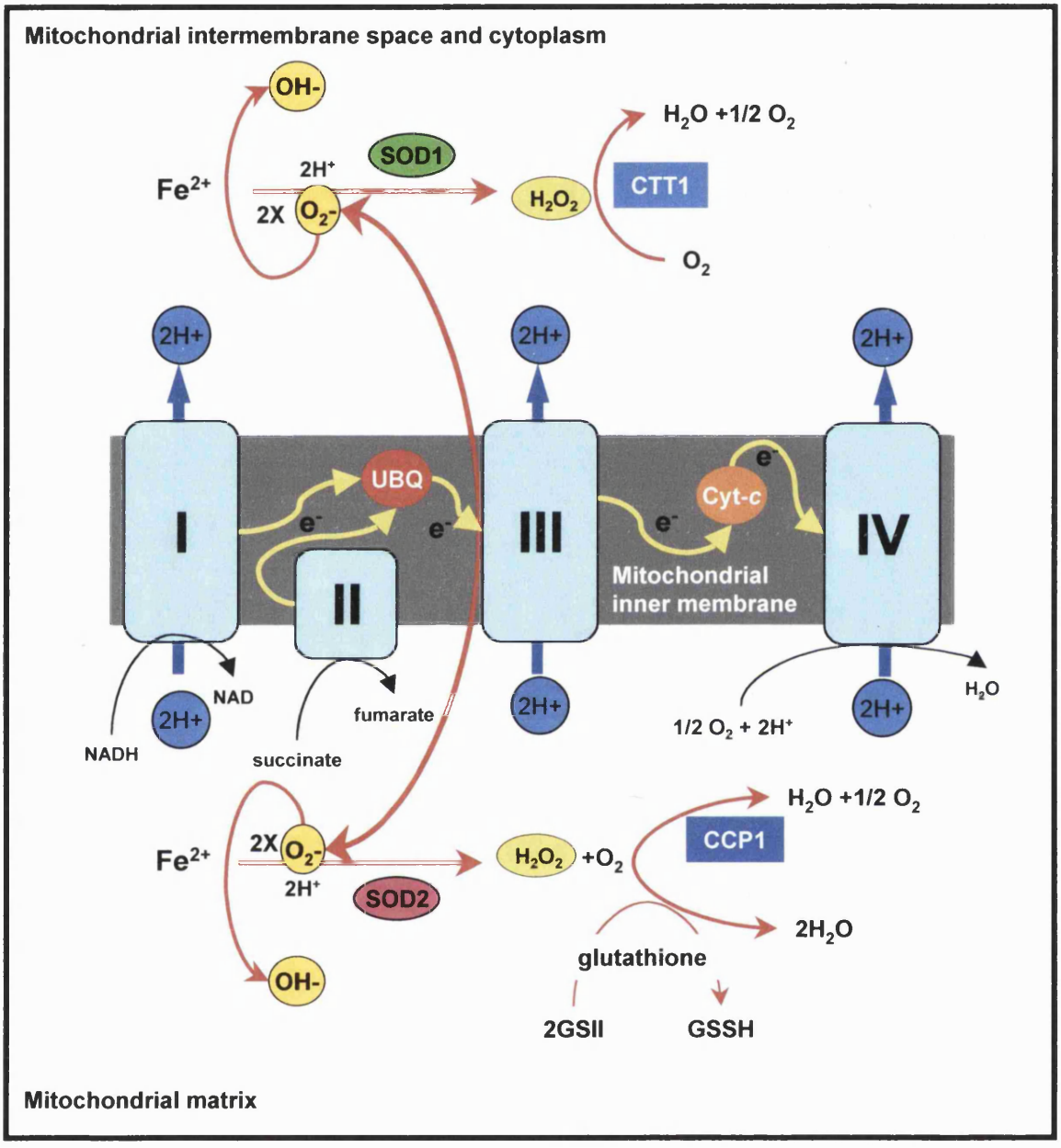
Mitochondrial intermembrane space and cytoplasm
OH-
Fe2+
2H+
SOD1
2X O2-
H2O2
CTT1
H2O +1/2 O2
O2
2H+
2H+
2H+
UBQ
e-
e-
e-
e-
Cyt-c
I
II
III
IV
Mitochondrial inner membrane
NAD
2H+
NADH
fumarate
succinate
2H+
2H+
1/2 O2 + 2H+
H2O
Fe2+
2X O2-
2H+
SOD2
H2O2 +O2
CCP1
H2O +1/2 O2
2H2O
glutathione
OH-
2GSH
GSSH
Mitochondrial matrix

4.2 Results 1: Overexpressing free radical scavenging enzymes in yeast.

4.2.1 Construction of yeast strains with elevated levels of antioxidant enzymes.

To see whether increased ROS scavenging can extend yeast chronological life span integrative cassettes for the overexpression of native major free radical-scavenging enzymes in *S. cerevisiae* were constructed. Initially cassettes were made for *ADH2* promoter-driven overexpression of the native mitochondrial Mn-Sod (Sod2p), mitochondrial catalase (cytochrome-c peroxidase Ccp1p), the cytoplasmic catalase (Ctt1p) and the cytoplasmic Cu,Zn-Sod (Sod1p). Each of these cassettes was then inserted into a haploid strain of S288c genetic background (FY1769-28c). The *ADH2* promoter was chosen for overexpression as this is a strong promoter in respiratory yeast (Denis and Audino, 1991), our earlier work having shown that it is stationary cultures well-adapted to respiratory maintenance that display the longest chronological life spans (MacLean et al., 2001).

As an initial step a 0.675kb *Eco*RI-*Xba*I fragment, containing the *ADH2* promoter and multiple cloning site of pWYG2L (Johnston, 1994), was ligated into *Eco*RI plus *Xba*I-cleaved pRS403 and pRS406 (Sikorski and Hieter, 1989) so as to give pRS403(ADH2) and pRS406(*ADH2*) respectively (Fig. 4.2a). Different genes were PCR amplified and subsequently inserted into these vectors, downstream of the *ADH2* promoter (Fig. 4.2b), so as to provide cassettes for overexpression of different antioxidant enzymes. PCR primers for the amplification of the antioxidant genes(Table 4.1) were designed with unique restriction sites, present in the multiple cloning site of pWYG2L, 5' of the ATG start codon and 3' of the stop codon.

Figure 4.2)

Schematic diagram of the construction of the pRS403/406-based integrative cassettes for overexpression of *SOD1* and *SOD2*. (a) A 0.675kb *Eco*RI-*Xba*I fragment, containing the *ADH2*-promoter and multiple cloning site of pWYG2L [Johnston, 1994 #546], (b) was ligated into *Eco*RI plus *Xba*I-cleaved pRS403 and pRS406 yielding pRS403(*ADH2*) and pRS406(*ADH2*). (c) Cassettes for *SOD1* and *SOD2* had been previously constructed whereby *SOD1* and *SOD2* had been cloned in front of a transcriptional terminator sequence derived from the 2-micron plasmid (2μT) (work done by P. Piper). These *SOD1* and *SOD2* regions including the 2μT sequence were removed on *Bam*HI/*Xba*I fragments and cloned into the pRS403/406(*ADH2*) plasmids.

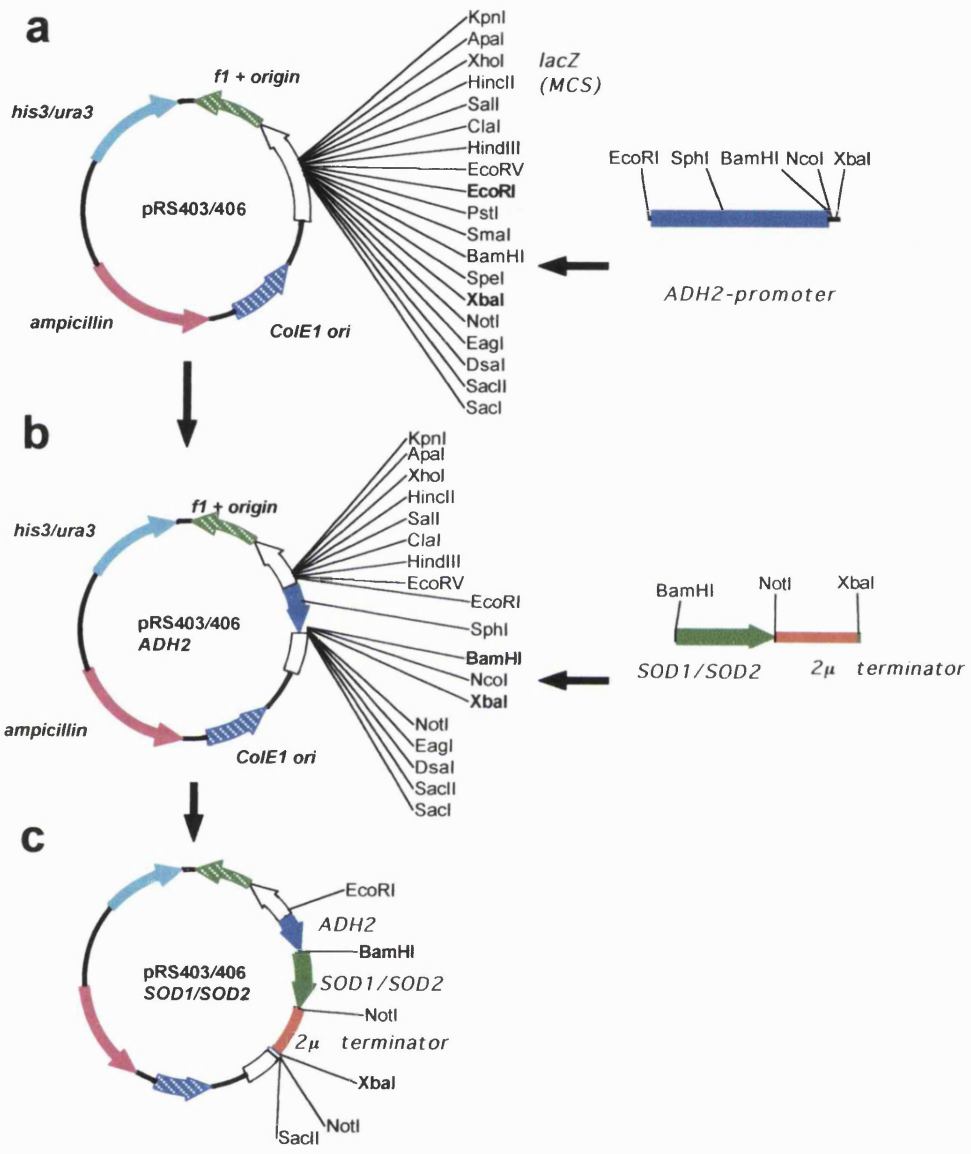
a
f1 + origin
his3/ura3
pRS403/406
ampicillin
ColE1 ori
KpnI
ApaI
XhoI
HincII
SalI
ClaI
HindIII
EcoRV
EcoRI
PstI
SmaI
BamHI
SpeI
XbaI
NotI
EagI
DsaI
SacII
SacI
lacZ
(MCS)
EcoRI SphI BamHI NcoI XbaI
ADH2-promoter
b
f1 + origin
his3/ura3
pRS403/406
ADH2
ampicillin
ColE1 ori
KpnI
ApaI
XhoI
HincII
SalI
ClaI
HindIII
EcoRV
EcoRI
SphI
BamHI
NcoI
XbaI
NotI
EagI
DsaI
SacII
SacI
BamHI
NotI
XbaI
SOD1/SOD2
2μ terminator
c
pRS403/406
SOD1/SOD2
EcoRI
ADH2
BamHI
SOD1/SOD2
NotI
2μ terminator
XbaI
NotI
SacII

Table 4.1) PCR primers used in study

FSOD1BamHI *(underline = restriction site)*	CTAGGATCCATAATGGTTCAAGCAGTCGC
RSOD1NotI	ATAGCGGCCGCCGCTATGAGATAAACCCGAA
FSOD2BamHI	CTAGGATCCAGGATGTTCGCGAAAACAGC
RSOD2NotI	ATAGCGGCCGCACAGCAATTGCCGAAAAC
FCTT1BamHI	CTAGGATCCTCATGCCAATAAGATCAATC
RCTT1XbaI	CGCTCTAGAAACTAACGAGTTGTGAA
FCCP1EcoRV	CACACACGTATATCTGATATCATGACTACTGC TGTTAGG
RCCP1XbaI	GTCTATTTCCATTGTGGAATCTAGAGCCCAAA AGA
FCCS1BamHI	CCCATTCGATCAGCGGATCCATGACCACGAAC GATACATACG
RCCS1NotI	TGTGCTATCTGCGGCCGCCTATTTGATGTTGTT GGCC
FSOD1N6HisBamHI *(Green = START* *Blue = 6xHIS tag)*	AAGCAATCGGGATCCATGCATCATCATCATCA TCATGGTATGGTTCAAGCAGTCGCAGTG
RSOD1N6HisNotI	GCCCGAGATCGGCGGCCGCCACATGGGTGGC ACGATG
FSOD1NotITERM	CTAACCAACTAAGCGGCCGCATAATATACTTG AATAAAAACCG
RSOD1SacIITERM	GCCCGAGATCGACCCGCGGCACATGGGTGGC ACGATG
FSOD1C6HisBamHI	AAACATAATTAAGGATCCATGGTTCAAGCAGT CGCAGTG
FSOD1C6HisNotI *(Red = STOP codon)*	TTACTTACATGCGGCCGCTTAATGATGATGAT GATGATGACCGTTGGTTAGACCAATGACACC

6xHISF AvaI/AscI	GGCCCCGGGGGTCATCATCATCATCATCATTA GGGCGCGCCGGC
6xHISRAscI/AvaI	GCCGGCGCGCCCTAATGATGATGATGATGATG ACCCCCGGGGCC
FSOD1C6xHisKanMX6 *(Magenta = vector annealing Black= genomic sequence)*	GGTCCAAGACCAGCCTGTGGTGTCATTGGTCT AACCAACGGGGGTCATCATCATCATCATCATT AGGGCGCG
RSOD1C6xHisKanMX6 *(Magenta = vector annealing Black= genomic sequence*	GGTGAAGTGATCAAGGACATAAATCTAAGCG AGGGAAATGAAAACGCGGCCGCATAGGCCAC TAGTGG
6xHISTAGseq	CGGGTGACCCGGCGGGGACGAGGC

Cassettes for *SOD1* and *SOD2* had been previously constructed whereby *SOD1* and *SOD2* had been PCR amplified from yeast genomic DNA on a *Bam*HI-*Not*I fragments, using primers *FSOD1BamHI* + *RSOD1NotI and FSOD2BamHI* + *RSOD2NotI* (Table 4.1), and cloned in front of a transcription terminator sequence derived from the 2-micron plasmid (2μ). *SOD1* and *SOD2* were removed together with the 2μ terminator sequence from these plasmids on *Bam*HI/*Xba*I fragments and ligated downstream of the *ADH2* promoter into the pRS403(*ADH2*) and pRS406(*ADH2*) plasmids digested with *Bam*HI/*Xba*I, thereby generating pRS403(*ADH2*)*SOD1* pRS406(*ADH2*)*SOD2* (Fig. 4.2c). Similarly the coding region of *CTT1* including the native downstream transcription termination sequences was PCR amplified from yeast genomic DNA using primers *FCTT1BamHI, RCTT1XbaI* (Table 4.1). After digestion with *Bam*HI-*Xba*I this was ligated into pRS403(*ADH2*)*SOD1* from which the coding sequence of *SOD1* and the 2μ terminator sequence had been removed with *Bam*HI-*Xba*I. The resulting plasmid therefore contained *CTT1* and its terminator sequence downstream of the *ADH2* promoter (Fig. 4.3a) *CCP1* was amplified with *FCCP1EcoRV* and *RCCP1XbaI* (Table 4.1). The coding sequence for *CCP1*, however contained both *Bam*HI and *Not*I sites and was therefore amplified using these primers and digested with *Eco*RV/*Xba*I before blunt end ligation into the same *Bam*HI-*Xba*I digested pRS403(*ADH2*)*SOD1* (Fig. 4.3b).

DNA digests were performed to verify these overexpression cassettes(Fig. 4.4). Finally these vectors were cleaved at their unique *Pst*I site prior to integrative transformation into *S. cerevisiae* FY1679-28c, selecting either for histidine prototrophy (pRS403-derived plasmids) or uracil prototrophy (pRS406-derived plasmids). Strains with a single integrated overexpression cassette were also transformed with either pRS403 or pRS406 so as to create a set of *HIS*$^+$ *URA*$^+$ isogenic strains (Table 4.2) with additional genes for oxidant scavenging enzymes, all under the ADH2 promoter control.

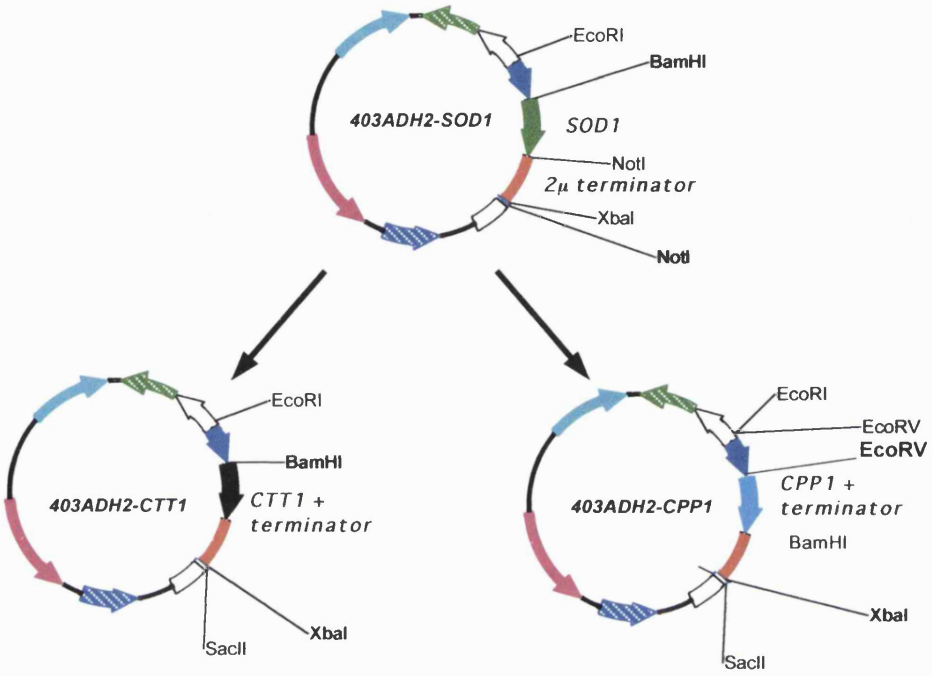

Figure 4.3)

Construction of the vectors for overexpression of *CTT1* and *CCP1*. The *SOD1* and 2μT sequences were removed from pRS403(*ADH2*)*SOD1* with *Bam*HI/*Xba*I prior to cloning of *CTT1* and *CCP1* downstream of the *ADH2* promoter of pRS403(*ADH2*). *CTT1* was inserted as a PCR amplified *Bam*HI/*XbaI* fragment (2327bp). *CCP1* was inserted on an *Eco*RV/*Xba*I (1552bp) fragment, which was then blunt end ligated into the pRS403(*ADH2*) backbone.

Figure 4.4)

DNA digests of the overexpression cassettes. *SOD1*, *SOD2*, *CTT1*, *CCP1* and *CCS1* were PCR amplified and cloned into the MCS of the pRS403/pRS406 intergrating plasmids, downstream of the *ADH2*-promoter.

Lanes 1 and 2: the *Eco*RI+*Bam*HI excised *ADH2*-promoter of both pRS403/pRS406 (305bp). 3, 4: the *SOD1* (465bp) and *SOD2* (702bp) gene fragments respectively, excised with *Bam*HI + *Not*I, from pRS403(*ADH2*)*SOD1* and pRS406(*ADH2*)*SOD2*..

CTT1 and *CCP1* were PCR amplified with their putative native transcriptional terminator regions and cloned into pRS403(*ADH2*), and hence the excised fragment is greater than the size of the gene. *CTT1* was amplified on a 2327bp *Bam*HI/*Not*I fragment (lane 5), containing the 1722bp of *CTT1* coding sequence and a 555bp downstream region cloned into pRS403(*ADH2*) . *CCP1* was amplified on a 1552bp *Eco*RV/*Xba*I fragment, containing 1086bp of coding sequence and 466bp of downstream sequence, which was blunt end ligated into the pRS403*SOD1* plasmid. Digestion of pRS403*CCP1* with *Eco*RV and *Xba*I (lane 6) yields the *CCP1* fragment and the *ADH2*-promoter which is on an *Eco*RV fragment (305bp).

CCS1 was amplified without its terminator sequence on a *Bam*HI/*Not*I fragment, and cloned into pRS403(*ADH2*) which contained a transcription termination sequence from *SOD1* (detailed in Fig. 4.7b). Digestion with *Bam*HI and *Not*I (lane 7) yields the 756bp gene fragment.

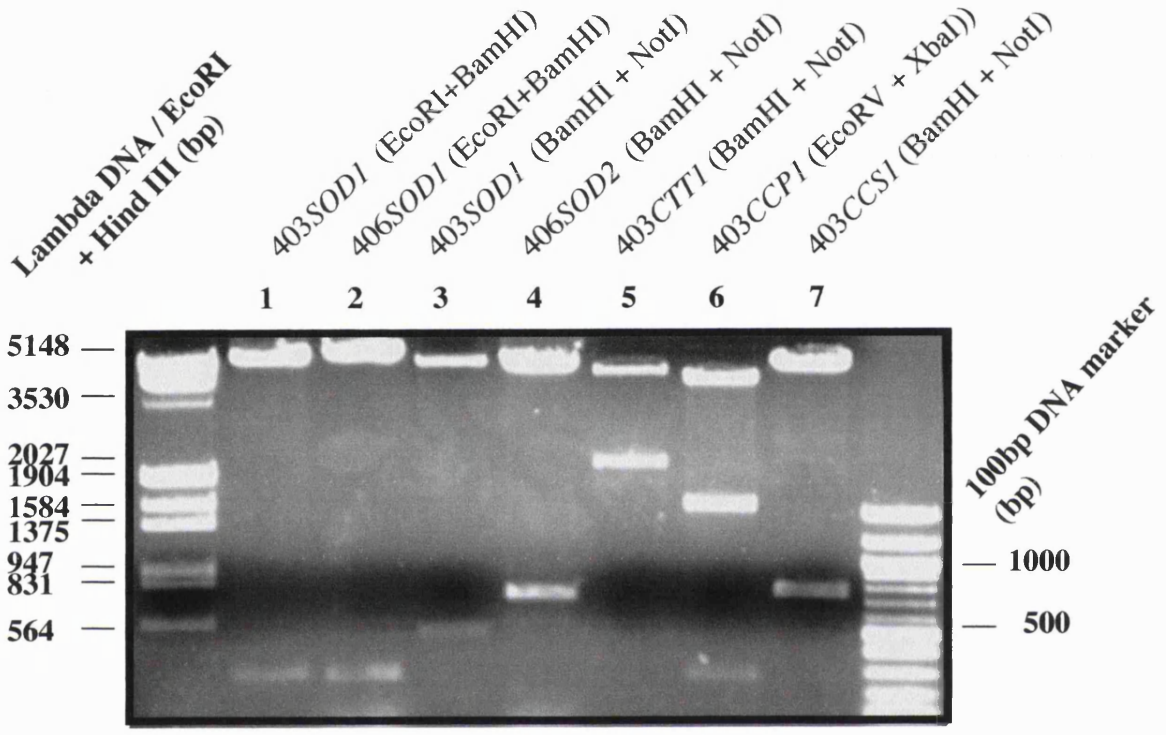
Lambda DNA / EcoRI + Hind III (bp)
403SOD1 (EcoRI+BamHI)
406SOD1 (EcoRI+BamHI)
403SOD1 (BamHI + NotI)
406SOD2 (BamHI + NotI)
403CTT1 (BamHI + NotI)
403CCP1 (EcoRV + XbaI))
403CCS1 (BamHI + NotI)
1
2
3
4
5
6
7
5148
3530
2027
1904
1584
1375
947
831
564
100bp DNA marker (bp)
1000
500

Table 4.2) Strains used in this study

Strain	Genotype	Source
FY1679-28c	MATa *his3-Δ200, ura3-52, leu2-Δ1, trp1-Δ63*	Euroscarf
FY*sod1Δ*	FY1679-28c *sod1ΔkanMX4*	(Piper, 1999)
FY*sod2Δ*	FY1679-28c *sod1ΔkanMX4*	(Piper, 1999)
FY*ctt1Δ*	FY1679-28c *ctt1ΔkanMX4*	This study
FY*wild type*	FY1679-28c *HIS3::[pRS403], URA3::[pRS406]*	This study
SOD1	FY1679-28c *HIS3::[pRS403], URA3::[pRS406(ADH2-SOD1)]*	This study
SOD2	FY1679-28c *HIS3::[pRS403], URA3::[pRS406(ADH2-SOD2)]*	This study
CTT1	FY1679-28c *HIS3::[pRS403(ADH2-CTT1)], URA3::[pRS406]*	This study
CCP1	FY1679-28c *HIS3::[pRS403(ADH2-CCP1)], URA3::[pRS406]*	
CCS1	FY1679-28c *HIS3::[pRS403(ADH2-CCS1)], URA3::[pRS406]*	This study
SOD1+CTT1	FY1679-28c *HIS3::[pRS403(ADH2-CTT1)], URA3::[pRS406(ADH2-SOD1)]*	This study
SOD2+CCP1	FY1679-28c *HIS3::[pRS403(ADH2-CCP1)], URA3::[pRS406(ADH2-SOD2)]*	This study
SOD1+CCS1	FY1679-28c *HIS3::[pRS403(ADH2-CCS1)], URA3::[pRS406(ADH2-SOD1)]*	This study
SOD1c6xHIS-kanMX4	FY1679-28c *SOD1c6xHIS kanMX4*	This study
SOD1c6xHIS-kanMX4 +SOD1c6xHIS	FY1679-28c *SOD1c6xHISkanMX4 HIS3::[pRS403], URA3::[pRS406(ADH2-SOD1c6xHIS)]*	This study
FY*mtGFP*	FY1679-28c *HIS3::[pRS403], URA3::[pRS406], TRP1::[pYX232-mtGFP]*	This study
SOD2 mtGFP	FY1679-28c *HIS3::[pRS403], URA3::[pRS406(ADH2-SOD2) TRP1::[pYX232-mtGFP]*	This study

4.2.2 Overexpression of the major free radical scavenging enzymes.

Consistent with the *ADH2* promoter being active only in respiratory cells the cassettes for *SOD2* and *CTT1* overexpression cassettes produced, respectively, 7–fold or 3-fold increases in either Mn-Sod activity or catalase activity (Fig. 4.5a, 4.5c). Sod activity in these extracts was measured either from its ability to inhibit the xanthine oxidase reaction *in-vitro* or its ability to inhibit reduction of nitro blue tetrazolium to formazan in PAGE gels (Flohe and Otting, 1984). Catalase activity was determined by the degradation of H_2O_2 by total cell extracts, and followed by the fall in absorbance at 280nm (Aebi, 1984) (methods 2.4.8; 2.4.9). It is improbable that any of this MnSod is active in the cytosol since, though the Mn-Sod precursor is synthesised on cytosolic ribosomes, removal of its 26-residue N-terminal leader sequence during import into the mitochondrion is a prerequisite for the formation of the active MnSod tetramer (Scandalios, 1992). The presence of the *SOD2* overexpression cassette also caused small increases in the cytosolic Cu,Zn-Sod and catalase activities of glycerol-grown cells (Fig. 4.5a). These may reflect stress induction of the chromosomal genes for Cu,Zn-Sod (*SOD1*) and catalase T (*CTT1*) (Moradas-Ferreira and Costa, 2000), possibly as a consequence of increased H_2O_2 production in mitochondria with excessive Mn-Sod activity. A catalase of the mitochondrion (Ccp1p) is known to be a vital component of the sensing of H_2O_2 stress in yeast (Charizanis et al., 1999).

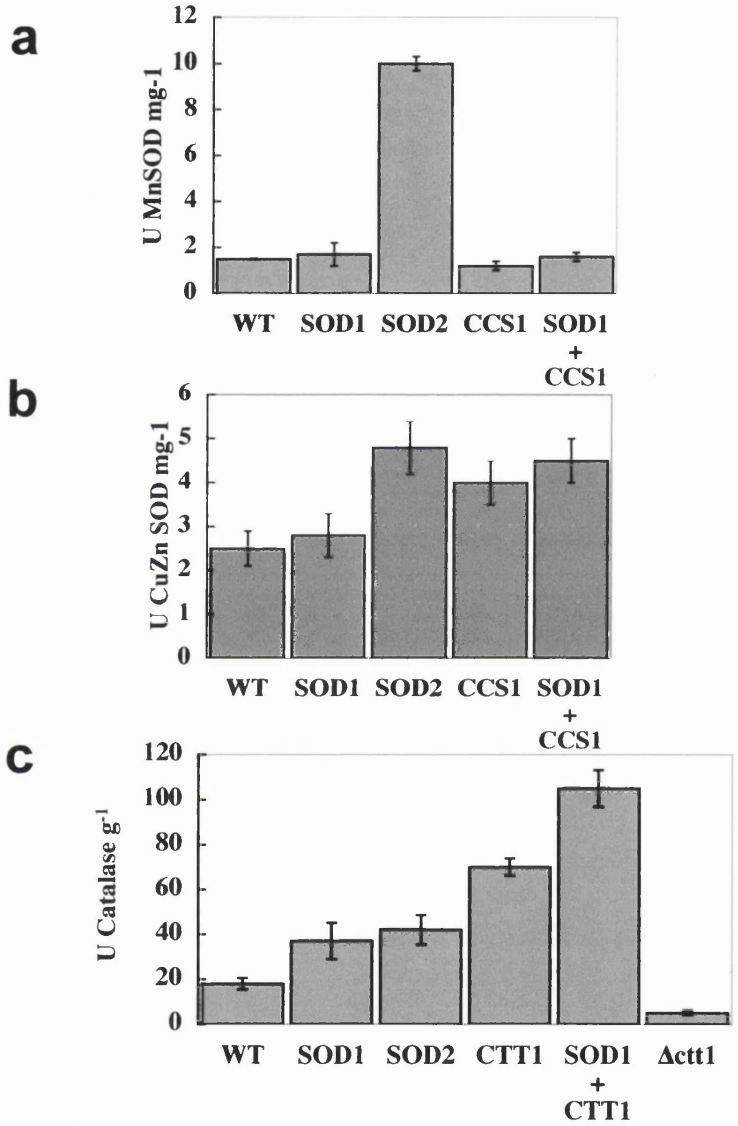

Figure 4.5)

Assays of (a)MnSod, (b)Cu,Zn-Sod and (c)catalase activities in total protein extracts from YP-glycerol cultures of the strains overexpressing the free radical scavenging enzymes.

4.2.3 SOD1 was not initially overexpressed.

The cassette that we constructed for *SOD1* overexpression did not increase Cu,Zn-Sod activity in our initial experiments (Fig. 4.5b). Surprisingly this strain showed a reduced growth compared to wild type on respiratory media at temperatures greater than 30°C and was slightly more sensitive to free radical generating drugs menadione and paraquat (Fig. 4.6). It was initially thought that this phenotype could be explained with Fenton chemistry. If superoxide dismutases are to be overexpressed then a subsequent increase in the hydrogen peroxide detoxifying enzymes could be required to cope with the increased levels of hydrogen peroxide. A cassette overexpressing *CTT1* was therefore introduced into these cells to see if it reversed this oxidative stress phenotype. The *CTT1* cassette typically gave a 3-fold increase in catalase activity and the *SOD1* cassette doubled catalase activity. (Fig. 4.5c). The combined overexpression of *CTT1* with *SOD1* gave a 5-fold increase in catalase activity, this did not however reverse the detrimental effects of increased *SOD1* , suggesting that the phenotype of the *SOD1* strain is not due to increases in cellular H_2O_2.

4.2.4 Verification of the overexpression of Sod1p from the pRS403-ADH2SOD1 cassette.

Others have also experienced problems augmenting Cu,Zn-Sod activity with overexpression of the *SOD1* gene in yeast (Stenlund and Tibell, 1999). To confirm that the Sod1p was overexpressed by the pRS403/406-*ADH2* cassettes, the levels of Sod1p in the wild type and *SOD1* overexpressing strains were determined by western blotting techniques. Due to a lack of an available antibody immunoreactive for yeast Sod1p, this protein was epitope tagged with a single glycine followed by a repeat of six histidine residues (6xHis-tag). pRS403/406-*ADH2* cassettes for overexpressing *SOD1*-6xHis were constructed (section 4.2.5).

Figure 4.6)

SOD1 overexpression is detrimental to respiratory growth (YPG). Cells overexpressing *SOD1* demonstrate an oxidatively stressed phenotype, these cells are less viable than wildtype when they are exposed to the free radical generating drugs paraquat, menadione and t-butyl-hydroperoxide (BHP). Co-overexpression of *CTT1* with *SOD1* does not reverse the SOD1 phenotype, suggesting that the oxidative stress is not as a result of excessive production of H_2O_2.Cells were grown to an OD_{600}=0.6 and 10-fold dilutions were replica plated onto YP-Glycerol media containing the indicated concentration of drug.

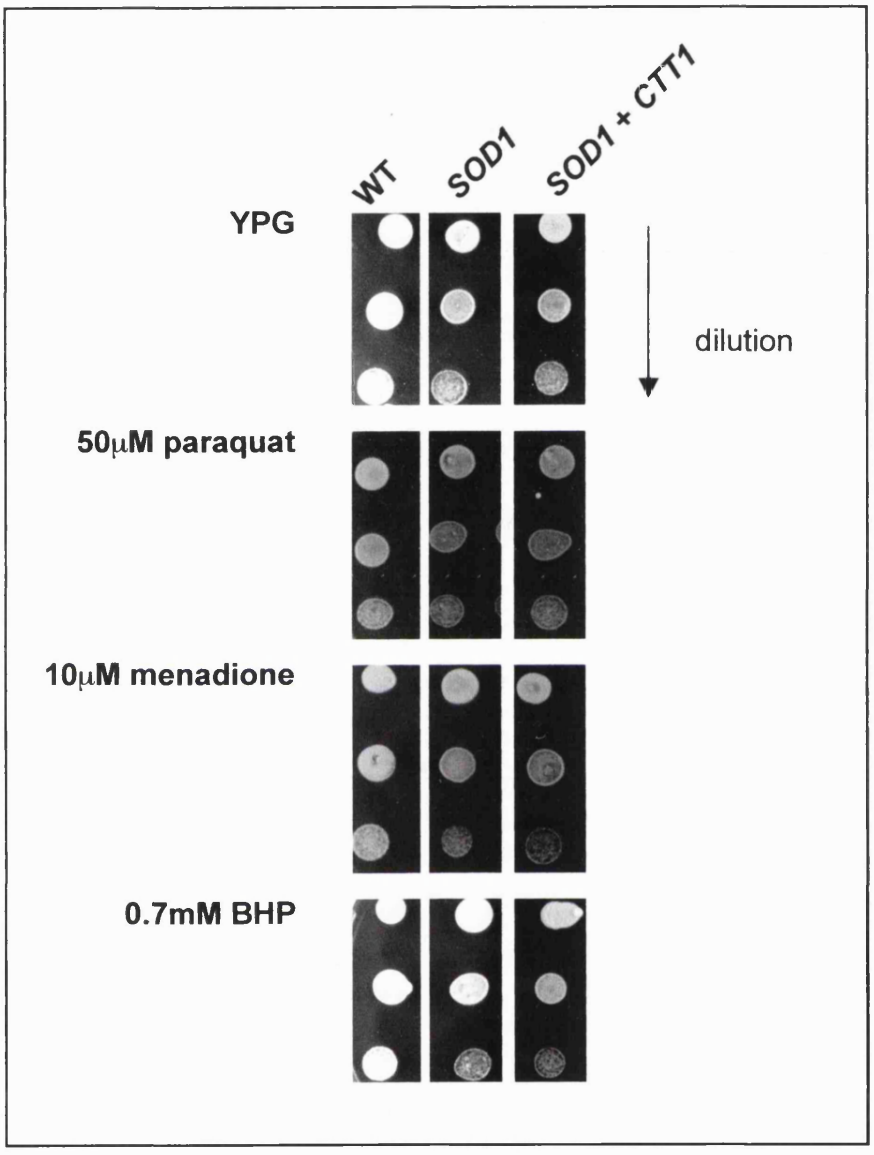
WT
SOD1
SOD1 + CTT1
YPG
dilution
50μM paraquat
10μM menadione
0.7mM BHP

4.2.5 Overexpression of SOD1-6xHis.

PCR was used to place a 6xHis tag on the product of the *SOD1* gene. Primers containing the sequence for this epitope tag were used to amplify *SOD1* This PCR product was cloned into pRS406(*ADH2*) and pRS403(*ADH2*)as a *Bam*HI/*Not*I fragment (Fig. 4.7a). Both the amino-termini (*N6xHis*) and the carboxy-termini (*C6xHis*) of *SOD1* were initially tagged. For amino-terminal tagging Sod1p the 6xHis-tag was in the forward primer *FSOD1N6HisBamHI* with *RSOD1N6HisNotI* as a reverse primer (Table 4.1). For carboxy-terminal tagging Sod1p the 6xHis-tag coding sequence was in the reverse primer *RSOD1C6HisNotI* with *FSOD1C6HisBamHI* as the forward primer (Table 4.1). Restriction endonuclease sites were also included in these oligonucleotides, *Bam*HI into the forward and *Not*I into the reverse primer, so that the amplified product could be ligated downstream of the *ADH2* promoter regions of pRS403/pRS406(*ADH2*) (Fig. 4.7b) (A pRS405(*ADH2*)*SOD1-C6xHis* was also created, by inserting the (*ADH2*)*SOD1-C6xHis from* pRS403(*ADH2*)*SOD1-C6xHis* into pRS405, with the *LEU2* gene as an auxotrophic marker.) *SOD1-N6xHIS* was amplified with its own transcriptional terminator 200bp region downstream of *SOD1*. For the *SOD1-C6xHIS* cassette the *SOD1* transcriptional terminator, a 200bp region immediately downstream of the *SOD1* gene, was amplified on a *Not*I/*Sac*II fragment with *FSOD1NotITERM and RSOD1SacIITERM* primers (Table 4.1) and cloned into the cassette 3' of *SOD1-C6xHis* (Fig. 4.7).

Functionality of these tagged Sod1 proteins was assessed by their ability to return Cu,Zn-Sod activity to FY1679-28c strain deleted for *sod1*(Fig. 4.8). Attempts to transform the *sod1* mutant were unsuccessful. The constructs were therefore introduced into the mutant by genetic crosses with wild type strains containing the *SOD16xHIS* constructs. The c-terminally tagged Sod1p was functional (Fig. 4.8a).

Figure 4.7)

a) Construction of the pRS403(*ADH2*)*SOD1*-N6xHIS vector The *SOD1* amino terminal-6xHIS fusion *(SOD1-N6xHIS)* was PCR amplified on a *Bam*HI/*Not*I fragment. The forward primer contained the Gly6xHis epitope tag and the reverse primer annealed 3' of the *SOD1* termination sequence. The resultant fragment was into the pRS403(*ADH2*) overexpression cassette. b) Construction of the pRS403(*ADH2*)*SOD1*-C6xHIS vector. The *SOD1* carboxy terminal-6xHIS fusion *(SOD1-C6xHIS)* was also PCR amplified on a *Bam*HI/*Not*I fragment. The reverse primer annealed directly 3' to the *SOD1* gene removing its stop codon, and contained the Gly6xHis epitope tag. The forward primer annealed to the 5' end of *SOD1*. To introduce the same transcription terminator sequence as the *SOD1-N6xHIS* *SOD1* Terminator sequence was PCR amplified on a NotI/SacII fragment which was ligated immediately 3' of the tagged *SOD1* coding sequence. This construct was functional (Fig. 4.8) the *ADH2-SOD1-C6xHIS* fusion and termination sequences were transferred into pRS405/406 vectors on *EcoRI\SacII* fragments.

a

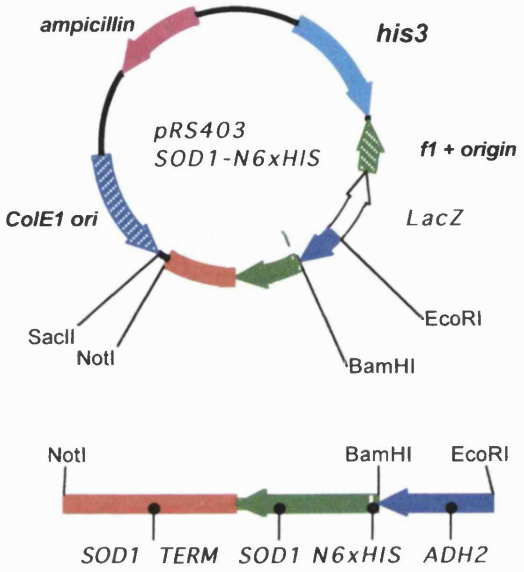
ampicillin
his3
pRS403
SOD1-N6xHIS
f1 + origin
ColE1 ori
LacZ
EcoRI
SacII
NotI
BamHI
NotI
BamHI
EcoRI
SOD1
TERM
SOD1
N6xHIS
ADH2

b

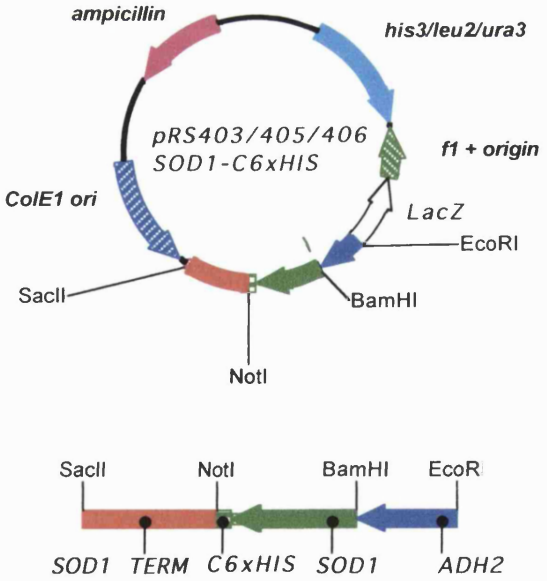
ampicillin
his3/leu2/ura3
pRS403/405/406
SOD1-C6xHIS
f1 + origin
ColE1 ori
LacZ
EcoRI
SacII
BamHI
NotI
SacII
NotI
BamHI
EcoR
SOD1
TERM
C6xHIS
SOD1
ADH2

Figure 4.8)

The tagged *SOD1* constructs were analysed for functionality. a) The Sod1p-C6xHIS fusion is functional, replacing the chromosomal *SOD1* gene with a single integrated copy of this gene under the *ADH2* promoter rescues the oxidatively stressed phenotype of the *sod1* delete grown on YP-glycerol. The Sod1p-N6xHIS does not rescue this phenotype (not shown). b) The pRS403(*ADH2*)-*SOD1-6xHIS* and pRS405(*ADH2*)-*SOD1-6xHIS* cassettes rescue the *sod1* phenotype on YP-glycerol and hence express functional Sod1p-C6xHIS. For reasons not determined the pRS406(*ADH2*)-*SOD1*-6HIS did not express functional Sod1p. The genomic *SOD1* gene replacement with the *SOD1-6xHIS* does not show an oxidative stressed phenotype and therefore its functionallity can be thought to be the same as that of wild type Sod1p. c) NBT in gel Sod activity demonstrates the activity of the cassettes, in extracts from glycerol grown cells however no increase in Cu,Zn-Sod activity is observed in the strains containing the pRS403(*ADH2*)-*SOD1-6xHIS* and pRS405 (*ADH2*)-*SOD1-6xHIS* overexpression cassettes when compared to *SOD1*-6xHIS gene under native promoter control.

a

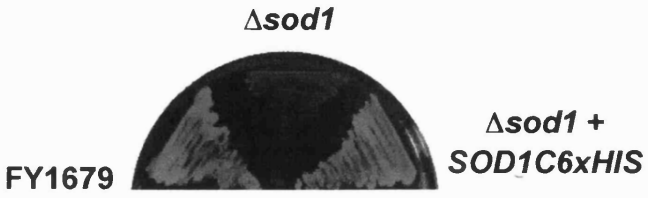

YP-Glycerol agar plates

b

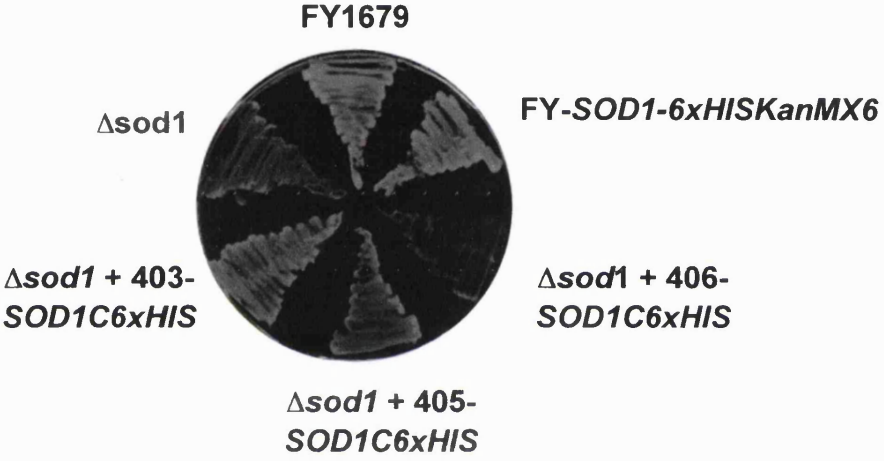

c

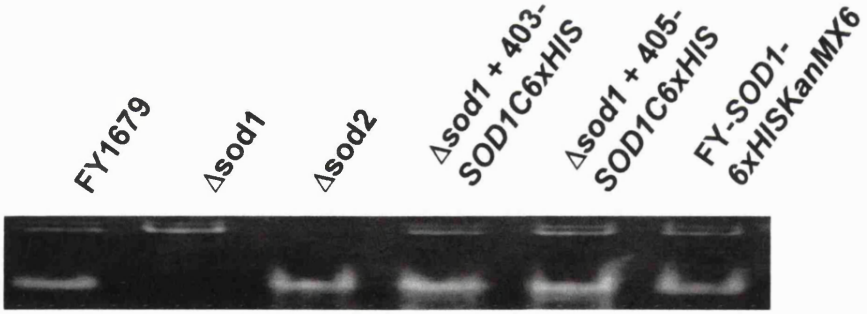

4.2.6 Replacement of the genomic SOD1 with SOD1-6xHis.

To quantify the level of overexpression of Sod1p from the *ADH2* promoter genomic *SOD1* was replaced with a *SOD1-c6xHis* fusion. The c-terminally tagged Sod1p is functional (Fig. 4.8a) so the method as described by Wach *et al.*, 1998 was used to insert the 6xHis-tag on the 3' end of the genomic copy of the *SOD1* gene by homologous recombination. No plasmids available facilitated the tagging of a gene with 6xHis using this method so the 3x Haemaglutinin coding sequence of the pFA6a-3xHA*kanMX6* (Wach et al., 1997) was replaced with the coding sequence for the 6xHis-tag (Fig. 4.9). Digestion of pFA6a3xHA*kanMX6* with *Ava*I and *Asc*I completely removes a 1.3kb fragment containing the 3xHA sequence, the remaining 2.9kb DNA fragment was purified and used to create the NpFA6a-6xHIS*KanMX6* plasmid. The glycine-6xhistidine coding sequence of the 6xHis-tag was synthesised as separate complementary oligonucleotide primers *(6xHISFAvaI/AscI 6xHISRAscI/AvaI)* (see methods section 2.3.8) containing the sequence of the 6xHis-tag aswell 5'*Ava*I and 3'*Asc*I restriction endonuclease sites (Table 4.1). The complementary oligonucleotides were annealed, digested and recircularised with the 2.9kb pFA6a3xHA*kanMX6* fragment. The resultant plasmid was sequenced across this region to verify the epitope tag sequence using *6xHISTAGseq* (Table 4.1).

The gene replacement was performed by amplifying the 6xHis-tag aswell as the kanamycin cassette from this plasmid and inserting this sequence directly behind the *SOD1* gene by homologous recombination (Fig 4.10). PCR primers *FSOD1C6xHisKanMX and RSOD1C6xHisKanMX* (Table 4.1) were used for the amplification of this region. (These primers also contained non complementary sequences corresponding to 3' end of the *SOD1* gene minus its TAA stop codon in the forward primer and a region 60bp downstream of the *SOD1* gene in the reverse primer.) These primers amplified the 6xHIS-Tag-KanMX6 fragment flanked by regions of homology at the 3' end and downstream of *SOD1* gene, so that when transformed into

Figure 4.9)

Schematic for the cloning of NpFA6a-6xHisKanMX6. 1) The 3xHaemaglutinin tag removed from pFA6a-3xHAKanMX6, with *Asc*I/*Ava*I restriction digest. 2) The Glycine-6xHistidine epitope tag was synthesised as oligo nucletotides FSOD1C6xHisKanMX6 / RSOD1C6xHisKanMX6. These were annealed and then digested with AscI/AvaI. The resultant fragment was cloned into the *Asc*I/*Ava*I digested pFA6a-3xHAKanMX6 plasmid yielding NpFA6a-6xHisKanMX6. The *6xHISTAGseq* sequencing primer was used to verify the correct insertion of the 6xHIStag coding region.

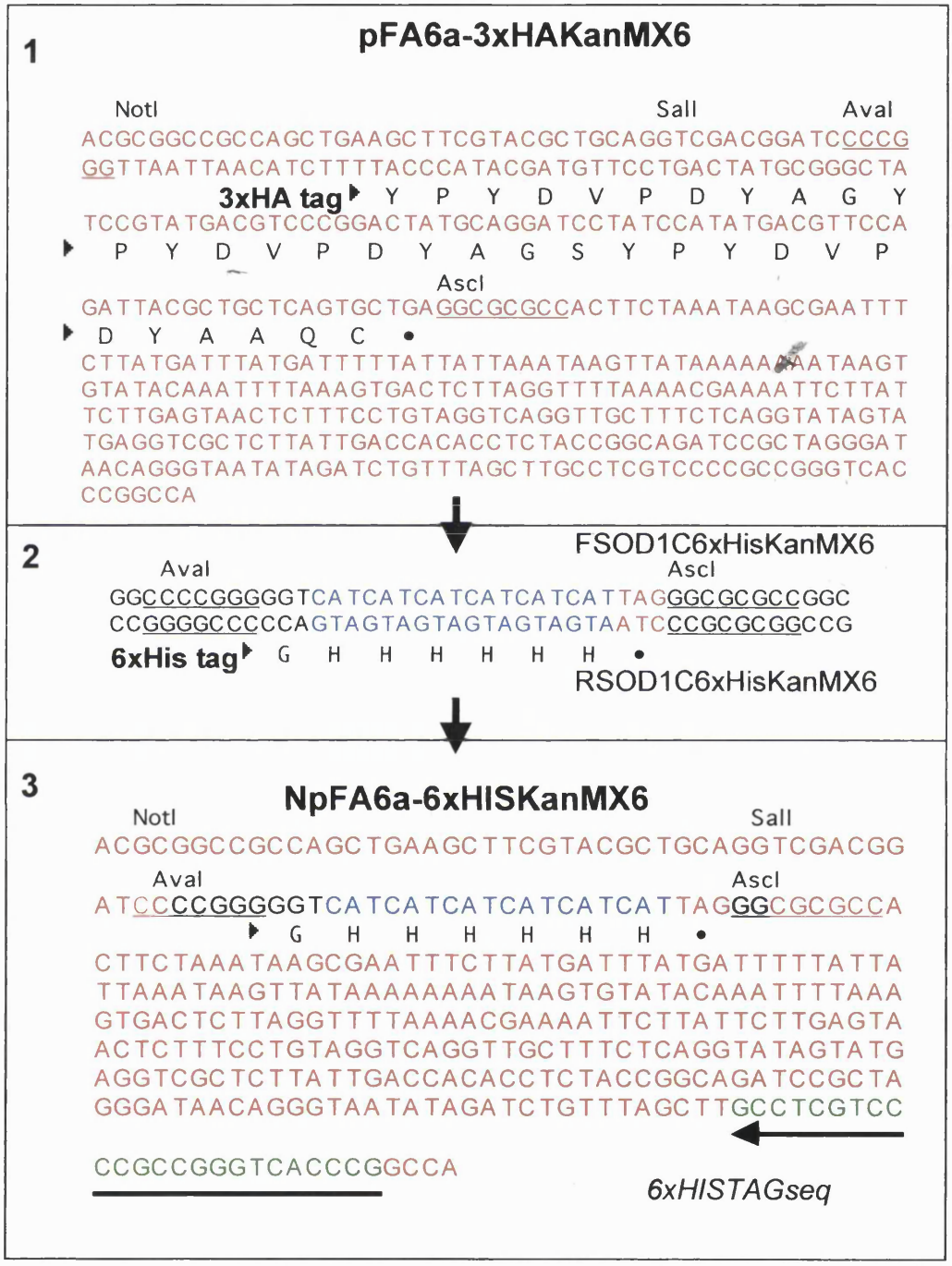
1
pFA6a-3xHAKanMX6
NotI
SalI
AvaI
ACGCGGCCGCCAGCTGAAGCTTCGTACGCTGCAGGTCGACGGATCCCCG
GGTTAATTAACATCTTTTACCCATACGATGTTCCTGACTATGCGGGCTA
3xHA tag
Y P Y D V P D Y A G Y
TCCGTATGACGTCCCGGACTATGCAGGATCCTATCCATATGACGTTCCA
P Y D V P D Y A G S Y P Y D V P
AscI
GATTACGCTGCTCAGTGCTGAGGCGCGCCACTTCTAAATAAGCGAATTT
D Y A A Q C •
CTTATGATTTATGATTTTTATTATTAAATAAGTTATAAAAAAAATAAGT
GTATACAAATTTTAAAGTGACTCTTAGGTTTTAAAACGAAAATTCTTAT
TCTTGAGTAACTCTTTCCTGTAGGTCAGGTTGCTTTCTCAGGTATAGTA
TGAGGTCGCTCTTATTGACCACACCTCTACCGGCAGATCCGCTAGGGAT
AACAGGGTAATATAGATCTGTTTAGCTTGCCTCGTCCCCGCCGGGTCAC
CCGGCCA
FSOD1C6xHisKanMX6
2
AvaI
AscI
GGCCCCGGGGGTCATCATCATCATCATCATTAGGGCGCGCCGGC
CCGGGGCCCCAGTAGTAGTAGTAGTAGTAATCCCGCGCGGCCG
6xHis tag
G H H H H H H •
RSOD1C6xHisKanMX6
3
NpFA6a-6xHISKanMX6
NotI
SalI
ACGCGGCCGCCAGCTGAAGCTTCGTACGCTGCAGGTCGACGG
AvaI
AscI
ATCCCCGGGGGTCATCATCATCATCATCATTAGGGCGCGCCA
G H H H H H H •
CTTCTAAATAAGCGAATTTCTTATGATTTATGATTTTTATTA
TTAAATAAGTTATAAAAAAAATAAGTGTATACAAATTTTAAA
GTGACTCTTAGGTTTTAAAACGAAAATTCTTATTCTTGAGTA
ACTCTTTCCTGTAGGTCAGGTTGCTTTCTCAGGTATAGTATG
AGGTCGCTCTTATTGACCACACCTCTACCGGCAGATCCGCTA
GGGATAACAGGGTAATATAGATCTGTTTAGCTTGCCTCGTCC
CCGCCGGGTCACCCGGCCA
6xHISTAGseq

Figure 4.10)

Strategy for the genomic replacement of *SOD1* with *SOD1-6xHIS* as described by Wach *et al.* (1997) 1) The 6xHIS epitope tag was PCR amplified from NpFA6a-6xHISKanMX6 on a fragment containing the KanMX6 cassette. Primers were designed with regions of homology to the 3' end of SOD1 and to downstream sequences. 2) The resultant PCR product is transformed into yeast whereby the fragment inserts into the genome by homologous recombination. 3) Successful transformants contain the *SOD1-6xHIS* gene and KanMX6 genetic marker. Southern blotting was used to verify the correct insertion into the genome.

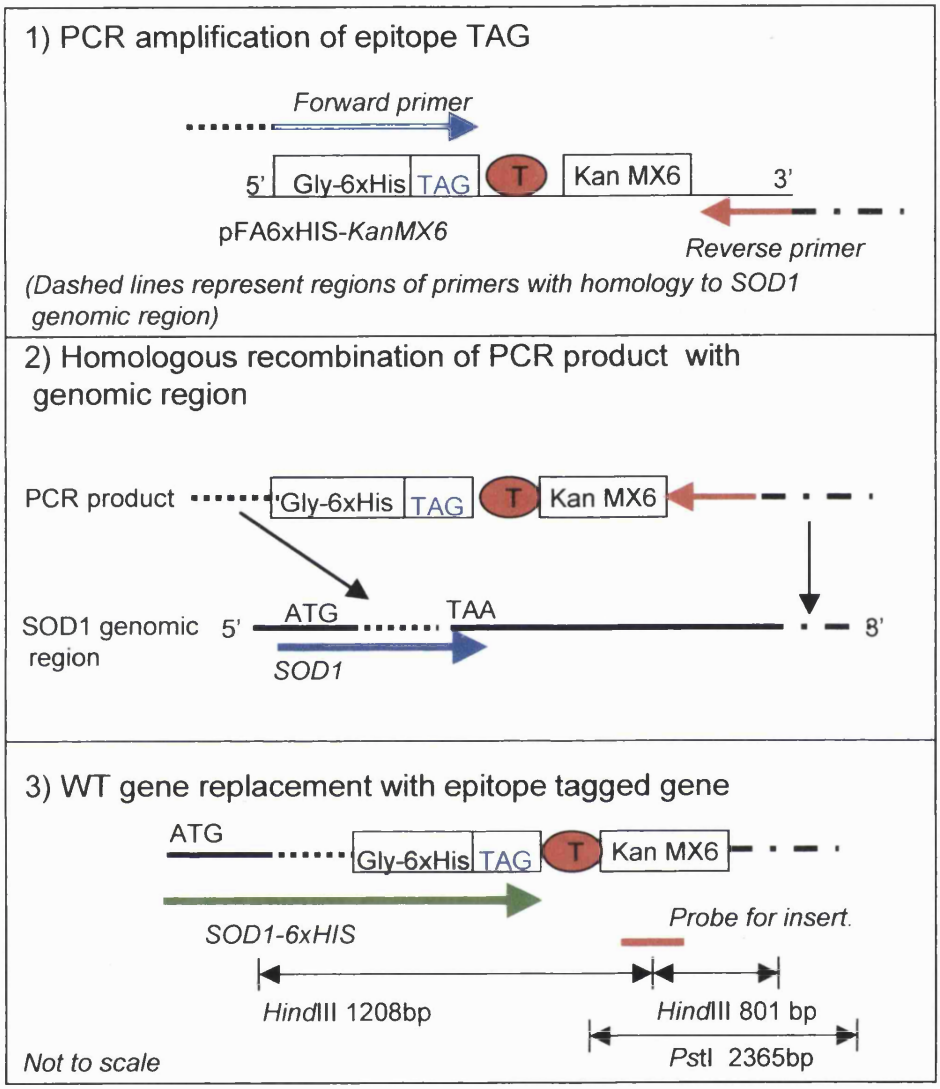
1) PCR amplification of epitope TAG
Forward primer
5'
Gly-6xHis
TAG
T
Kan MX6
3'
pFA6xHIS-KanMX6
Reverse primer
(Dashed lines represent regions of primers with homology to SOD1 genomic region)
2) Homologous recombination of PCR product with genomic region
PCR product
Gly-6xHis
TAG
T
Kan MX6
SOD1 genomic region
5'
ATG
TAA
3'
SOD1
3) WT gene replacement with epitope tagged gene
ATG
Gly-6xHis
TAG
T
Kan MX6
SOD1-6xHIS
Probe for insert
HindIII 1208bp
HindIII 801 bp
PstI 2365bp
Not to scale

yeast this, PCR fragment would replace the 3'end of the *SOD1* gene with the 6xHIS tagged version (Fig. 4.10).

Transformants were selected by G418 resistance afforded to them by the KanMX6 cassette included on the PCR fragment. 8 positives were assayed for Cu,Zn-Sod activity (Fig 4.11a) and the presence of the Gly-6xHis epitope tag (4.11b), the latter using an antibody immunoreactive to 6xHIS . The genomic location of the insertion in each was also checked using southern blot analysis (4.11c). Total genomic DNA was digested with *Hind*III and *Pst*I yielding 1208 and 801 bp and 2365 bp fragments respectively when probed for a sequence within the KanMX6 cassette (Fig. 4.10_3). Transformants 1,3 and 8 showed a correct genomic insertion of the epitope tag on the 3' end of *SOD1* yielding a functional 6xHIS-tagged Sod1p (Fig. 4.11). Transformants 4, 5 and 7 had no functional Sod1p and no expression of the tag was detected. As the southern analysis suggests a correct location for the insert in these transformants, these are likely to have arisen from an out of frame insertion which removed the stop codon from the gene resulting in a non-functional protein with a nonsense tag (Fig. 4.11). In transformant 2 the *SOD1*-6xHIS confers G418 resistance and Sod1p is still functional but, not tagged (Fig. 4.11).

4.2.7 An increase in Sod1p was detected using the 6xHistidine epitope tagging method, however no corresponding increase in Cu,Zn-Sod activity is detected.

During respiratory growth the levels of Sod1-6xHISp were at higher levels in cells containing the pRS403*SOD1-6xHIS* overexpression cassette when compared to cells with just the chromosomally-tagged *SOD1* gene. However this was not reflected in a corresponding increase in Cu,Zn-Sod activity when compared to levels of wild type and *SOD1-6xHIS-KanMX6* gene replacement strains (Fig. 4.12). It can therefore be concluded that the expression system is functioning to increase the cellular level of Sod1p, but that this is not causing increased Cu,Zn-Sod activity.

Figure 4.11)

Transformants of FY1679 obtained with the *SOD1*-6xHIS PCR product tested for a) Cu,Zn -Sod activity with the PAGE-NBT assay; b) the expression of the 6xHIS tag by immunodetection with an antibody for the 6xHIS repeat; c) the location of the correct genomic insertion by probing of a southern blot of total genomic DNA digested with *Hind*III or *Pst*I. Fragments were detected by the hybridisation of a radiolabelled probe for the KanMX6 sequence. Transformants 1, 3 and 8 had a successful replacement of genomic *SOD1* with the *SOD1*-6xHIS-KanMx6 PCR product, in these the Sod1p remained functional and was epitope tagged with 6xHIS.

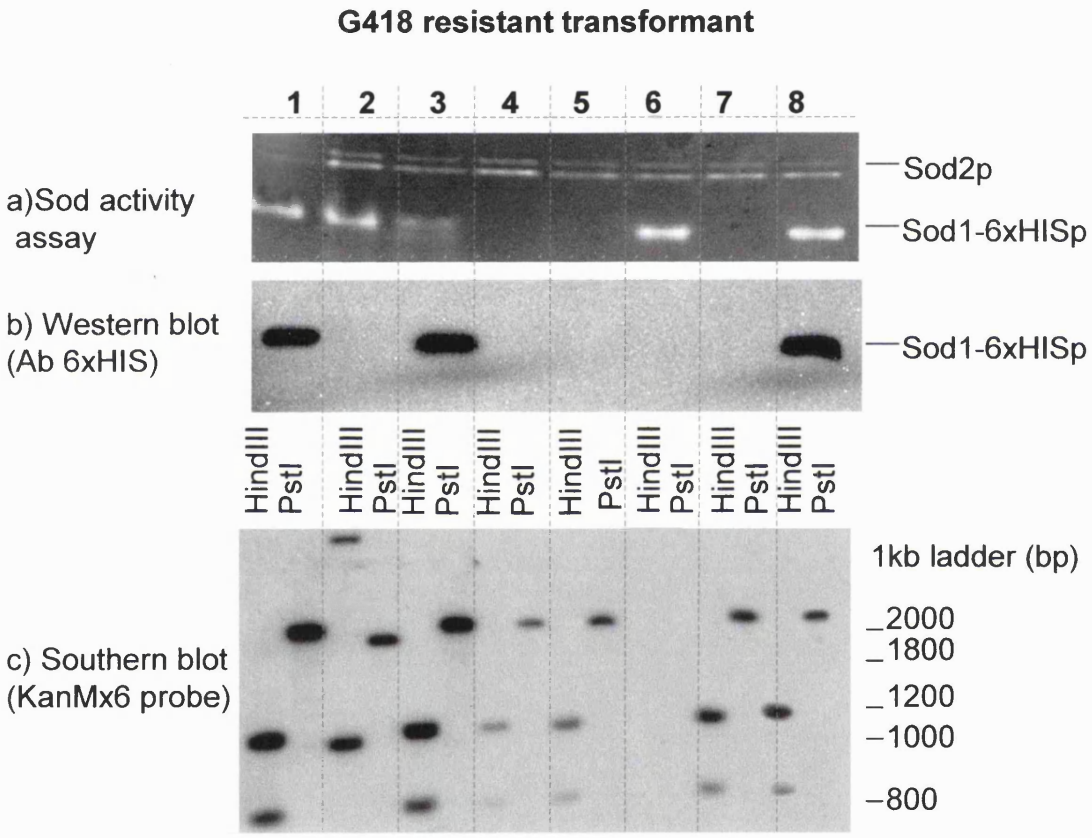
G418 resistant transformant
1
2
3
4
5
6
7
8
a)Sod activity assay
Sod2p
Sod1-6xHISp
b) Western blot (Ab 6xHIS)
Sod1-6xHISp
HindIII
PstI
c) Southern blot (KanMx6 probe)
1kb ladder (bp)
2000
1800
1200
1000
800

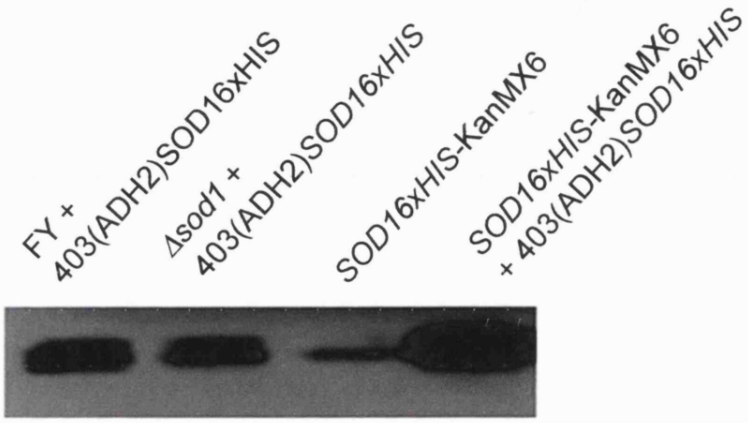

Figure 4.12)

Western blot of total cell extracts of cells containing the epitope tagged versions of Sod1p, probed with an antibody for 6xHis. Overexpression of the Sod16xHISp from the pRS403/406(*ADH2*) cassettes was successful. Densitometric analysis of the bands indicated a 10-fold increase in the level of Sod1-C6xHISp in cells containing the *SOD1-C6xHIS* overexpression cassette when compared to cells with just the tagged chromosomal copy of this gene. Cells were grown in YP-glycerol media and 10μg of total cell extract was separated on a 12% PAGE. Proteins were transferred to nitrocellulose and the Sod1-6xHIS fusion protein was detected with a 6xHIS antibody.

4.2.8 SOD1 activity is limited by the availability of copper.

As with *E. coli* engineered to overexpress eukaryotic Cu,Zn-Sod enzymes (Stenlund and Tibell, 1999), our *S. cerevisiae* containing the *SOD1-6xHIS* overexpression cassette could overexpress active Cu,Zn-Sod to higher levels than the wildtype strain, when the growth medium was supplemented with a high level of Cu^{2+} (Fig. 4.13). This indicated a problem in loading the overexpressed Cu,Zn-Sod *apo*protein with Cu^{2+} ions. Since Cu^{2+} engages in Fenton chemistry (Halliwell and Gutteridge, 1998) we were reluctant to introduce high levels of Cu^{2+} into our life-span measurements.

4.2.9 Increasing the activity of Cu,Zn-Sod genetically.

The prooxidant nature of copper necessitates a co-ordinated cellular regulation of its import, trafficking and its delivery into target metalloenzymes. This regulation is extreme; intracellular [Cu] free levels are maintained at less than one free copper ion per cell (Rae et al., 1999). To date three copper chaperones, *CCS*, *ATX1* and *COX17*, have been reported (O'Halloran and Culotta, 2000). *CCS1* (copper chaperone for SOD) (Culotta et al., 1997) delivers copper to Sod1p, *ATX1* (Lin et al., 1997; Pufahl et al., 1997; Valentine and Gralla, 1997) and *COX17* (Glerum et al., 1996) deliver copper to the secretory pathway and mitochondria respectively (Fig. 4.14).

In *S. cerevisiae CCS1* was originally isolated in a screen of lysine auxotrophs, and named *LYS7* (Horecka et al., 1995). Δ*ccs1* mutants are defective in *SOD1* expression and sensitive to oxidative stress, yet their defect can be largely overcome with Cu^{2+} supplementation (Gamonet and Lauquin, 1998).It was therefore investigated if the lack of increased Cu,Zn-Sod activity with the overexpression cassette could be overcome by increasing the levels of Ccs1p, the chaperone dedicated to the loading of the Cu,Zn-Sod apoprotein with Cu^{2+} (Culotta et al., 1997).

Figure 4.13)

Sod activity gel assay. Cu,Zn-Sod and Mn-Sod activity is determined by the intensity of the clear band in the NBT stained gels. (a) Cu,Zn-Sod migrating as the fastest single band and can be distinguished from the Mn-Sod which migrates slower as a doublet as indicated by the absence of the corresponding bands in the deleted strains. (b) Cu,Zn-Sod activity can be increased upon addition of copper. The activity of Cu,Zn-Sod in the strain overexpressing *SOD1* can be increased to a greater level with 5mM $CuSO_4$ than that of wild type, indicating that the activity of Cu,Zn-Sod is limited by copper availability.

Cells were harvested during exponential growth phase. 10μg of total cell extracts was separated on non-denaturing, 12% polyacrylamide gels. The gels were stained for Sod activity with NBT and a second gel was stained with coomassie as a loading control.

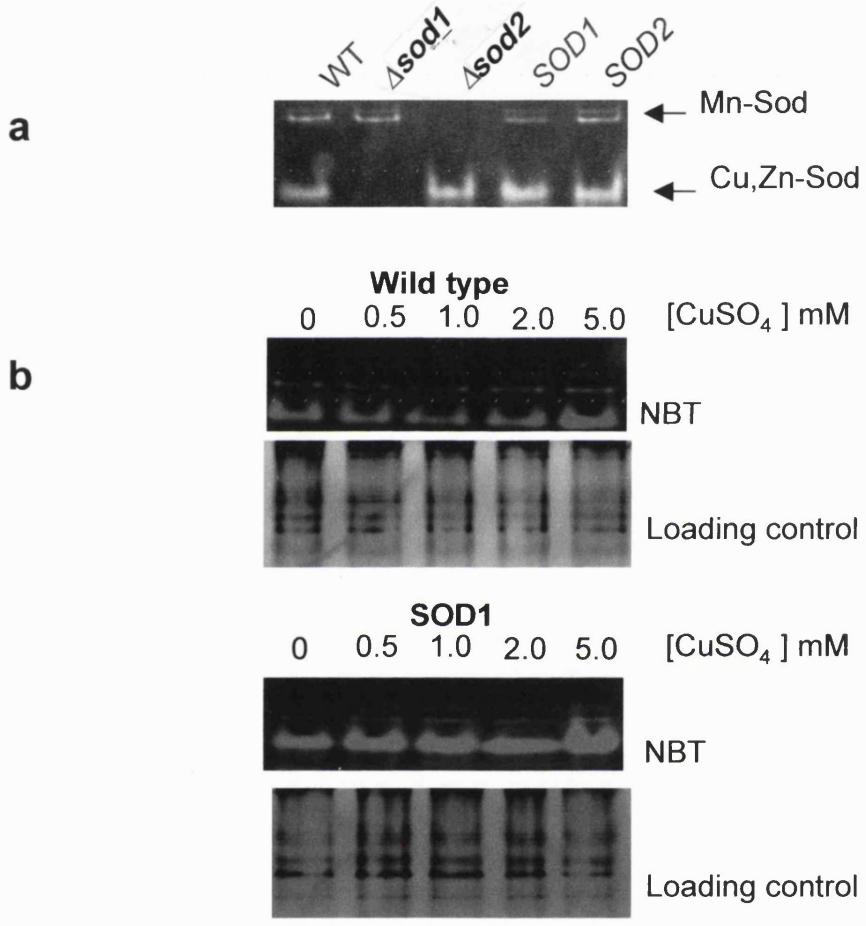
a
WT
Δsod1
Δsod2
SOD1
SOD2
Mn-Sod
Cu,Zn-Sod
b
Wild type
0 0.5 1.0 2.0 5.0 [CuSO4] mM
NBT
Loading control
SOD1
0 0.5 1.0 2.0 5.0 [CuSO4] mM
NBT
Loading control

Figure 4.14)

Copper transport and distribution in *S. cerevisiae*. Copper is first reduced from Cu[II] to Cu[I] by cell surface reductases Fre1/Fre2p prior to uptake. High affinity Cu ion uptake is mediated by Ctr1p. Within the cell Cu is bound to the known cytosolic Cu chaperones Atx1p, Cox17p and CCS1p for specific delivery to the secretory pathway, mitochondria and Cu,Zn-Sod, respectively. Within the secretory pathway, Ccc2p accepts Cu from Atx1p, followed by incorporation of Cu to the multicopper ferroxidase, Fet3p in a manner facilitated by the Gef1p chloridechannel. Fet3p forms a complex with the iron permease Ftr1p and both proteins are responsible for high affinity iron uptake at the plasma membrane. In mitochondria Cu delivered by Cox17p is incorporated into cytochrome oxidase, a process that requires the integral inner-membrane protein Sco1p and possibly its homologue, Sco2p. CCS1p delivers Cu specifically to Cu,Zn-Sod in the cytosol. Currently it is not known whether specific chaperones are required for incorporation of Cu to the metallothioneins Cup1p and Crs5p in the cytosol, or the nuclear Cu-metalloregulatory transcription factors Ace1p and Mac1p or the vacuole, which is important for proper Cu detoxification. (As reviewed in Pena, *et al.*, 1999)

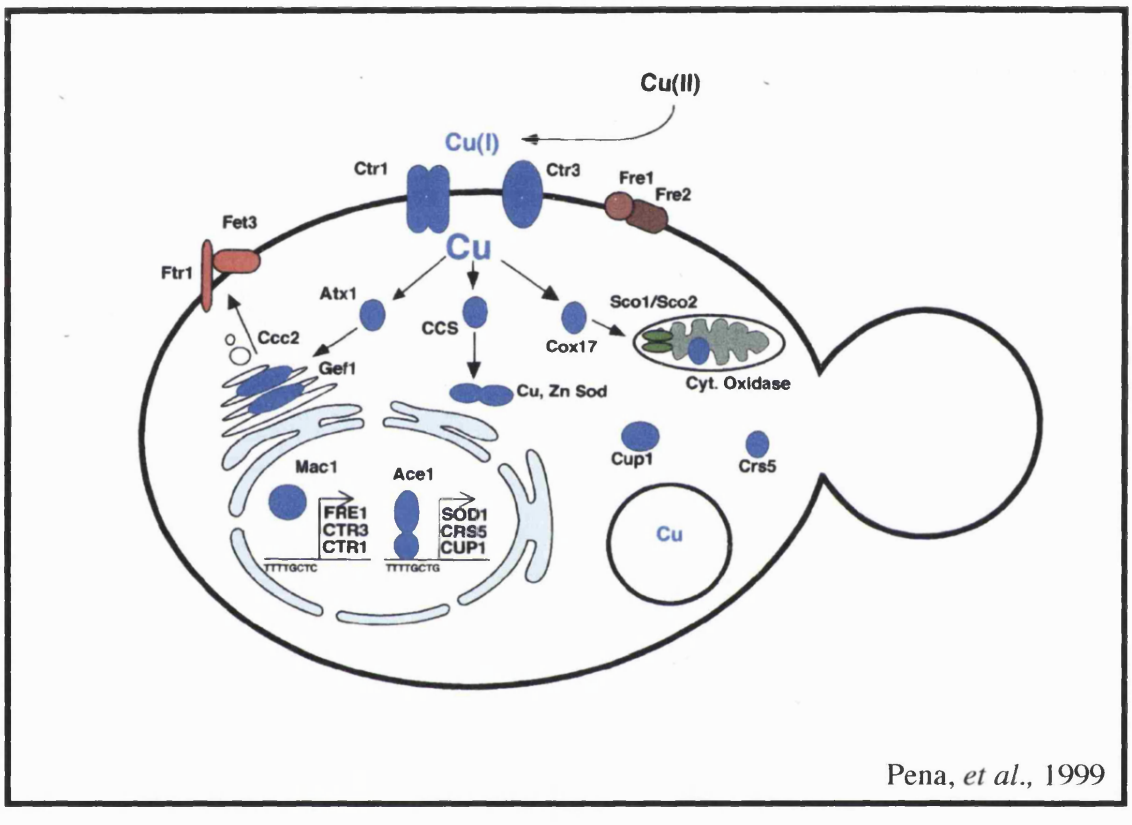

Pena, *et al.*, 1999

4.2.10 An increase in Cu,Zn-Sod activity requires the simultaneous overexpression of Cu,Zn-Sod and the Sod1p-specific Cu $^{2+}$ chaperone (Ccs1p).

The *CCS1* sequence was PCR amplified *(FCCS1BamHI, RCCS1NotI)* (Table 4.1) and cloned into the pRS403(*ADH2*) as *Bam*HI/*Not*I fragment (Fig. 4.15). The subsequent plasmid was *PstI* digested and integrated into FY1679-28c strains, with and without the *SOD1* overexpression cassette. Surprisingly, this *CCS1* overexpression cassette could increase Cu,Zn-Sod activity even in the absence of the *SOD1* overexpression cassette (Fig. 4.16), indicating the levels of the Ccs1p chaperone are normally limiting for Cu,Zn-Sod expression, at least in respiratory yeast cultures. Above all, the presence of this cassette enabled us to achieve a Cu,Zn-Sod overexpression in respiratory cells without the need for Cu^{2+} supplementation of the medium.

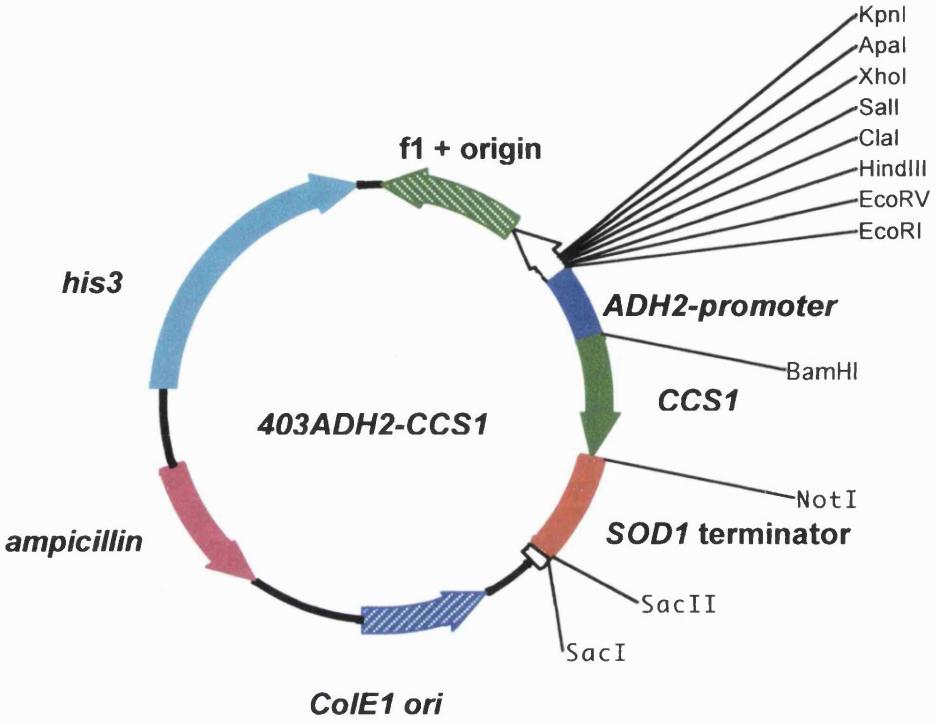

Figure 4.15)

Schematic of the pRS403(*ADH2*)*CCS1* integrative cassette. This cassette was constructed from the pRS403(*ADH2*)*SOD16xHIS* plasmid. The *SOD1*6xHIS coding region was removed on a *Bam*HI/*Not*I fragment and was directly replaced with the coding sequence of *CCS1* leaving the *SOD1* terminator sequence down-stream of the *CCS1* gene.

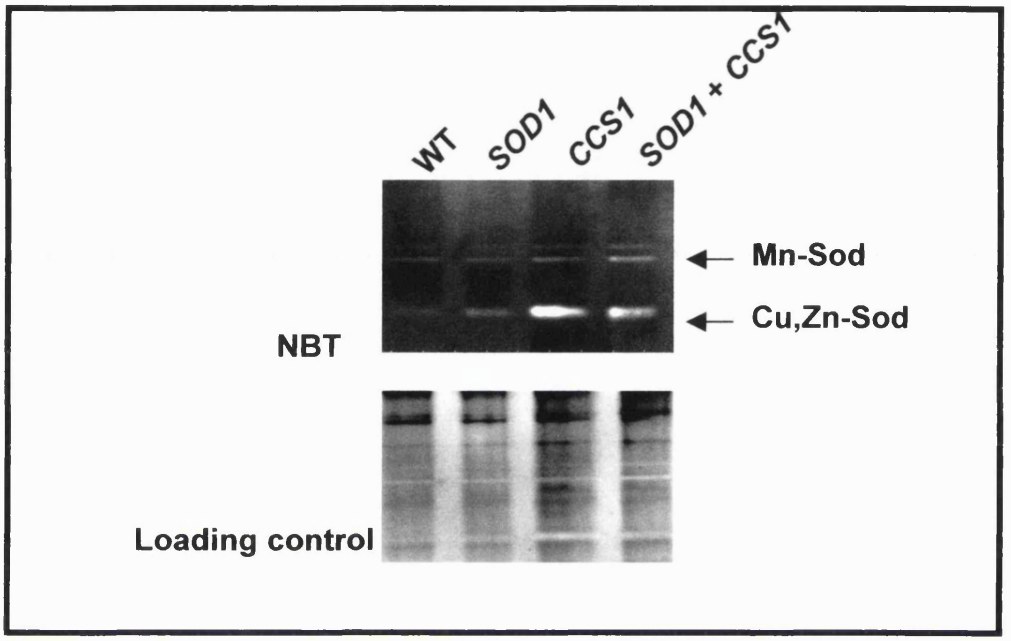

Figure 4.16)

NBT PAGE Sod assay. The *CCS1* overexpression cassette could increase Cu,Zn-Sod activity even in the absence of the *SOD1* overexpression cassette, indicating that levels of the copper chaperone are normally limiting for Cu,Zn-Sod expression in respiratory cultures. Cu,Zn-Sod activity is not increased by the introduction of the *SOD1* overexpression cassette unless cells are grown in media supplemented with copper (Fig. 4.13). The Ccs1p serves to load copper into Cu,Zn-Sod, co-overexpression of *CCS1* with *SOD1* increases the copper availability for Sod1p and hence results in an increase in the Cu,Zn-Sod activity.

4.3 *Results 2: Chronological Life span measurements*

4.3.1 Increased cellular antioxidant activity extends chronological life span.

Maximisation of the *S. cerevisiae* chronological life span requires prior growth of the cells to stationary phase on a respiratory carbon source (MacLean et al., 2001). Cultures prepared this way can be maintained aerobically for months at 30°C with little viability loss although, so that we can conduct survival measurements over a reasonable time span, we routinely measure survival at the more stressful temperature of 37°C (MacLean et al., 2001). As with aging of *Drosophila* (Zwaan et al., 1991) survival is much shorter at a higher temperature. Efficient adaptation to respiratory maintenance also ensures that the replicative potential of the cells is substantially maintained during stationary maintenance, even the 2% of stationary wild type cells surviving a 5d 37°C ageing enjoy a full replicative life span when they reenter the cell cycle (Fig. 4.17). This contrasts with cells pre-grown on glucose, which survive less well in stationary phase (MacLean et al., 2001) and show a shortened replicative life span when they reenter the cell cycle after a period of stationary arrest (Ashrafi et al., 1999)

Of the strains for antioxidant enzyme overexpression that we constructed (Table 4.2), it was those overexpressing active Mn-Sod or Cu,Zn-Sod that displayed appreciable increases in chronological life span (Fig. 4.18). The extensions to chronological life span, with overexpressions observed at 37°C were also apparent at lower temperatures (Fig. 4.19), a further indication of the role of oxidative stress in *S.cerevisiae* lifespan. Losses of these oxidant scavenging enzymes are known to *decrease* the stationary survival of glucose-grown cells (Longo et al., 1996; Longo et al., 1999), while increasing Cu,Zn-Sod in the intermembrane space of the mitochondrion generates a small *extension* to this life span (Sturtz et al., 2001). The survival of glucose-grown cells in G_0 arrest is also increased with the loss of Sch9, a protein kinase that is the yeast homologue of the Akt/PKB protein kinase involved in insulin signalling in mammals (Fabrizio et al., 2001). However this is the first time that increased chronological life spans have been shown for yeast adapted to efficient respiratory maintenance. It reveals that it is oxidative stress that limits the longevity of these stationary cells.

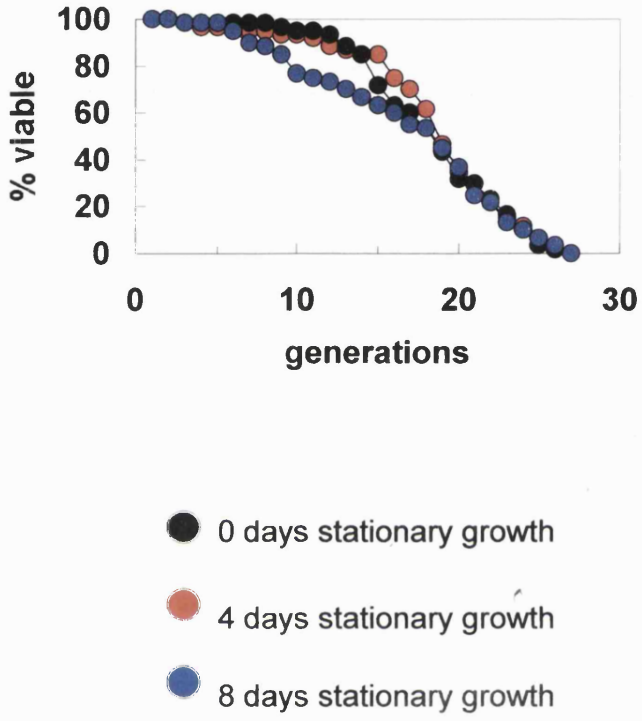

Figure 4.17)

Replicative lifespans of the FY1679-28c after periods of chronological ageing in the G0.

Figure 4.18)

Chronological life spans at 37°C of the strains with increased antioxidant activities used in this study. The *SOD2* (a) overexpressor has an extended life span. The *SOD1* overexpression cassette (a) did not increase life span, but was instead detrimental reducing life span. The detrimental effects of the *SOD1* overexpression were not as a result of the reduction of H_2O_2 to the OH^- radical via the fenton reaction as no restoration of the *SOD1* chronological life span back to wild type levels was observed when *CTT1* was co-overexpressed with *SOD1* (b). Overexpression of the cytoplasmic *CTT1* activity alone produced a small increase in chronological life span (a). Overexpression of the mitochondrial *CCP1* gene had no effect on the chronological life span (a), but when co-overexpressed with *SOD2* the life span was severly reduced, reversing the benefit of the *SOD2* overexpression (c). The*SOD1* overexpressor has higher levels of *apo*Sod1p than wildtype cells (Figs. 4.12, 4.13). Upon loading of copper into the Cu,Zn-Sod, by the overexpression of the *CCS1* the greatest extension to chronological life was achieved.

a

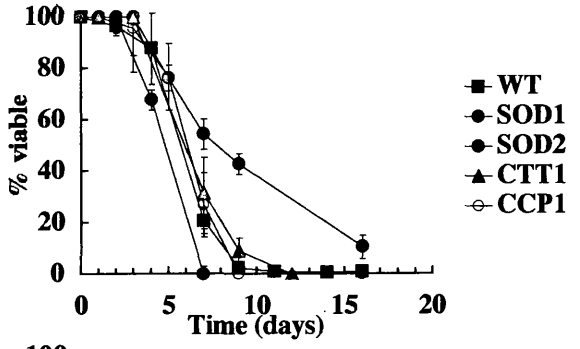
100
80
60
40
20
0
% viable
0
5
10
15
20
Time (days)
WT
SOD1
SOD2
CTT1
CCP1

b

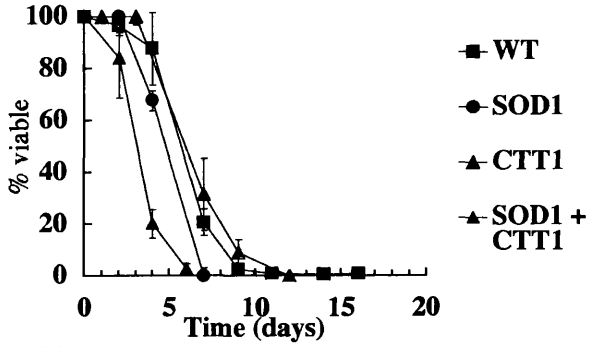
100
80
60
40
20
0
% viable
0
5
10
15
20
Time (days)
WT
SOD1
CTT1
SOD1 +
CTT1

c

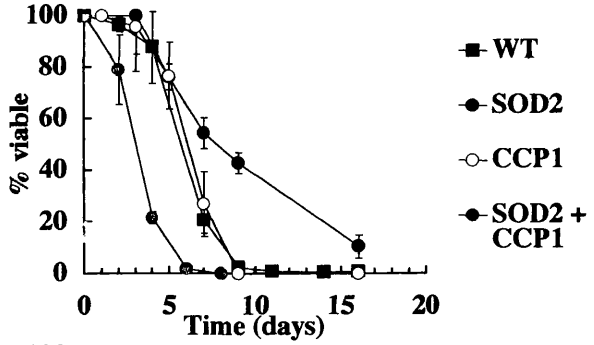
100
80
60
40
20
0
% viable
0
5
10
15
20
Time (days)
WT
SOD2
CCP1
SOD2 +
CCP1

d

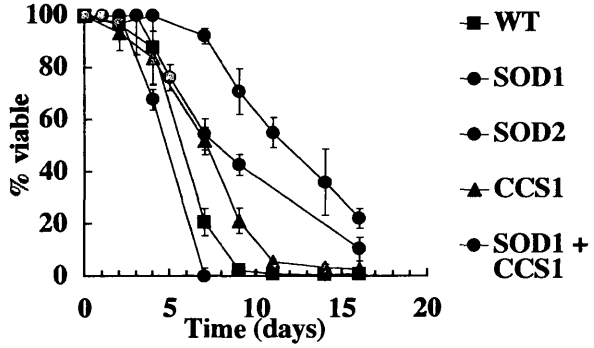
100
80
60
40
20
0
% viable
0
5
10
15
20
Time (days)
WT
SOD1
SOD2
CCS1
SOD1 +
CCS1

4.3.2 The effect of Sod activity on chronological life span.

The greatest extension to chronological life span (almost a doubling of the mean survival (Fig. 4.18d)) was from a combined *SOD1+CCS1* overexpression, but even *CCS1* overexpression alone produced a small extension to this life-span (Figs. 4.18d, 4.19) that can probably be attributed to its ability to elevate levels of active Cu,Zn-Sod resulting from the *SOD1* gene under native promoter control that exists in the genome of all of these strains (Fig. 4.18d). Mn-Sod overexpression (strain *SOD2*) also increased survival, but to a lesser extent than a combined *SOD1+CCS1* overexpression (Figs. 4.18a, 4.19). This may reflect Mn-Sod being only in the mitochondrial lumen and proportionally a smaller fraction of the total Sod activity of respiratory cells than Cu,Zn-Sod (Gralla and Valentine, 1991; Moradas-Ferreira and Costa, 2000; Sturtz et al., 2001; Westerbeek-Marres et al., 1988).

However, in contrast to the dramatic lifespan extension of a combined *SOD1+CCS1* overexpression, the *ADH2-SOD1* cassette alone (strain *SOD1*) led not just to no appreciable Cu,Zn-Sod *activity* increase (Fig. 4.5) but impaired survival (Fig. 4.18a). The latter appears not due to excessive H_2O_2 production, since it is not rescued by the simultaneous overexpression of catalase (*SOD1+CTT1*; Fig. 4.18b). Instead this impaired survival of the *SOD1* strain may be a reflection of the high endogenous oxidative stress that is a feature of this strain (section 4.5; Fig. 4.21). This endogenous oxidative stress may arise from the majority of the Sod1p being present in the *apo*Sod1p form (Figs. 4.12, 4.13)

4.3.3 The effect of catalase overexpression on chronological lifespan

The role of catalases, both the major cytoplasmic *CTT1* and the mitochondrial equivalent cytochrome-c-peroxidase (*CCP1*), in yeast chronological life span were determined. A very slight increase in stationary phase viability over time was afforded to the cells when *CTT1* was overexpressed (Fig. 4.18b) and no change in life span was noted for those cells with

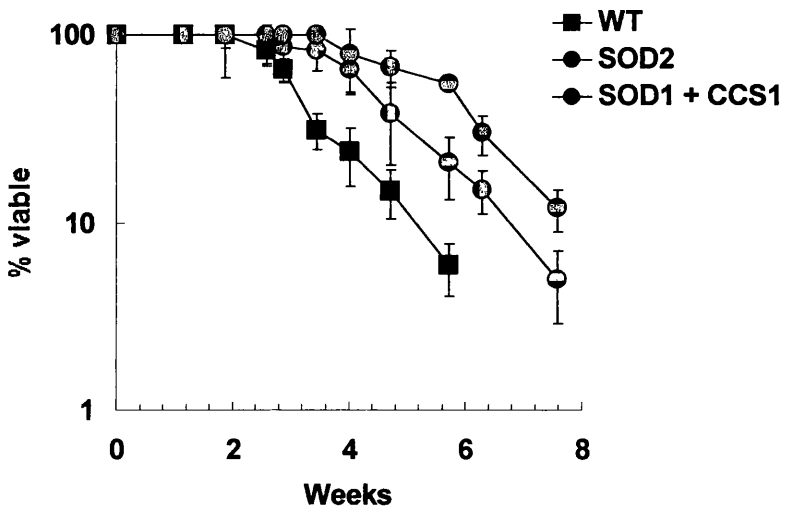

Figure 4.19)

Chronological life spans measured at 30°C. The extensions to lifespan correspond to those carried out at the 37°C (Fig 4.18) although the extensions are not quite as great. This reflects a reduced rate of respiration by the cells and hence the internal oxidative stress is reduced.

the *CCP1* overexpression cassette (Fig 4.18c) (increases in *CCP1* expression/activity were not determined). The co-overexpression of *CCP1* with *SOD2* reduced the life span of the *SOD2* overexpressing strain to a level far below that of wild type, hence reversing the advantageous effects of *SOD2* overexpression alone (Fig. 4.18c).

The small increase in chronological life span of increased catalase activity can be explained as increased scavenging of H_2O_2. However, cells with increased Sod activity demonstrated significantly greater increases in chronological life span, indicating that the major limiting pro-oxidant for long term stationary phase survival is the superoxide anion.

The activity of the *ADH2*-promoter driven cassette for *CCP1* were not under question because *CCP1* co-overexpression with *SOD2* generated a dramatic change in the *SOD2*-overexpressor phenotype. The reason for the detrimental affects of *SOD2/CCP-1* co-overxpression was not determined. It could be a consequence of a problem with the increased protein transport into the mitochondria. If there is a skewed distribution towards high levels of Sod2p and Ccp1p import then there could be a situation whereby important proteins, those in the electron transport chain for example, would be hindered on their passage into the mitochondria. The cells would therefore be less able to sustain viability in stationary phase.

4.3.4 Overexpression of active Cu,Zn-Sod delays the acquisition of large-scale protein oxidation damage.

Cells optimised for G_0 survival survive longer at 30°C, yet the beneficial effects of overexpressing active MnSod or Cu,Zn-Sod are still apparent even at this less stressful temperature (Fig. 4.20a). Cell inactivation in such cultures is essentially biphasic, an initial very limited loss of viability being followed by a period of much more rapid cell death ((MacLean et al., 2001); Fig. 4.20a). During natural aging, cells become steadily more prooxidant (Sohal and Weindruch, 1996). This results in increased oxidative damage, measurable by the formation of protein carbonyls (Levine et al., 2000; Levine et al.,

1995). At the point where stationary yeast starts to show appreciable losses of viability there is a dramatic increase in such protein oxidation (Fig. 4.20b). This increase in protein carbonyl content is substantially delayed in cells that overexpress both *SOD1* and *CCS1* (Fig. 4.20b). Increasing Cu,Zn-Sod activity therefore delays the acquisition of high levels of oxidative damage, this delay to large-scale damage accumulation being a plausible explanation for the increased longevity of the *SOD1+CCS1* overexpressor (Figs. 4.18d, 4.19).

This delay to the acquisition of high-level protein oxidative damage was not seen with cells that overexpress Mn-Sod (Fig. 4.20b). Nevertheless Mn-Sod is only active in the mitochondrial lumen and mitochondrial proteins are only a small fraction of those analysed in figure 4.20b. Also the effects of Mn-Sod overexpression on chronological life span are considerably less than those of the combined *SOD1+CCS1* overexpression (Figs. 4.18d, 4.19).

Figure 4.20)

a) Chronological lifespans of the longlived yeast strains aged at 30°C. Lifespans of these cells follows a pattern whereby an initial periodof very limited loss of viability is followed by a period of much more rapid cell death when inactivation adopts essentially first order kinetics. The point at which the cells show appreciable loss in viability corresponds with a massive increase in total cell protein oxidation (below). b) Carbonyl assay for determination of oxidatively modified proteins over time. Wild type and *SOD2* overexpressors show a dramatic increase in total cellular protein oxidation at the point they start to lose viability. This oxidation is delayed in the *SOD1* + *CCS1* overexpressor. Cells were aged at 30°C and 10μg of total cell protein extracts were separated by PAGE and blotted onto nitrocellulose (loading control gels were coomasie stained), oxidised proteins were detected using an antibody for DNP, see methods. (Work done in collaboration with Vitor Costa).

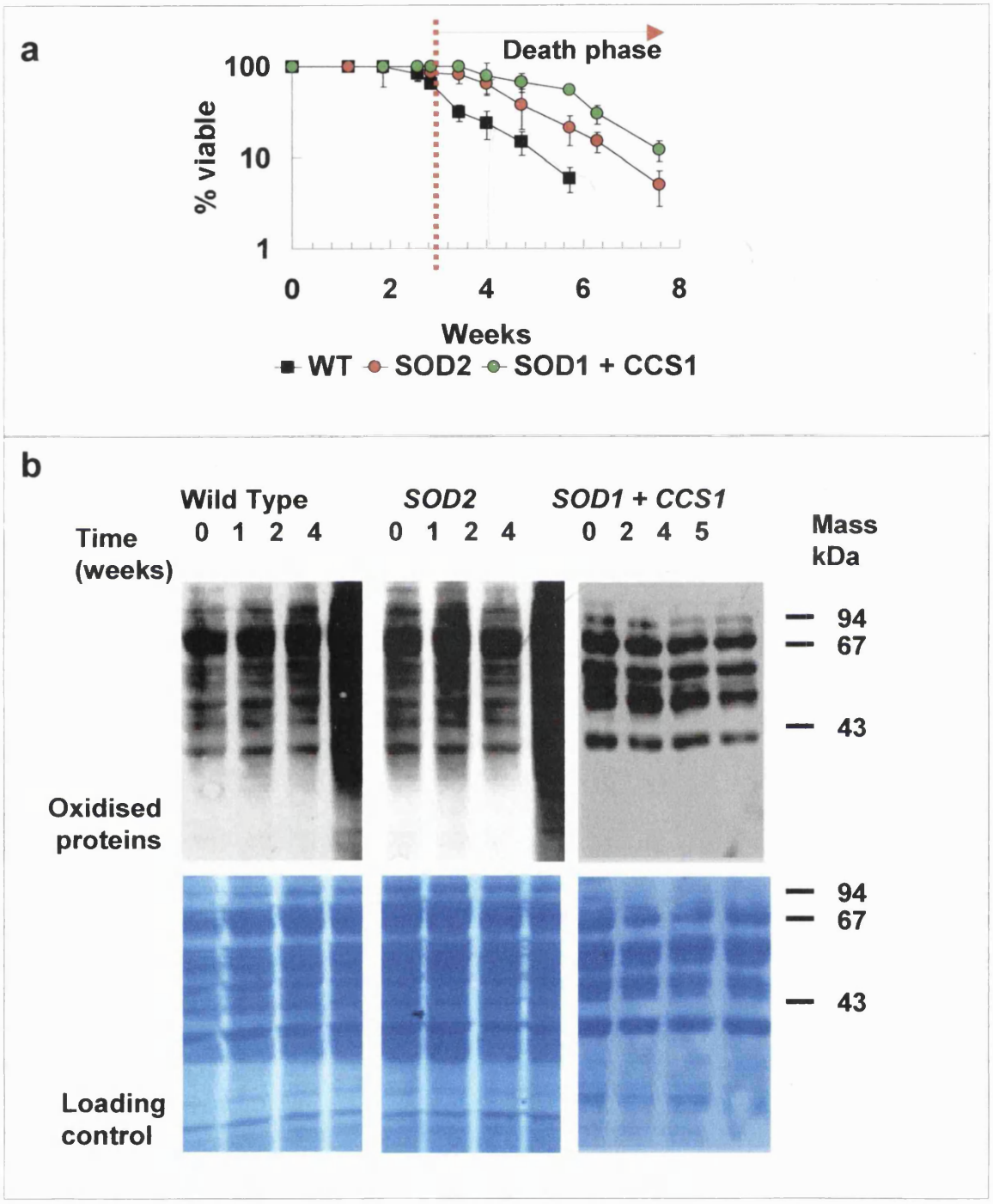
a
Death phase
100
10
1
% viable
0
2
4
6
8
Weeks
WT
SOD2
SOD1 + CCS1
b
Wild Type
SOD2
SOD1 + CCS1
Time (weeks)
0 1 2 4
0 1 2 4
0 2 4 5
Mass kDa
94
67
43
Oxidised proteins
94
67
43
Loading control

4.4 Results 3: Replicative life span and antioxidant activity.

4.4.1 Increased Cu,Zn-Sod activity has no effect on replicative life span

Previous studies have shown yeast cells that lack Sod or catalase activities have reduced generational life span (Barker et al., 1999; Nestelbacher et al., 2000; Wawryn et al., 1999). None of the overexpressions studied here extended this life span. Cells with increased levels of *apo*Sod1p had reduced replicative life spans (Fig 4.21a) but when the Cu,Zn-Sod activity was increased by simultaneous overexpression of *CCS1* a normal replicative life span was observed (Fig. 4.21b)

The reduced generational life span of the *CCS1* overexpressor is interesting. It suggests that the disruption in copper homeostasis by biasing the copper chelation towards *CCS1* is detrimental in someway to replicative life span. Increased Ccs1p, was beneficial to non-dividing cells maintained in aerobic culture which may relate to its ability to increase active Cu,Zn-Sod due to expression of the chromosomal *SOD1gene* (Fig. 4.21b). The same is not the case for replicative life span and suggests oxidant scavenging in the dividing cell is not limiting the latter life span.

4.4.2 Increased Mn-Sod activity reduces replicative life span.

Reduction in replicative life span was most marked for the *SOD2* overexpressor, this was not rescued with simultaneous overexpression of *CCP1* (Fig. 4.21c). This severe reduction in replicative life span of the *SOD2* overexpressor was not present when the strain was grown on glucose (Fig 4.22). Only a small reduction in replicative life span was observed when the cells were grown on glucose, when there is only a small amount of *ADH2*-promoter activity.

4.4.3 The SOD2 overexpressor does not accumulate ERCs.

The replicative life span of yeast is probably limited by the accumulation of ERCs (Sinclair and Guarente, 1997) (as discussed section 1.2.2). It is unlikely that the increased ROS scavenging would slow the accumulation of these ERCs. It can therefore be concluded that damage to the cell by ERC accumulation occurs before that of

Figure 4.21)

Replicative lifespans of the strains containing overexpression cassettes for the ROS scavenging systems. The overexpression of *SOD1*, *SOD2* and *CTT1* is detrimental to a full replicative potential (a). Overexpression of *SOD2* causes the most severe reduction to the replicative lifespan. Overexpression of *SOD1* has been shown to cause intracellular oxidative stress (section 4.5), this is the probable cause of the reduction in replicative lifespan in this strain. Co-overexpression of *CCS1* increases the activity of Cu,Zn-Sod, and restores replicative lifespan to that of the wildtype strain. *CCS1* alone is detrimental to replicative lifespan. (c) The negative affect of *SOD2* overexpression (not seen in this strain when grown on YPD (Fig. 4.22)) is not reversed by the co-overexpression of *CCP1* and hence the negative effect of *SOD2* overexpression is not due to excessive H_2O_2 production in the mitochondria. Replicative lifespans were determined by the analysis of over 60 virgin cells per strain tested. The cells were grown on YPGlycerol agar and dissected with a micromanipulator (Singer Instruments).

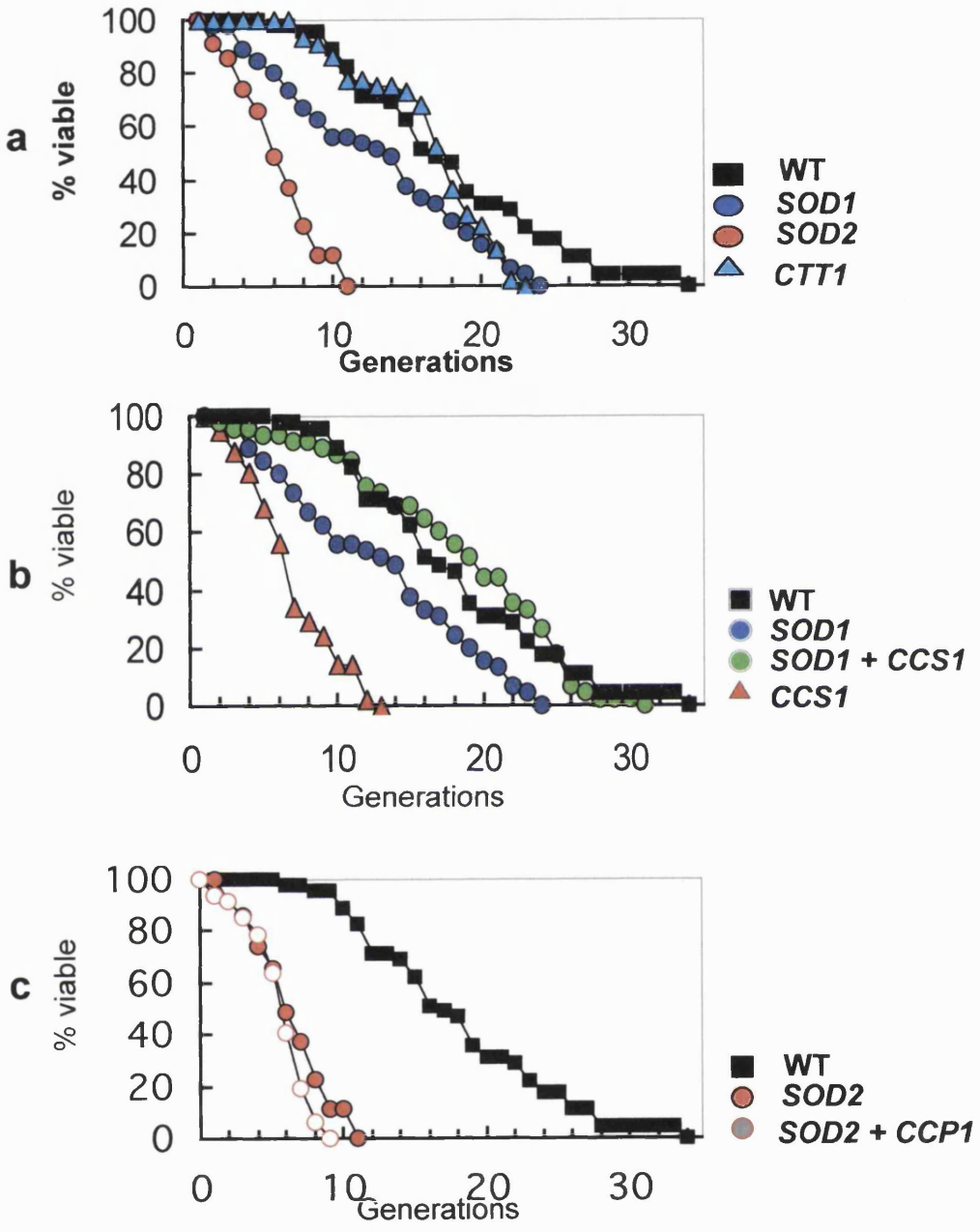
a
% viable
100
80
60
40
20
0
0
10
20
30
Generations
WT
SOD1
SOD2
CTT1
b
% viable
100
80
60
40
20
0
0
10
20
30
Generations
WT
SOD1
SOD1 + CCS1
CCS1
c
% viable
100
80
60
40
20
0
0
10
20
30
Generations
WT
SOD2
SOD2 + CCP1

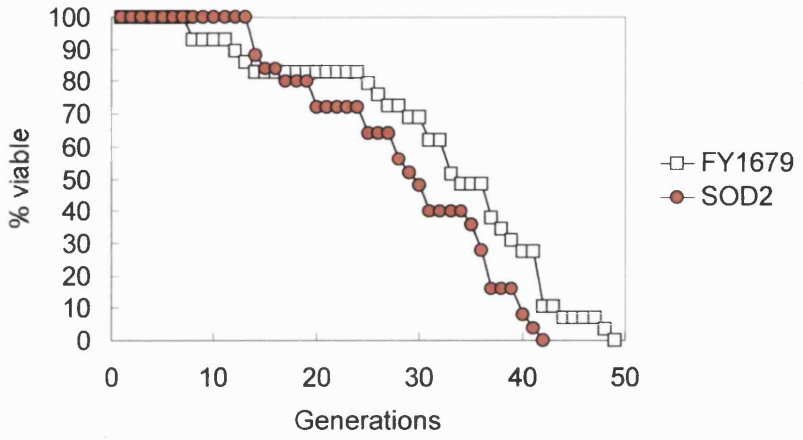

Figure 4.22)

Replicative life span of the *SOD2* overexpressor grown on 2% glucose (YPD). The *SOD2* strain does not have a severly reduced replicative life span when grown on glucose.Sod2p is not expressed in these conditions because of the glucoserepression of the The ADH2 promoter of this strain is glucose repressed and hence under these conditions the Sod2p is not elevated above wild type levels. A small decrease in the replicative potential of the glucose grown *SOD2* overexpressor can be explained by a very small level of *ADH2* promoter activity. Overexpression of *SOD2* is very detremental to the replicative life span of the cell that a minimal level of increased expression is the probable cause of the small reduction of viability seen in this experiment.

oxidative stress. The number of ERCs in the *SOD2* overexpressing strain was determined at the 5th division and compared to wild type to determine whether the much reduced generational life span of this strain was as a result of an accelerated ERC accumulation. Yeast cells were purified from culture after 5 divisions using a magnetic sorter (Smeal et al., 1996) and ERC number was determined by southern blot (Methods 2.5.5.4). No difference in ERC number could be determined, the shortened life span of this strain was therefore as a result of the detrimental effects of the Mn-Sod (Fig. 4.23).

4.4.4 Is the reduction in replicative life span of the SOD2 overexpressor caused by a disruption of mitochondrial inheritance?

A reduced replicative life span of the *SOD2* overexpressor could be due to a problem with the mitochondria. The 7-fold increase in Mn-Sod activity indicates an increase in Sod2p, which requires import into the mitochondria. The 7-fold increase in detectable Mn-Sod may not be a true reflection of Sod2p levels. The Sod2p levels may be much higher as some of the Mn-Sod may not be active as is the case observed for the Cu,Zn-Sod (see section 4.2.8). Levels of Mn-Sod in the *SOD2* overexpressor were not determined because no antibody, immunoreactive to the yeast Sod2p, was available. The increased levels of import required for the excess of Sod2p may affect the turnover and inheritance of the mitochondria in the dividing cell. To test for this fluorescent microscopy was used.

4.4.5 Mitochondria were followed throughout the life span of the SOD2 overexpressor.

The mitochondria of young and old cells of both wild type and *SOD2* overexpressing strains were observed. Young cells were harvested from a mid-logarithmic YEPG culture. Cells were biotin labelled and then magnetically reisolated after growth on YEPG for five doublings, with streptavadin coated magnetic beads. The mitochondria of these cells were fluorescently stained or labelled and observed using an Axioplan 2 fluorescent microscope equipped with a Plan-Neofluar 100x/1,30 Ph3 oil objective and a 100W mercury lamp microscope (Carl Ziess Jena GmbH, Germany).

Figure 4.23)

Southern blot for the detection of ERC accumulation throughout the replicative life span of the *SOD2* overexpressing strain. The accumulation of ERCs in the old mother cells was not accelerated by the overexpression of *SOD2*. This demonstrates that the reduced replicative life span of the *SOD2* strain was not as a result of ERC accumulation. Old mother cells were harvested after the fifth division, which is the point at which 50% of the *SOD2* overexpressing cells cease to divide.

Total cellular DNA was extracted from a mid-log culture for generation 1 cells and cells magnetically harvested from a culture, grown for five doubling times, for generation 5 cells. All cultures were grown in YPG, 20μg of DNA was separated on a 1% agarose gel (1V/cm for 30 hrs) and transferred to nitrocellulose membrane. ERCs were detected by hybridising the blot with a probe for yeast rDNA sequence.

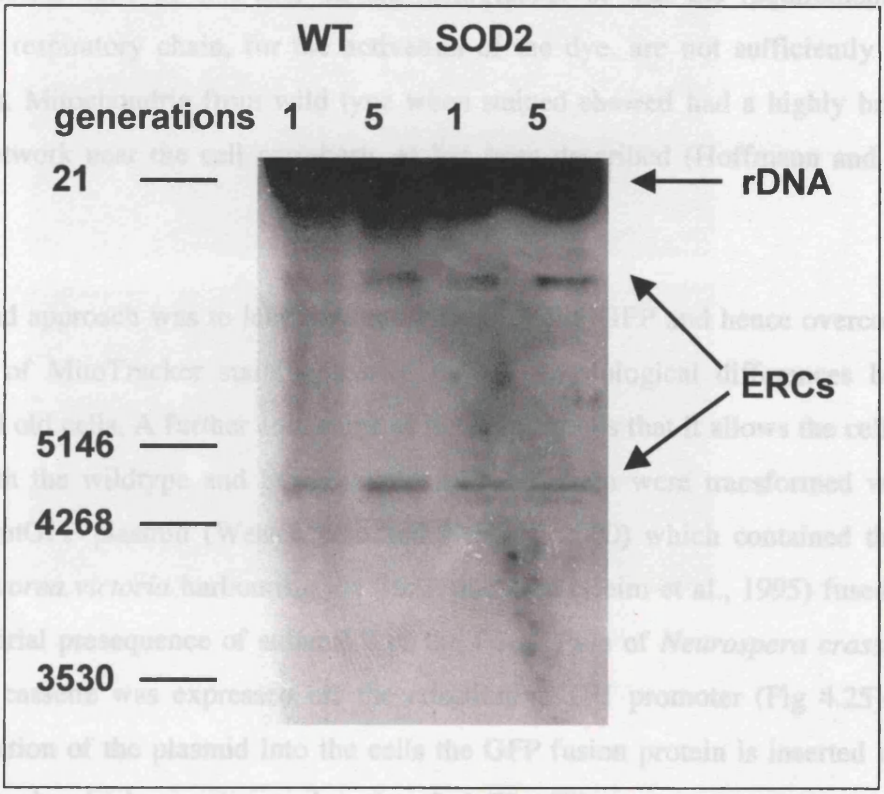
WT
SOD2
generations 1 5 1 5
21
5146
4268
3530
rDNA
ERCs

MitoTracker (Molecular probes Ltd, UK) was initially used to follow the mitochondria throughout the life span of the cell (Fig 4.24). This method however, was unreliable for the detection of old mother cell mitochondria. A possible reason for this could be that the old mother cells do not take up the MitoTracker or that the requirements of a functional respiratory chain, for the activation of the dye, are not sufficiently met in these cells. Mitochondria from wild type when stained ~~showed~~ had a highly branched tubular network near the cell periphery, as has been described (Hoffmann and Avers, 1973)

The second approach was to label the mitochondria with GFP and hence overcome the problems of MitoTracker staining caused by the physiological differences between young and old cells. A further advantage of this approach is that it allows the cells to be fixed. Both the wildtype and SOD2 overexpressing strain were transformed with the pYX232-mtGFP plasmid (Westermann and Neupert, 2000) which contained the GFP from *Aequorea victoria* harbouring the S65T mutation (Heim et al., 1995) fused to the mitochondrial presequence of subunit 9 of the F0-ATPase of *Neurospora crassa*. This Su9-GFP cassette was expressed off the constitutive TP1 promoter (Fig 4.25). Upon transformation of the plasmid into the cells the GFP fusion protein is inserted into the outer mitochondrial membrane by the Su9-F0-ATPase presequence, and hence fluorescently tags the mitochondria (Westermann and Neupert, 2000).

4.4.6 Increased levels of Mn-Sod in the dividing cell causes problems with mitochondrial inheritance and morphology.

Mitochondria labelled with GFP present the same morphology (Fig 4.26) as those stained with MitoTracker (Fig 4.24), indicating that this method is reliable for observing the mitochondria and that the inclusion of GFP into the outer mitochondrial membrane does not disrupt their phenotype.

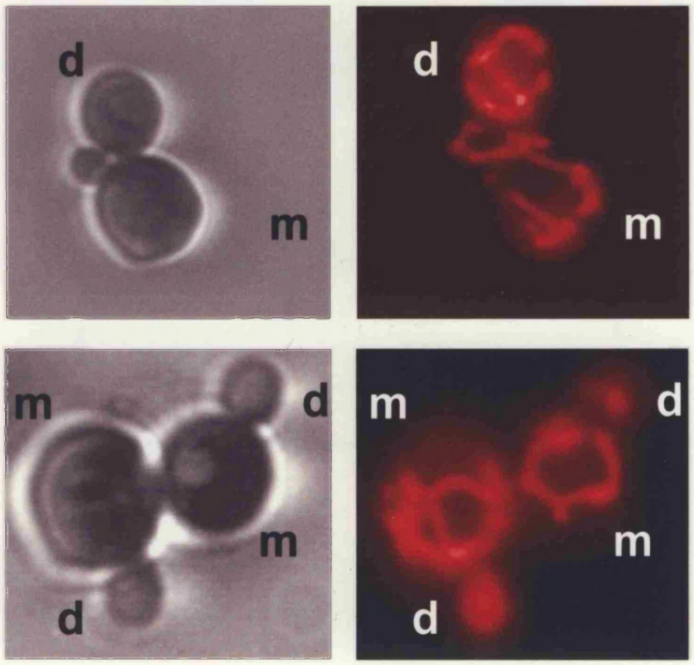

Figure 4.24)

Wildtype FY1769 cells stained for mitochondria with MitoTracker dye and observed with a fluorescent microscope. The mitochondria is clearly visible, stained red, the mitochondrial morphology is, as described in the literature, a tubular network below the cell cortex (Hoffman and Avers, 1973; Stevens, 1982). Background staining is however a limitation of this technique. In the lower panel the mitochondrial structure of the daughter cells is obscured by background glare. Cells were grown to mid-logarithmic phase harvested and incubated with 10μM MitoTracker for 30 mins at 37°C.

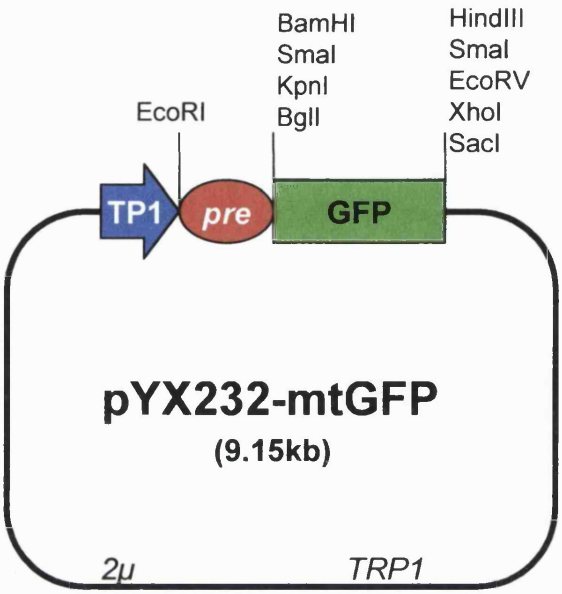

Figure 4.25)

Schematic of the pYX232-mtGFP plasmid (Westerman *et al.*, 2000). The Su9 mitochondria pre sequence-GFP fusion protein is constitutively expressed from the TP1 promoter. The FY1679 and *SOD2* strains were transformed with the plasmid and selected for TRP auxotrophy. For old mother analysis cells were grown in minimal SD media + 3% glycerol + 0.5% cassamino acids for maintenance of the plasmid and activation of the ADH2 promoter driven expression of *SOD2*

Figure 4.26)

GFP-staining of the mitochondria in young (unsorted) and 5-generation old (sorted) cells from YPglycerol cultures of the wild type and *SOD2* overexpressor strains. The mitochondria of wild type old mother cells (m) retain a morphology and inheritance similar to that seen in young cells. The mitochondria in old *SOD2* overexpressor cells are in contrast either lost completely to the daughter (d) and grand daughter (gd), not inherited by the daughter, or seen to undergo massive proliferation. The spherical particles of uniform size and fluorescence in the old cell images are streptavidin coated magnetic beads used for the isolation of these cells, mother cells are identified on the basis of size and their attachment to these beads.

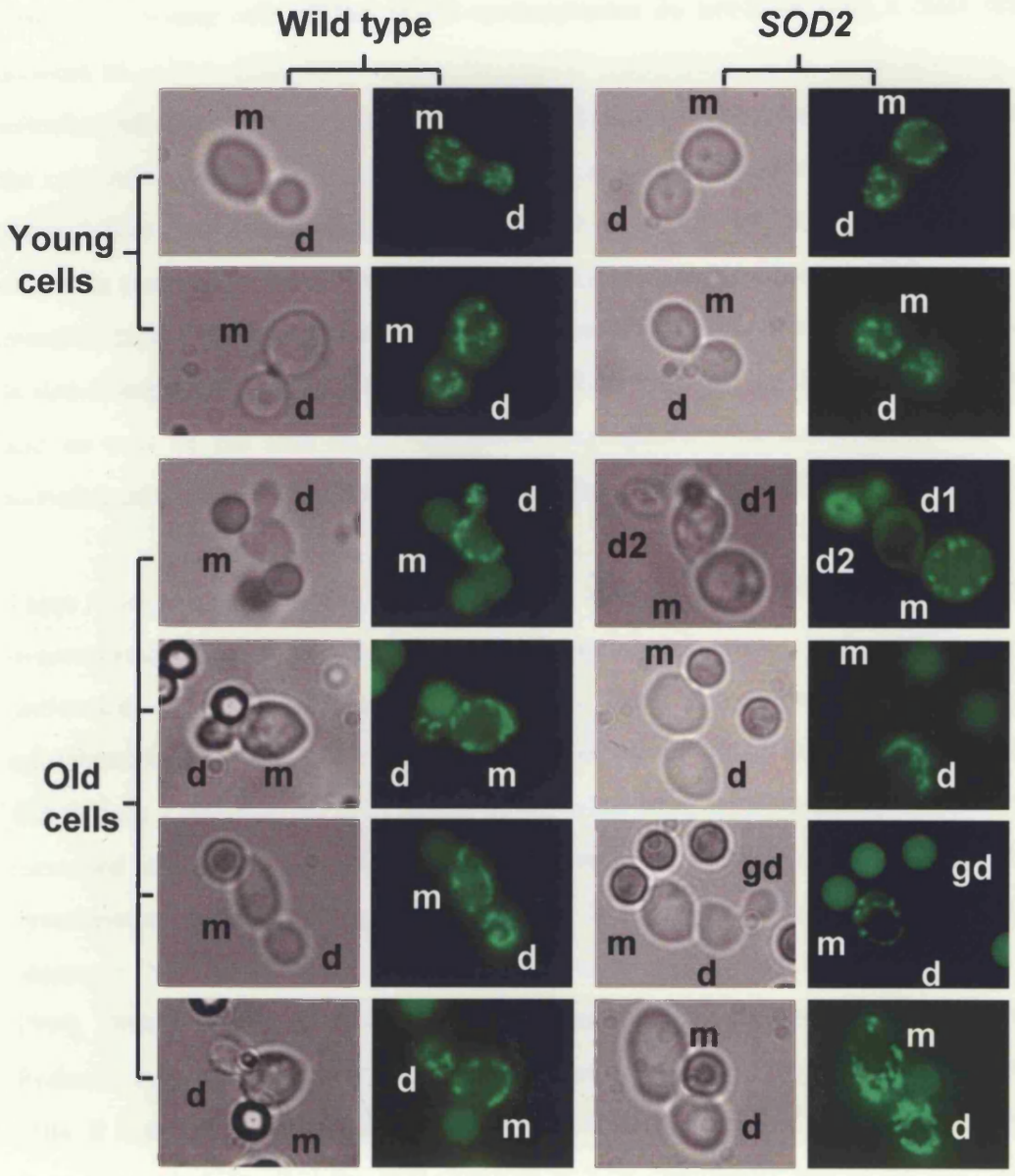
Wild type
SOD2
Young cells
Old cells
m
d
d1
d2
gd

After five divisions the wild type cells are more swollen than younger cells, a phenotype commonly associated with old mother cells. Mitochondrial segregation into the daughter cells remains unchanged (Fig 4.26). This is in contrast to the *SOD2* overexpressing strain. The young cells of the *SOD2* overexpressor do not have such a clear tubular network of
mitochondria. The mitochondria in these cells is more swollen and less spread through the cell. After five generations 50% of the old mother cells are not viable. These cells show defects in cellular morphology cells are generally swollen and have irregular shape. In some cases the *SOD2* old cells fail to complete cytokinesis and daughter cells remain attached these cells leaving a cluster of attached cells. Mitochondrial inheritance is also disrupted (Fig 4.26). Total loss of mitochondria from the mother cell is observed and as well as the lack of mitochondrial segregation into the daughter cells. The mitochondria in these cells is also less tubular than the wildtype (Fig 4.26).

These results suggest that the reason for such a reduced replicative life span of the *SOD2* overexpressing strain is due to a mitochondrial inheritance defect. The assay is performed on respiratory media and hence, the dividing cell absolutely requires mitochondria. The atypical circular blebs of mitochondria in the *SOD2* strain suggest that there is a defect in the cells ability to move the mitochondria throughout the cell. An increased import of a protein into the mitochondria may hinder its association with the cytoskeleton. Genetic evidence shows that *S.cerevisiae* requires both intermediate filaments (McConnell et al., 1990) and the actin cytoskeleton (Bereiter-Hahn and Voth, 1994; Drubin et al., 1993) for efficient mitochondrial morphology and inheritance. Reduced mitochondrial mobility would hence hinder their segregation into daughter cells. It is therefore conceivable that the reduced replicative life span could simply arise from the probability that the mitochondria will be completely lost to the daughter cell. The disrupted cellular morphology of the 5 generation *SOD2* mother cells however suggests that the mitochondrial mobility defect is damaging to the cell.

4.4.7 Normal physiological antioxidant activity of yeast appears to be optimal for their replicative life span.

We found that the replicative potential of cells grown to stationary phase on a respiratory carbon source is substantially maintained during subsequent stationary maintenance. Even the 1% of stationary wild type cells surviving a 5d 37°C ageing mostly exhibit a full replicative life span (Fig. 4.27b). In contrast dividing cells overexpressing antioxidant activities displayed, to varying extents, reductions in their generational life span. Nevertheless cells overexpressing *CCS1* and *SOD1*, despite their considerably improved stationary survival, exhibited a dramatic shortening of replicative potential with a period of stationary maintenance. This shortened life span was not exhibited by the wild type or the daughter cells of these *CCS1*/*SOD1* overexpressors and is therefore not an inheritable trait. This result strongly indicates that the normal physiological antioxidant activity of the yeast is optimal for replicative life span.

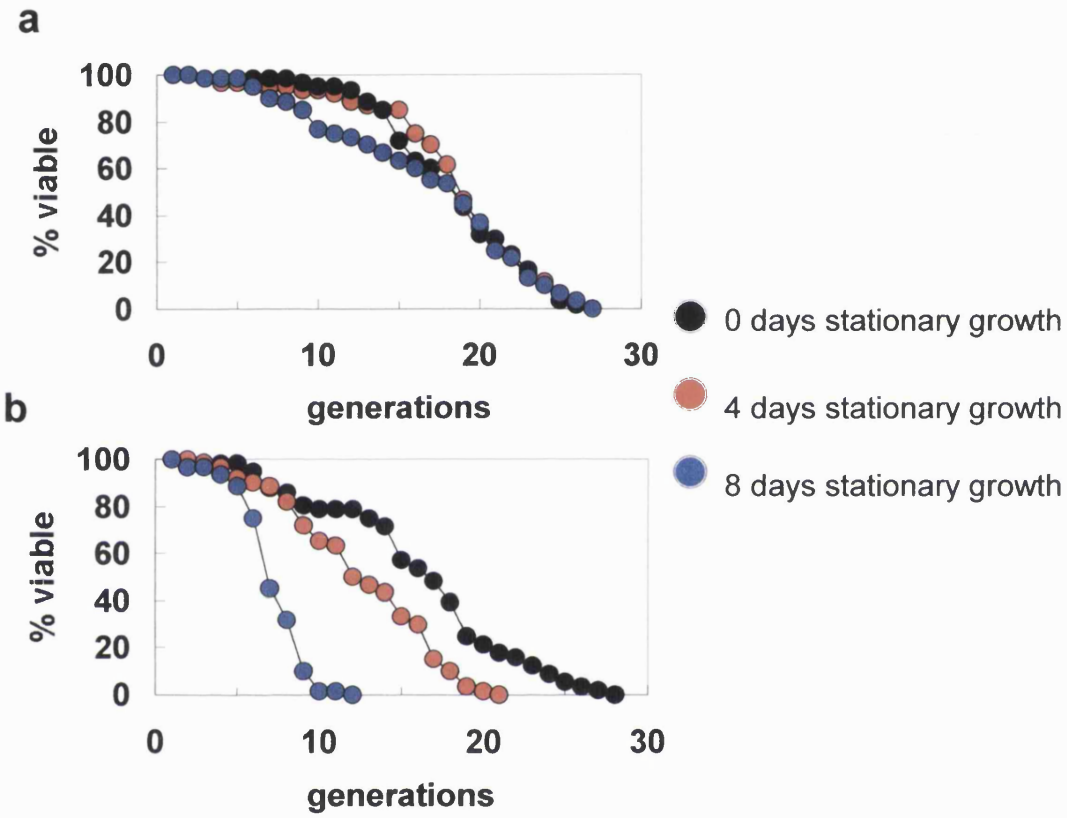

Figure 4.27)

Replicative lifespans of the (a) WT and (b) SOD1+CCS1 overexpresing strains, after periods of chronological ageing in the G0.

4.5 Results4: Overexpression of the Sod1 apoprotein increases endogenous oxidative stress.

4.5.1 Cells with increased levels of Sod1 apoprotein had greater levels of endogenous oxidative stress as indicated by the fluorescent dye DHR

The unexpected detrimental effect on both the chronological and replicative life spans of overexpressing the Cu,Zn-Sod *apo*protein (Sod1p) in the absence of a simultaneous *CCS1* overexpression (the *SOD1* strain; Figs. 4.18,4.21) was investigated. We found this *SOD1* strain exhibits very high endogenous ROS production during growth on glycerol.

The endogenous oxidative stress in the strains overexpressing the free radical scavenging enzymes were measured using the oxidation sensitive dye dihydrorhodamine123 (DHR). This lipophillic nonfluorescent indicator is deacetylated upon its passive diffusion into the cell. It is oxidised by ROS to the fluorescent dye rhodamine123 (Cowen, 2002; Tarpey and Fridovich, 2001). After a one hour incubation with 50mM DHR 123 the cells were observed down a fluorescent microscope. The image was captured and fluorescence measurements were taken from the total area of the cell. 75 cells were scored per strain in three independent experiments.

To verify the assay a *sod1* delete was compared to the wild type. An expected increase in internal ROS was demonstrated, a 99% fold increase (Fig 4.28a). Cells overexpressing the Sod1 *apo*protein displayed an increase of 68% ROS compared to wildtype, at a level similar to that of the *sod1* delete strain 99% (Fig. 4.28a). This was reversed when Ccs1p was co-overexpressed, demonstrating that the increased ROS of the *SOD1* strain can be directly attributed to an inefficient Cu^{2+}-loading of the overexpressed Sod1 protein. Cells with increased levels of the superoxide dismutases had significantly reduced levels of internal ROS. *SOD1/CCS1*, *CCS1* and *SOD2* had 45%, 48% and 39% reductions in internal ROS respectively (Fig 4.21a).

a

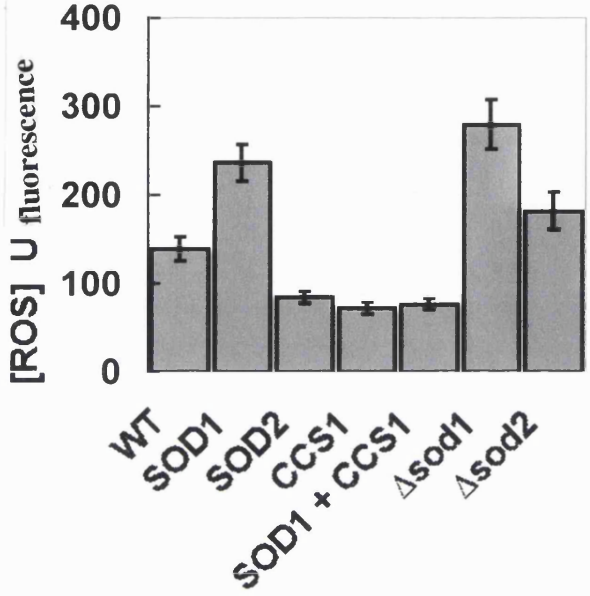

b

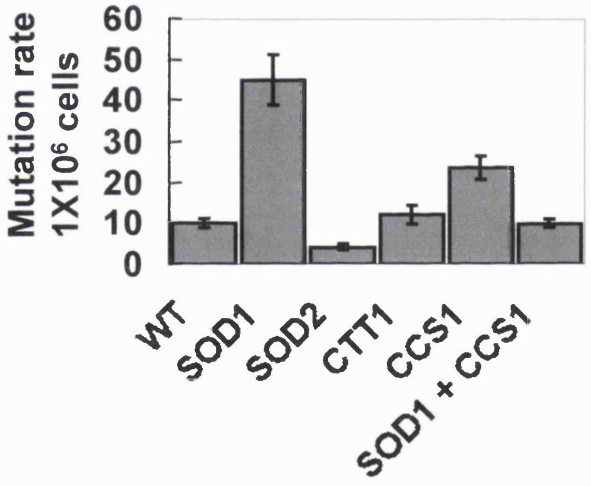

Figure 4.28)

(a) Endogenous ROS production by the wild type, *SOD1*, *SOD2*, *CCS1* and *SOD1+CCS1*strains, as well as *sod1*Δ, *sod2*Δ mutants, during room temperature glycerol growth. (b) Rates of mutation to canavanine resistance.

4.5.2 *Increased levels of Sod1 apoprotein cause increases in the spontaneous mutation rate of nuclear DNA*

Further to the direct measurement of internal oxidative stress, the spontaneous mutation rate of the cells nuclear DNA was measured, from which an indication of internal oxidative stress can be inferred. Cells with increased Sod1 *apo*protein displayed a greater *CAN1*^{s} to *can1*^{r} mutation rate when serial dilutions of a mid-logarithmic YPGlycerol culture were spread on agar plates containing the toxic ortholog of arginine, canavanine (Fig. 4.28b). This can be correlated with the pro-oxidant nature of the Sod1 apoprotein overexpression here measured with DHR (Fig. 4.21a). In cells which had a simultaneous overexpression of Ccs1p with Sod1p a restoration to wild type levels of endogenous ROS and mutation rates (Fig. 4.28).

4.5.3 *Increased levels of Sod1 apoprotein reduce the maximum growth temperature of the cell.*

The enzyme overexpressions studied here also have other notable phenotypic effects. Cells with increased Sod1 apoprotein further demonstrated an oxidatively stressed phenotype with a reduced maximum growth temperature (Fig. 4.29b). The overexpression cassettes that elevate Sod activity levels (*SOD2*, *CCS1* and *SOD1+CCS1*) give an improved respiratory growth in the presence of ethanol and sorbic acid (Fig. 4.29a), chemical stress agents that exert a strong prooxidant effect on cells by causing increased superoxide production by the respiratory chain (Costa et al., 1997; Piper, 1999). In addition the Mn-Sod overexpression causes a remarkable increase in the maximum temperature of growth (by about 1°C; Fig. 4.29b). This is a strong indication that endogenous oxidative stress due to mitochondrially-generated superoxide is a major factor determining the upper temperature limits of yeast growth. It is Mn-Sod, not Cu,Zn-Sod, that is thought to be the major protection against the superoxide generated by the respiratory chain (Moradas-Ferreira and Costa, 2000).

Figure 4.29)

a) Phenotypes of cells containing the antioxidant enzyme overexpression cassettes.(a) Cells with increased levels of Cu,Zn-Sod, Mn-Sod and catalase are more resistant to the Ethanol and Sorbate, chemical agents that exert a strong prooxidant effect on cells by enhancing free radical production by the respiratory chain (Costa et al.,1997; Piper, 1999). (b) In addition to this Mn-Sod overexpression *increases* the maximum growth temperature of the cells by about 1°C . Cells were grown in liquid YPG media held in a 96well-plate. A temperature gradient was maintained across this plate using a gradient PCR block, cells were grown for 48-hours and were replica plated onto YPD agar to test viability.

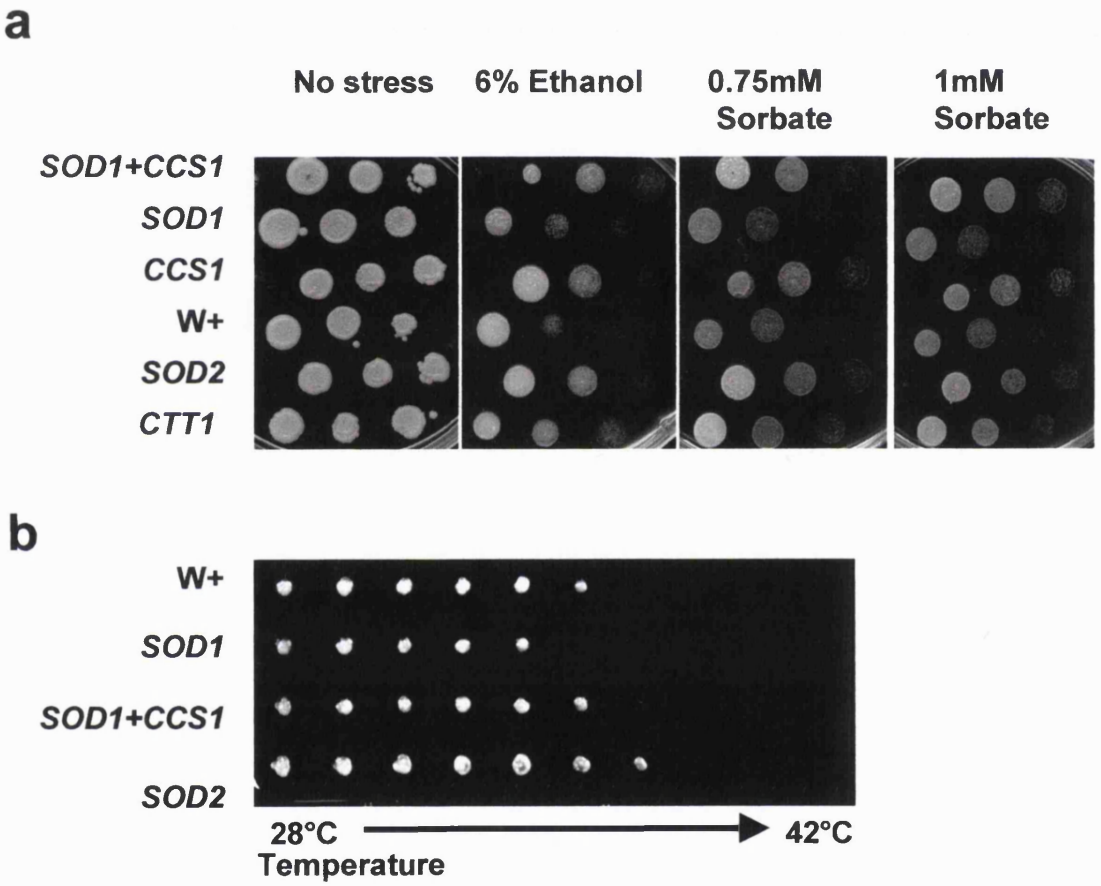
a
No stress
6% Ethanol
0.75mM Sorbate
1mM Sorbate
SOD1+CCS1
SOD1
CCS1
W+
SOD2
CTT1
b
W+
SOD1
SOD1+CCS1
SOD2
28°C
42°C
Temperature

4.6 Conclusion

This work has demonstrated that as is the case for *C.elegans* and *Drosophila* an increase in free radical scavenging can slow the chronological ageing of *S. cerevisiae.* The chronological life span of yeast can be extended by up to two-fold with increases in the activity of Cu,Zn-Sod and to lesser extents by the Mn-Sod and catalase enzymes. This is a clear indication that the major life span limiting process for cells optimised for G_0 survival is the release of free radicals from the respiratory chain and the damaging effects that these cause to cellular components. In cells with increased Cu,Zn-Sod (the longest lived strain) the onset of cellular protein oxidation is delayed. It has been demonstrated that the timing of increased levels of cellular protein oxidation coincides with a major loss in viability of the cells. The oxidation of proteins occurs rapidly, and is probably as a result of a total collapse in cellular protection from free radicals. The delay in this protein oxidation, resulting from an increased free radical protection with elevated Cu,Zn-activity, extends life span.

In addition to this life span data it has been shown that copper is limiting for Cu,Zn-Sod activity in respiratory adapted cells. To achieve an the increased activity of Cu,Zn-Sod the copper inserting chaperone *CCS1* had to be simultaneously expressed. Overexpression of *SOD1* alone, leads to an increase in cellular levels of *apo*Sod1p. This form of the Sod1p is detrimental to survival in G_0, and the cells demonstrate an oxidatively stressed phenotype.

No increase in the replicative potential of cells was observed with increased free radical protection from the *SOD1+CCS1* overexpressing strain. The life span limiting effects of ERC accumulation must therefore become toxic to the cells before damage to the cell by free radicals can occur. Overexpression of Sod1p Sod2p and Ccs1p reduce the replicative life span, surprisingly overexpression of the Sod2p is the most detrimental to replicative life span. Increased levels of *apo*Sod1p in the cell may be limiting to replicative life span for the same pro-oxidant reasons as for its limitations to

chronological life span. Increased Mn-Sod activity extends chronological life span and therefore a trade off between the advantageous affects of Mn-Sod activity on chronological life span and its inhibitory affects on replicative life span must exist. Further investigation demonstrated that the increased level of Sod2p inhibits mitochondrial inheritance, whereby mitochondria can be lost completely to the daughter cell.

5 A screen for prosenescence genes in the yeast genome.

5.1 Introduction

As described in Chapter 1 nondividing (G_0 phase) yeast cells provide a genetically tractable model of the mechanisms whereby stress resistances influence chronological life span. The final part of the project was to develop a method to select long lived mutants of *S. cerevisiae* directly, by exploiting the fact that this organism has a stable haploid state. A mutant screen can be expected to identify nonessential and nonredundant genes whose loss is somewhat detrimental for propagation of the species yet beneficial for long-term maintenance of nondividing cells. Thus it should be possible to reveal whether such "prosenescence" functions exist in a simple eukaryotic genome.

Evolutionary pressure is exerted mainly on the young individuals of a species. As a result the force of natural selection declines dramatically with age. This can provide strong selection for prosenescence functions, genes beneficial in young individuals but detrimental for older individuals (Kirkwood, 2002). For most organisms, stress protection and repair systems are not optimal for the maximisation of life span, raising the important issue of why natural selection acts to prevent the higher constitutive expression of stress genes whereby life spans would be maximal. Unfortunately mutations in prosenescence genes are generally recessive, with the result that many out breeding models of ageing (e.g. *Drosophila*) do not lend themselves very readily to the direct selection of mutants in such functions. *C. elegans* is an exception, and the only organism in which prosenescence genes have been directly selected to date. The *age* mutants of *C. elegans* from C. Kenyon's original screen have proved to be instrumental in revealing the importance of dauer-larval signalling to life span determination in this species (Kenyon et al., 1993). Yeast, with its stable haploid state, should also allow the direct selection of mutants with longer chronological life spans. It should therefore be useful in determining prosenescence functions that are present within a simple eukaryotic genome.

The aim of developing this screen was to identify genes whose mutation is somewhat detrimental for propagation of the species yet beneficial for long-term stationary maintenance (clearly a mutant would not be selected if the former effect is too severe). Chapters 3 and 4 describe different genetic alterations which enhance stress resistance in *S. cerevisiae*. In Chapter 3, it was shown that cells that display elevated expression of heat shock genes due to the E381K mutation in the Hsp90 chaperone display slowed growth and reduced replicative life span, yet a large increase in stress resistance and a small increase in stationary survival (Harris et al., 2001). In Chapter 4, strains overexpressing Mn-Sodp, Cu,Zn-Sodp/Ccs1p, and Ctt1p were shown to have an increased oxidative stress resistance and stationary survival, yet a reduced replicative life span. Yet another reported situation of increased stress resistance and stationary survival is the *sir4-42* mutation (Kennedy et al., 1995). It can therefore be expected that screening for long lived mutants will identify prosenescence genes which should highlight novel pathways involved in the regulation of the yeast chronological life span.

5.2 Results

5.2.1 Development of a strategy to isolate mutants with extended life span.

To perform the screen a system has to be used whereby a pool of mutants can be followed throughout their life span and the longest survivors easily identified. Mutants with the longest life span could be selected from the Euroscarf collection of single gene deletants (all of which are barcoded (Shoemaker et al., 1996) Alternatively a pool of tagged minitransposon inserts could be generated using the mTn-3xHA/*LacZ* minitransposon (mTn) insertion library created in the laboratory of M Snyder (Ross-Macdonald and et.al., 1999). A pool of yeast mutants created from this library, can then be screened for a long life span, the location of the disruption being identified by sequencing from within known DNA sequence of the minitransposon into the genomic regions adjacent to the mTn3 insertion site. (Ross-Macdonald and et.al., 1999). This mTn approach has the advantage that not all insertions lead to gene inactivation; some cause altered gene function.

A pool of mutants created by the mTn approach has been previously used to screen for prosenescence genes. mTn insertions in two genes, *SCH9* and *CYR1*, were shown to increase longevity over time of cells grown to stationary phase on glucose (Fabrizio et al., 2001) (discussed in section 1.4.1.). There are however, several problems with this earlier study. Firstly, this study did not use cells optimised for G_0 maintenance. Ageing studies should generally use conditions that give long life spans, longevities close to the maximum for the organism under study. If this condition is not met, such work is more in the sphere of "fitness" rather than ageing. As shown by other work in the laboratory (MacLean et al., 2001), respiratory adapted cells have the longest chronological lifespans. Therefore in a screen for genes with a prosenescence function respiratory adapted cells must be used. The above two mutants were isolated from cells grown in glucose, conditions not optimal for a full life span. Secondly, this screen reduced the huge task of screening the very large pool of mutants required for a full representation of the mutagenised library, by first selecting for mutants that survived a 1-hour heat stress at 52°C or resistance to 1mM paraquat (Fabrizio et al., 2001). Such an approach can therefore not identify any prosenescence function that does not operate through elevated stress resistance. Lastly, the transposon insertion library affects nearly 2000 annotated genes, representing about one-third of the 6200 predicted genes in the yeast genome (Ross-Macdonald and et.al., 1999). It is therefore probable that not all genes with prosenescence functions are represented within this insertion library. In the screen conducted below all except the last of the above problems were addressed.

5.2.2 Screening for prosenescence, using the mTn-3xHA/LacZ library genes and selection of long lived-respiratory adapted cells.

A pool of mTn mutants was created in the haploid FF18733 *ura3* minus yeast strain. FF18733 was used because in our hands it had demonstrated the longest stationary phase survival (MacLean et al., 2001). The subsequent screen for long term survivors was performed on cells which were grown to stationary phase in respiratory growth media

(3%) glycerol. No pre-selection for stress resistance was performed, and a pool of all mutants created from the insertion library mutagenesis were screened,

5.2.3 Creation of the mTn-3xHALacZ insertion library in FF18733

The mTn-3xHA/*LacZ* insertion library was received in 10 pools of DNA each comprising a separate mTn-3xHa/*lacZ* mutated library held on the pHSS6 plasmid from the M Snyder laboratory (http://ygac.med.yale.edu/mtn/insertion_libraries.stm). These had been created as follows. A yeast genomic library cloned into plasmids on *Not*I fragments in *E.coli* was mutagenised using mTn-3xHA/*LacZ*. Individual plasmids were then purified and organised in 96-well format. To use the library the disrupted genomic fragments are removed with *Not*I and subsequently transformed into yeast, each fragment integrating at its corresponding genomic locus by homologous recombination, placing a mTn insertion at this position. It has been demonstrated by transforming a diploid yeast strain that the library contained insertions in 1917 annotated ORFs distributed over all 16 chromosomes of the yeast genome, thus representing about a third of all the known yeast ORFs (Ross-Macdonald and et.al., 1999).

The pooled plasmid DNA library was propagated in *E.coli* DH5α and the plasmid pool prepared using a maxiprep plasmid purification kit (QIAGEN). The purified plasmid pools were then digested with *Not*I, agarose gel analysis revealing a 2.1kb band corresponding to the vector DNA and a smeared broad band in the 8kb region corresponding to the yeast-DNA-mTn insertions (Fig 5.1a). The resultant digest was directly transformed into *S. cerevisiae* , FF18733 selecting for uracil prototrophy.

In order to gain a 95%, degree of confidence, of successful gene replacement with all the disrupted alleles, 30,000 transformants were selected (3000 transformants for each of the10 mutagenised library pools). Typically the lithium acetate transformation method generated 1000 transformants per 10ng of the digested DNA library (Gietz et al., 1995), but the DNA concentration was kept at minimal levels for the efficiency required so as to reduce the possibility of multiple insertions. Once removed from the plates used for

Figure 5.1)

a) *Not*I digest of an aliquot of the pooled mTn3-3xHA/*lacZ* insertion library DNA. The large band around 8kb contains fragments of yeast genomic DNA containing mTn3-3xHA/*lacZ* insertions. The lower 2.1kb band corresponds to vector DNA. b) Total genomic DNA extracted from a pool of mTn3-3xHA/*lacZ* insertion transformants, digested with NotI and run on a 1% agarose gel for 18hrs at 1V/cm. DNA was transferred by southern blot and probed with a radiolabelled sequence of mTn3-3xHA/*lacZ*. The probe hybridised to a broad region around 8kb indicating that the mutant library contained many insertions.

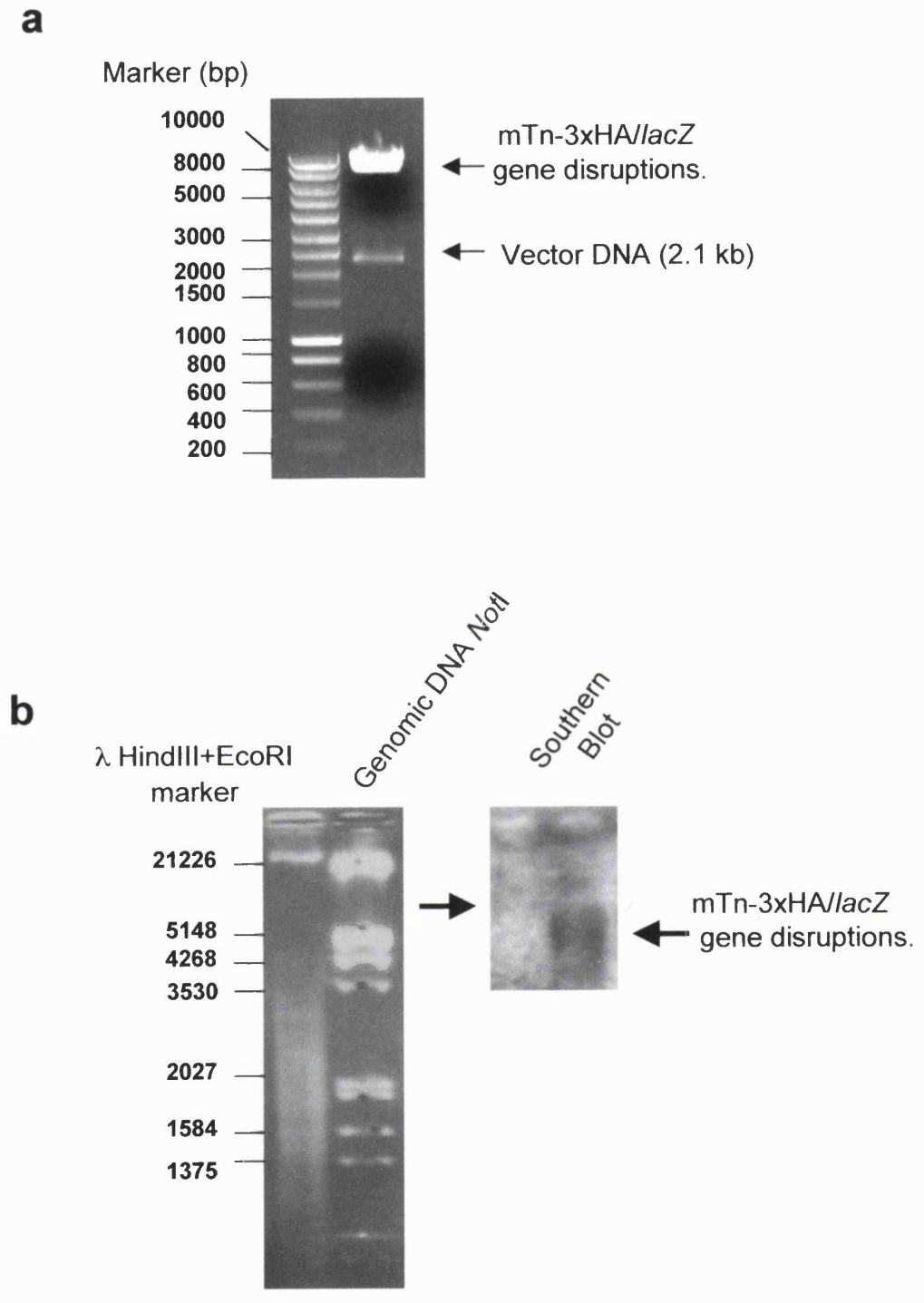
a
Marker (bp)
10000
8000
5000
3000
2000
1500
1000
800
600
400
200
mTn-3xHA/lacZ
gene disruptions.
Vector DNA (2.1 kb)
b
λ HindIII+EcoRI
marker
Genomic DNA NotI
Southern
Blot
21226
5148
4268
3530
2027
1584
1375
mTn-3xHA/lacZ
gene disruptions.

selection , the yeast mutants were grown for four generations before being pooled together and aliquoted into five separate pools for storage at -70°C.

5.2.4 Screening the mTn-3xHA/LacZ insertion mutants for prosenescence functions.

For this prosenescence screen 10 separate pools of the library were grown to stationary phase on respiratory (YP-glycerol) medium, then transferred to water and maintained at 30°C until these cultures had attained less than 5% viability. The surviving mutants were recovered, by growing in rich media to stationary phase. This process was repeated three times, with the intention of selecting mutants that survive well in stationary phase.

After the final ageing step the pools of aged cultures were recovered on uracil deficient SD minimal agar plates. From these plates 500 mutants (50 mutants from each pool) were collected for life span determination.

5.2.5 Identification of a single genetic disruption.

To determine the efficiency of the selection process the mutants were pooled and genomic DNA was extracted. This DNA was digested with *Not*I restriction endonuclease, the mTn3 insertion library was created in a library of *Not*I yeast genomic DNA fragments hence the digest would remove the original fragment used in mutant generation. A southern blot of this digest was probed for a sequence within the mTn-3xHA/*LacZ*. If the screen had been successful then distinct *Not*I fragments containing the selected mTn-3xHA/*LacZ* insertion would be visible. A similar southern blot analysis on the entire pool of mutants gives a broad band of DNA in the 8kb region (Fig 5.1b). The southern analysis performed on the pooled long-lived mutants identified a single excised band. Surprisingly this band was of very high molecular weight (Fig 5.2). Southern analysis was performed on 10 individual mutants, one from each pool with the same results (data not shown). It therefore appeared that the screen for prosenescence might have selected a single mTn-3xHA/*LacZ* insertion event.

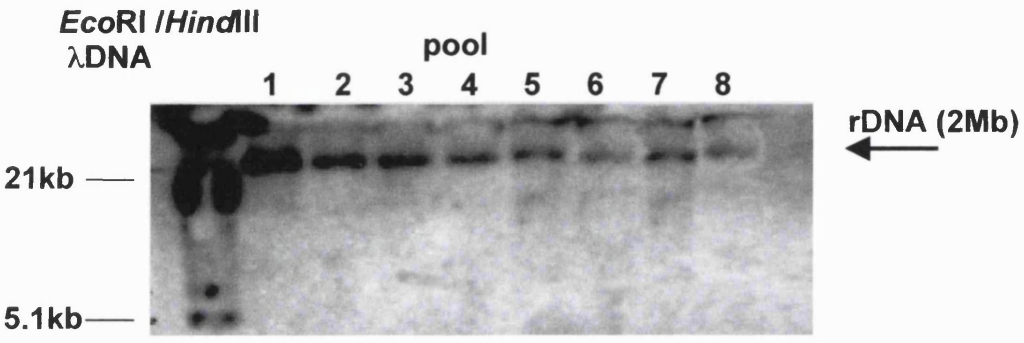

Figure 5.2)

Southern blot for mTn-DNA sequences in the genomic DNA of the yeast selected for prosenescence. Total genomic DNA was extracted from the eight pools of mutants which had been subjected to 3 successive periods of stationary phase inactivation to 5% cell viability. Genomic DNA, of these pools was digested with *Not*I, southern blotted and probed with mTn-3xHA-*lacZ* sequence. In all cases the probe hybridised to a genomic region greater than 2Mb (containing no *Not*I sites in all cases). For technical reasons pools 9 and 10 are not shown, analysis of these two was performed separately with the same results.

5.2.6 Identification of the insertion site

Because the southern blot data suggested that a single genetic insertion might have been selected, 10 mutants, one from each pool, were chosen for further analysis. Interestingly these mutants had different resistances to a 52°C heat shock (Fig 5.3). The location for the mTn-3xHA/*LacZ* insertion was however very large, and the differences in stress resistance may be explained by different insertions into different genes within this region.

For these 10 mutants the genomic site of mTn-3xHa-*lacZ* insertion was identified by the plasmid rescue strategy detailed in (Fig. 5.4). All the rescued plasmids when analysed by double digestion with *Kpn*I and *Bam*HI yielded a 2.85kb band of vector sequence plus similar size insert fragments. The sequence of the latter, is adjacent to the lacZ-derived sequence, and were sequenced using a primer (*prosenseq*) (Fig. 5.4) which was complementary to the 5' end of the transposon.

These sequences were searched against the *S. cerevisiae* Genome Database (SGD) using BLAST. All 10 mutants had mTn-3xHA/*LacZ* insertions on the right arm of chromosome XII within the ribosomal DNA (rDNA). This result therefore, agrees with the southern analysis carried out on the mutants. The rDNA region contains 100-200 tandem copies of a 9.1-kb repeat and spans about 2Mb of DNA (described in section 1.2.2). However the rDNA repeat lacks a *Not*I site, such that the *Not*I fragment contains the entire rDNA region from the genome (Fig. 5.2) (containing the mTn-3xHa-*lacZ* insertion).

Each rDNA repeat contains the genes for 5S, 5.8S, 25S and 18S rRNAs. All except the 5SrRNA gene are transcribed by RNA polymerase I as a single precursor, the 35S pre-rRNA (Venema and Tollervey, 1999). The rDNA is represented by several SGD entries. The *RDN1* locus represents the entire 1-2Mb repeat region. *RDN37* represents the primary transcript that is processed into the 25S, 18S and 5.8S rRNAs. *RDN25*, *RDN18*,

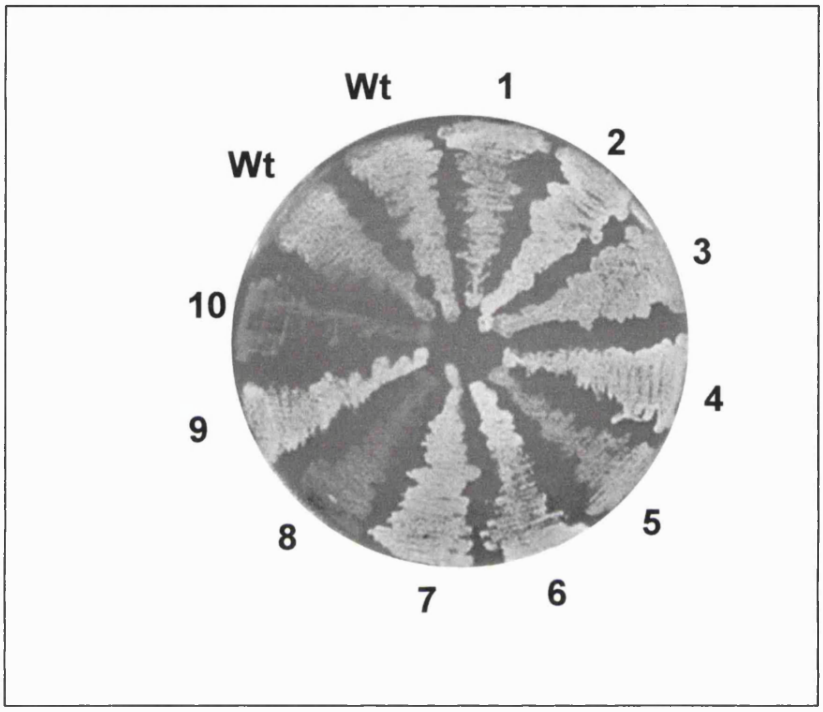

Figure 5.3)

Mutants from the ten prosenescence selection screens were assayed for resistance to a 52°C heat shock. The strains were grown on a YPG plate at 30°C O/N before replica plating onto YPD, this plate was subjected to a heat shock of 52°C for 2-hours, plates were cooled and incubated at 30°C O/N. The mutants have varied heat stress tolerances despite having the same mTn-3xHA/*LacZ* genomic disruption.

Figure 5.4)

Plasmid rescue strategy for retrieval of genomic sequences adjacent to the mTn-3xHA/*lacZ insertion*. To introduce an origin of replication (*ori*), a plasmid marked with *LEU2* (pRSQ2-*LEU2*, accession No. U64693) was used to replace part of the mTn by recombination between plasmid- and transposon-borne copies of the *lacZ* sequences. pRSQ2-*LEU2* was linearised with Bam*HI* and transformed into the yeast strain containing mTn-3xHA/lacZ. Transformants are selected for with the *LEU2* marker. Genomic DNA is then recovered from the yeast transformants and digested with *Bam*HI and*Kpn*I. (*Kpn*I cuts within the polylinker of pRSQ2-*LEU2*) to excises a fragment of DNA which contains the *E.coli ori* from pRSQ2 -*LEU2*, the *AMP* gene, the 5' terminal repeat of mTN-3xHA/*lacZ* and the adjacent genomic DNA up to the first *Kpn*I site. This fragment is recircularised and recovered in *E.coli*. The recovered plasmid is checked with a double digest between *Bam*HI and *Kpn*I yielding a 2.8kb fragment. Sequencing using the *prosenseq* primer reveals the genomic DNA adjacent to at the site of mTn-3xHa/*lacZ* insertion. Retrieved sequences are searched against SGD using BLAST.

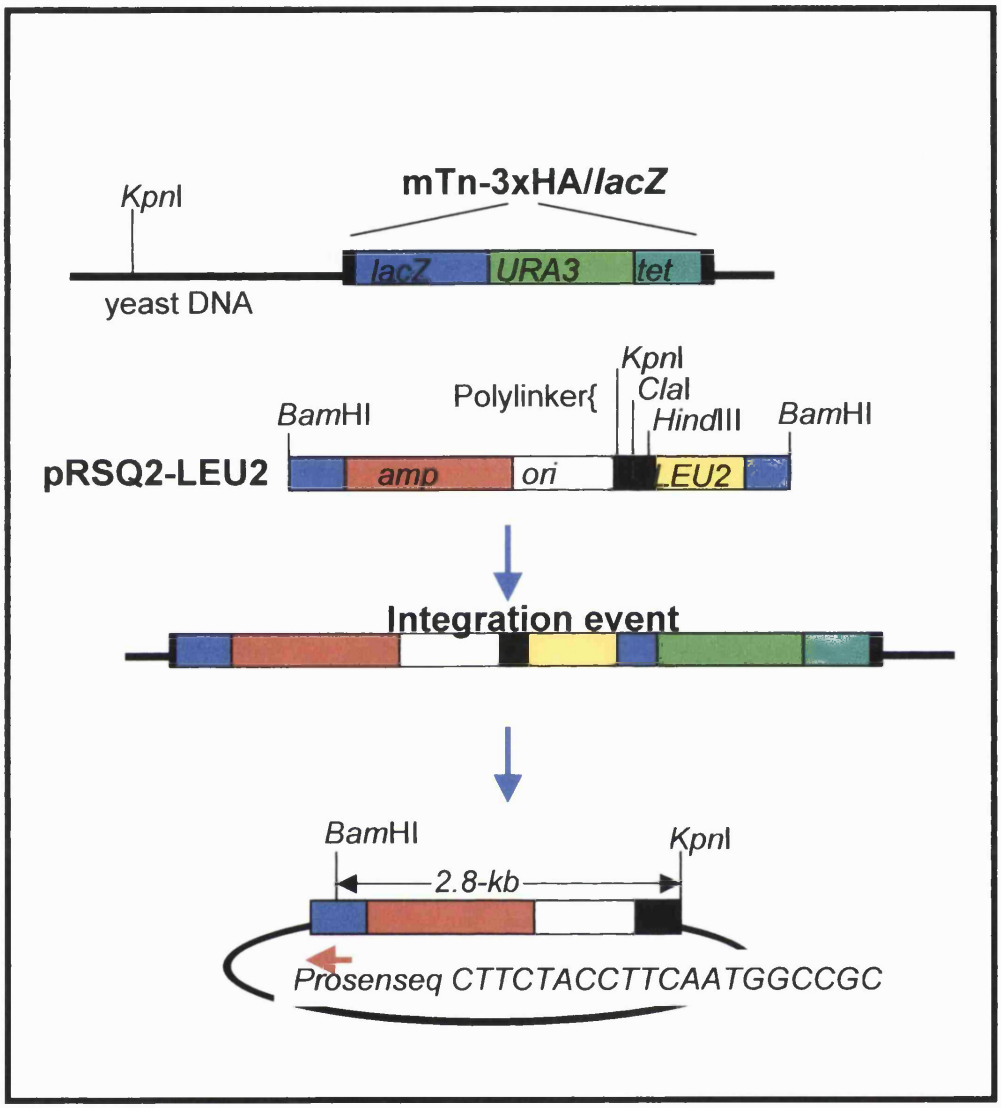
mTn-3xHA/lacZ
KpnI
lacZ
URA3
tet
yeast DNA
KpnI
ClaI
Polylinker{
BamHI
HindIII
BamHI
pRSQ2-LEU2
amp
ori
LEU2
Integration event
BamHI
KpnI
2.8-kb
Prosenseq CTTCTACCTTCAATGGCCGC

and *RDN58* represent the 25S, 18S, and 5.8S rRNAs, respectively, and *RDN5* represents the 5S rRNA. The *RDN5*, *RDN37*, *RDN58*, *RDN25* and *RDN18* loci therefore represent the rRNA-encoding regions within each repeat (Venema and Tollervey, 1999). The 10 mutants analysed had mTn-3xHa-*lacZ* clustered in three separate locations towards the 3' end of *RDN25* (Fig. 5.5).

5.2.7 Lifespan is not extended in the RDN25 insertion mutants

Measurements of chronological life spans of individual mutants corresponding to the three different mTn-3xHa-*lacZ* insertion sites, unexpectedly revealed their life spans were no longer than the wild type strain. The screen of mTn insertions for a prosenescence phenotype had therefore been unsuccessful (Fig 5.6).

5.2.8 A large representation of rDNA genes within the insertion library led to the selection of the RDN25 locus in this screen.

The above screen did not select for long life span. The mTn-3xHa-*lacZ* insertion library was chosen because it was reported to have a reasonably non-biased distribution throughout the yeast genome (Ross-Macdonald and et.al., 1999). The very repeated nature of the rDNA sequence however lends itself to an insertion bias, such that the mTn-3xHa-*lacZ* library contains multiple clones representing inserts in rDNA repeats. The *RDN25-1* gene is represented by over 1300 different clones, while protein-coding genes in the library are often represented by only single or double disruptions, (for example *ACT1* is represented as only a single mTn-3xHA-*lacZ* insertion) (http://ygac.med .yale.edu/triples /triples.htm\). The large number of insertions in rDNA represented in the library is also a result of the high levels of recombination which are known to occur within the rDNA (Defossez et al., 1999).

This over representation of mTn-3xHA-*lacZ* inserts in rDNA within the library is the probable reason for isolation of these inserts in the prosenescence screen. The library was successively aged together as a mixed culture of different mutants. This leads to an advantageous bias for any mutant which has no detrimental effect on chronological

Figure 5.5)

a) Map of the *RDN37-1* locus. b) Map of the three independent mTn insertions into the *RDN25* locus identified by vector rescue (Fig. 5.4). Mutants 5, 8 and 10 had insertions at mTnI-1; mutants 1, 2, 3 and 4 had insertions at mTn-2; mutants 6, 7, and 9 had insertions at mTn-3.

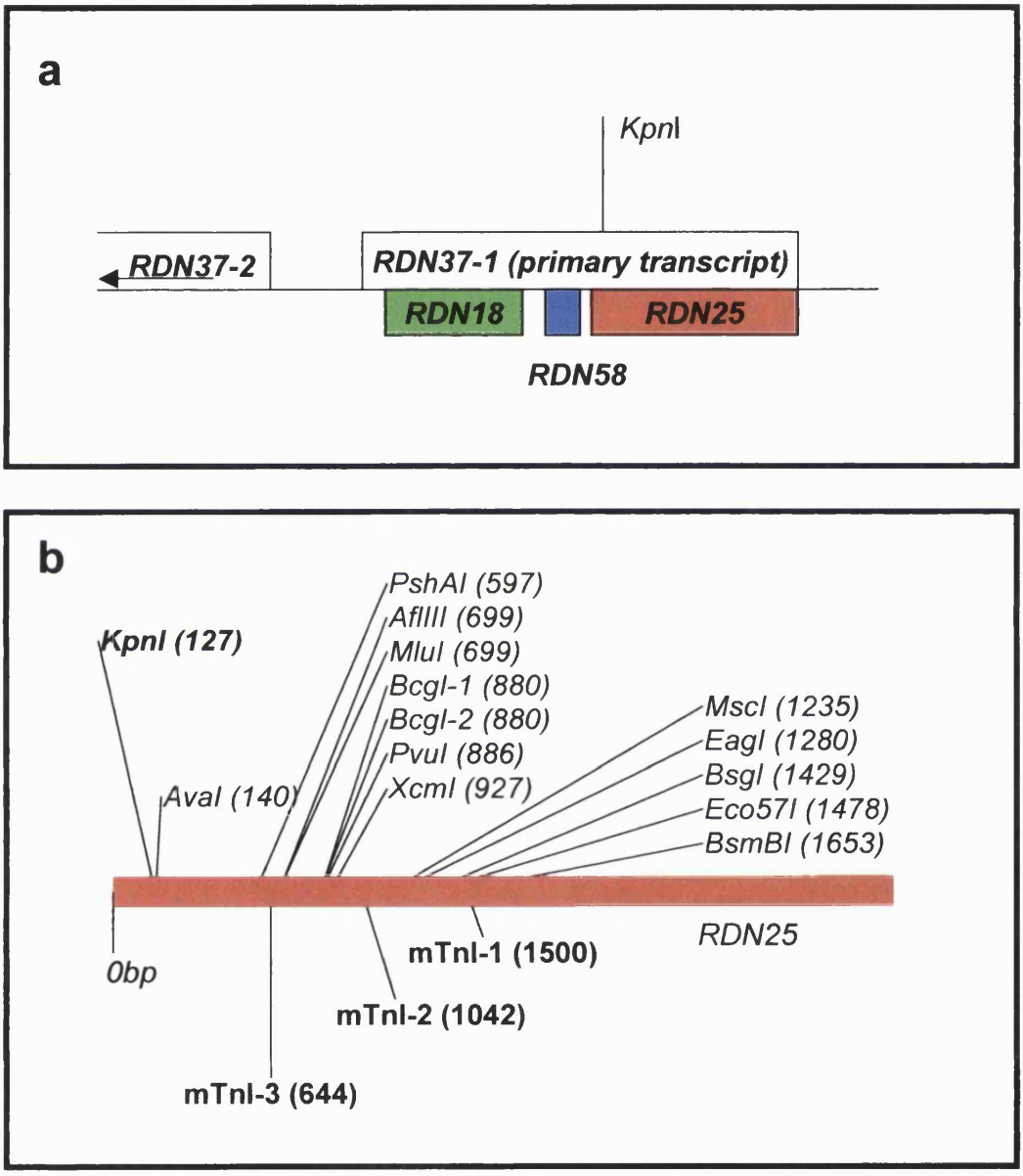
a
KpnI
RDN37-2
RDN37-1 (primary transcript)
RDN18
RDN25
RDN58
b
PshAI (597)
AflIII (699)
MluI (699)
BcgI-1 (880)
BcgI-2 (880)
PvuI (886)
XcmI (927)
KpnI (127)
AvaI (140)
MscI (1235)
EagI (1280)
BsgI (1429)
Eco57I (1478)
BsmBI (1653)
0bp
mTnI-1 (1500)
RDN25
mTnI-2 (1042)
mTnI-3 (644)

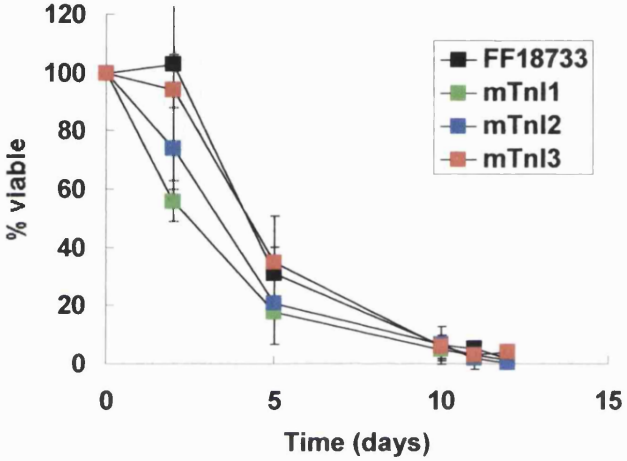

Figure 5.6)

Chronological lifespan measurements (37°C) for the three mutants with mTn insertions in the *RDN25* locus. mTnI1, mTnI2 and mTnI3 correspond to the three insertions identified (Fig. 5.5).

lifespan but is present in much greater numbers in the culture than other mutants. The greater number of these cells increases the probability that they will be revived after a period of stationary phase maintenance to less than 5% viability. Successive rounds of the ageing screen would only serve to amplify the selection of this mutant.

5.3 Improving the prosenescence screen.

The major drawbacks of the prosenescence screen conducted on the *mTn-3xHA/LacZ* insertion library were found to have been firstly; that the insertion library does not contain all the 6200 predicted yeast ORFs. Secondly; that screening of this mixed culture of mutants leads to a bias whereby over-represented mutants are selected over and above those which are much less abundant. An improved screen would be one where lifespans could be individually measured for each individual mutant.

The remaining part of this chapter describes the development of a system whereby yeast mutants in 96 well arrays can be individually measured for stationary phase survival. This has been developed with the intention that it can be applied to the Euroscarf collection of yeast deletant strains. The latter was constructed as part of the EUROFAN II project whereby the systematic deletion of the 6000 predicted ORFs of the yeast genome was undertaken by a consortium of European and American laboratories. The collection of deletion strains is available from Euroscarf (Frankfurt, Germany) (http://www.uni-frankfurt.de/fb15/mikro/euroscarf) in the BY strain genetic background (isogenic to S288c). Mutants were constructed using a PCR-based gene disruption and the capacity of S. cerevisiae to promote homologous recombination after transformation (Winzeler et al., 1999). Gene disruption cassettes included unique 20bp "barcode" thus allowing for strain identification (Shoemaker et al., 1996). This collection allows the functional analysis of novel genes from *S. cerevisiae* in genome-wide approaches by growing pools of mutants under a large variety of conditions, and hence is the best collection of yeast mutants available for the screen of nonessential, nonredundant genes whose loss generates a prosenescence phenotype. The homozygous diploids of each gene deletant should be used for this purpose, since there is a small chance that a second copy of the disruption cassette has integrated elsewhere in the genome.

5.3.1 Screening the Euroscarf delete collection on 96-well microtitre plates.

The Euroscarf library is maintained on 80 96-well microtitre plates, the location of each delete on the plates corresponding to a known gene disruption. The proposal for the prosenescence screen is therefore to perform the ageing experiments in these plates. The mutants can be grown to stationary phase on YP-glycerol in the 96-well format, the cell washing steps, transferal to water and the stationary phase maintenance over time all being performed in the wells of the plate. This way the mutants are aged individually thus preventing the problems encountered in the first screen for prosenescence mutants discussed above. To test the viability of these 6000+ cultures a Biomek 2000 Workstation equipped with a 96-well high density replicating tool (96-HDRT) (Beckman Coulter) was used to replica plate from the liquid cultures in 96-well plates onto YPD agar-filled omnitrays (Nunc #242811) to measure viability at time intervals. The pins of the 96-HDRT would transfer a small number of the cells from each culture onto the YPD agar. With subsequent incubation of the YPD agar the viable cells would exit G_0 and form visible colonies. As cultures become senescent the number of viable colonies would reduce. Any colonies out-surviving the wild-type could then be recorded and analysed for chronological life span by more conventional methods of serial dilution and plating.

5.3.2 Testing the proposed method.

Using the Sod overexpressor strains created in Chapter 4 (Table 4.2) the practicality of a 96-well plate automated chronological life span assay was tested. Chronological life span measurements of these cells with elevated Cu,Zn-Sod and Mn-Sod activities, aswell as cells with increased levels of the Ccs1p, had demonstrated life span extensions compared to wild type. In contrast the *SOD1* overexpressing strain had a reduced stationary phase survival (Fig. 4.18). The known life span increases and decreases of these strains provided a system by which robotic life span measurements could be validated. The variations in these life spans also enabled determination of the degree of life span difference that could potentially be detected by this approach.

The test was performed on four 96-well plates, 8wells of these plates carrying each tester strain as shown in figure 5.7. The test assay therefore included 32 repeated replica platings for each strain. Initially the plates were inoculated by hand into 150μl of YPG, the latter in the wells of 96v-well plates (Nunc #249662). These were grown to stationary phase (4d at 30°C) in an orbital shaker at 200rpm. The cells were collected in the bottom of the v-wells by centrifugation at 1000rpm, the growth media was removed by rapid inversion of the plate. The cells were resuspended in sterile H_2O, the cells were collected in the bottom of the wells and the water was tipped off again. This was repeated three times to ensure adequate washing of the cells and complete removal of any remaining media from the wells. Cells were aged in 100μl of sterile H_2O at 37°C in an orbital shaker at 200rpm. Viability measurements were made every three days by replica plating the 4 96well plates, with the 96HDRT, onto a single YPD agar plate in a 384 (4x96) format. Each well position on the 96 well plate corresponding to a square of 4 colony regions on the 384 format plate) (Fig 5.7b). The YPD plate was incubated at 30°C for three days

5.3.3 The 96-well chronological life span assay can be used to measure stationary phase survival of yeast.

The yeast chronological life spans as measured by this automated assay (Fig. 5.8a) directly correlate with earlier results obtained by diluting samples from 5ml cultures, plating and then determining viability by colony counting (Fig 5.8b). The first strain that was unrecoverable on rich media after incubation in the 96-well plate was the short lived *SOD1* overexpressor. This lost any ability to form colonies after 6 days of stationary phase maintenance (the viability for this strain at this time point was measured at less than 1% (Fig 5.8b) in previous experiments). The next strain to senesce was the wild type, which survived up to day 12 in this assay. Again this follows measurements taken for WT viability (Fig. 5.8b). In this assay *SOD2* just outlived the *CCS1* strain, while the longest lived strain was the *SOD1+CCS1* combined overexpressor, was still viable after 27 days. The robotically-measured viability measurements for the latter three strains were not in quite as close agreement with the earlier viability measurements (Fig. 5.8b) as for the *SOD1* strain and wild type. This may be explained by the shape of the survival

Figure 5.7)

The 96-well-format test of chronological ageing, organised so as to perform 32 repeats of each strain in the ageing assay. (a) shows the pattern in which strains were innoculated into the four plates (FY = wildtype; S1 = *SOD1*; S2 = *SOD2*; CS = *CCS1*, SC = *SOD1* + *CCS1*). Empty wells were left adjacent to the culture wells to determine whether any cells were inadvertantly transferred into different wells during the assay, though these wells remained sterile throughout the assay (data not shown). (b) Viability test at day 0 on a YPD agar filled omnitray. The four 96 well plates were replicated into a 384 (4x96) well format.

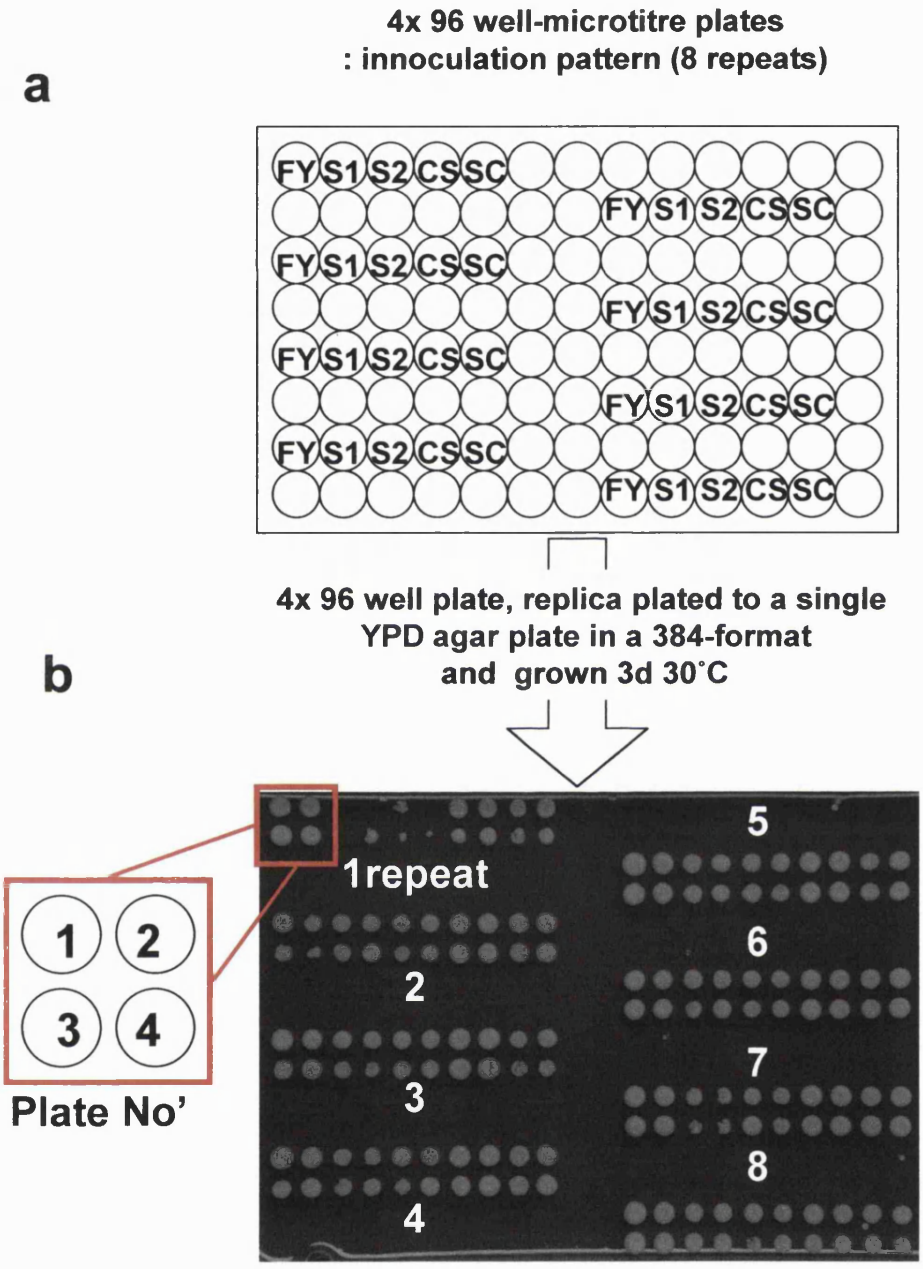
a
4x 96 well-microtitre plates
: innoculation pattern (8 repeats)
FY S1 S2 CS SC
4x 96 well plate, replica plated to a single
YPD agar plate in a 384-format
and grown 3d 30°C
b
1repeat
1
2
3
4
Plate No'
5
6
7
8

Figure 5.8)

Validation of 96-well chronological ageing using the strains created in Chapter 4. These strains had varying lifespans, shorter *SOD1* and longer *SOD2, CCS1*, and *SOD1+CCS1* than the parent strain FY1679. The life spans as determined by automated replica plating onto YPD agar in the 384-format (a) closely correlate to the earlier results obtained by manual dilution and replica plating from Chapter 4 (b).

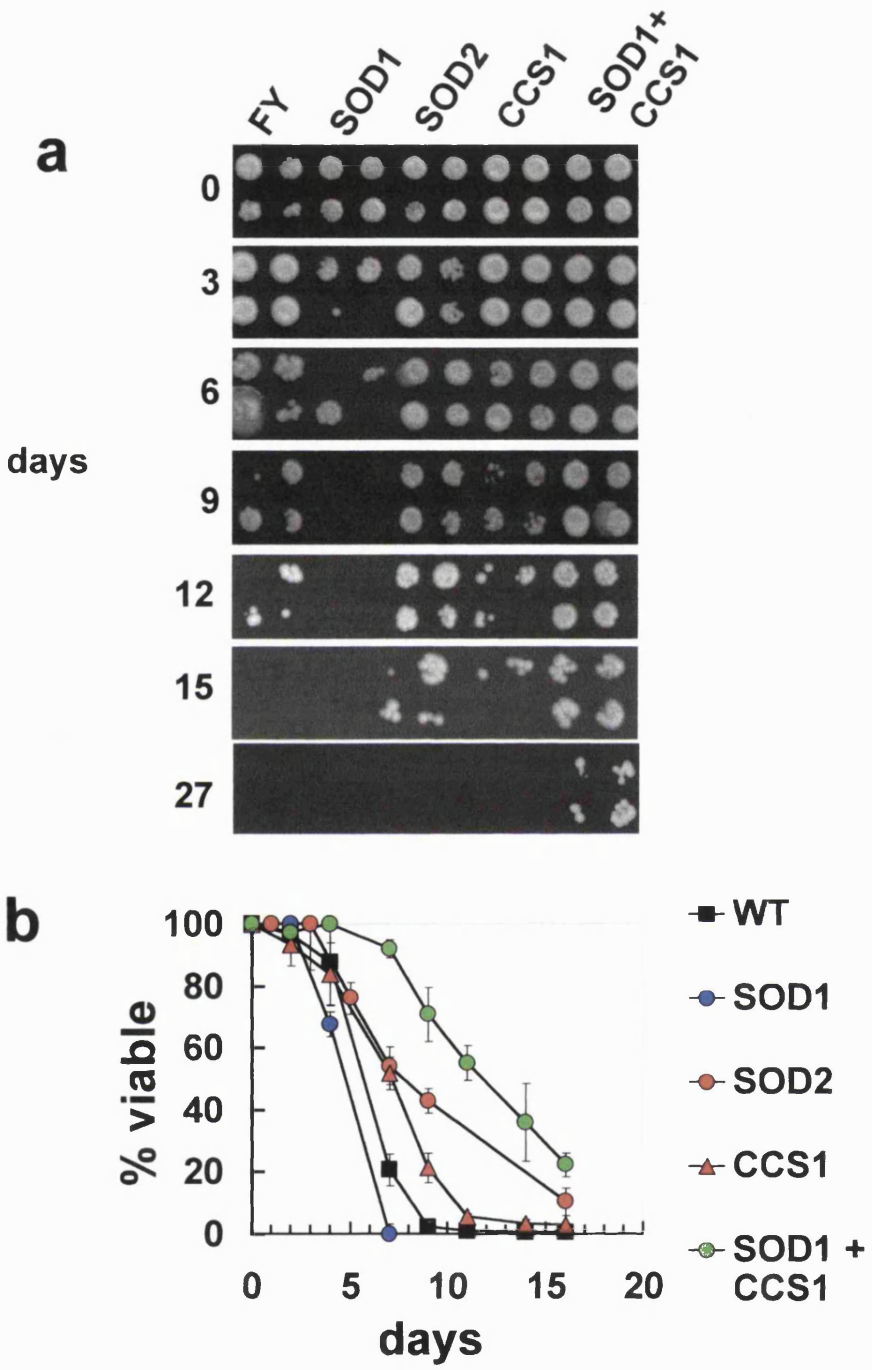
a
FY
SOD1
SOD2
CCS1
SOD1+ CCS1
0
3
6
days
9
12
15
27
b
100
80
60
40
20
0
% viable
0
5
10
15
20
days
WT
SOD1
SOD2
CCS1
SOD1 + CCS1

curve. The long lived strains tend to senesce at a slower rate which could possibly result in a few cells surviving a very long time, a scenario which is more likely to be seen in the 96-well assay. The order of senescence is however preserved.

5.4 Conclusion

The work in this chapter revealed the limitations of the mTn-3xHA/*lacZ* insertion library in screening for potential prosenescence mutants, also the need for a more rigorous approach for such a screen. While the work was in progress the Eurofan collection of deletant strains was completed, allowing for screening of any nonessential, nonredundant genes whose loss extends chronologial life span. The 96-well plate chronological life span assay was developed as part of this work to screen the Euroscarf library of mutants individually for a prosenescence function. This new method was tested on yeast strains with increased free radical scavenging capabilities, described Chapter 4. The life span data for these strains collected by robotic replica plating of cultures in 96-well format closely matched that obtained by laborious manual plating of serial dilutions as described in section 4.3. The assay was therefore validated laying the basis for a screen of the Euroscarf library for long lived mutants. Unfortunately due to time restraints, however this screen was not completed as part of this study.

6 Discussion

The initial aim of this study was to determine the role of stress resistance in the replicative and chronological life spans of *S. cerevisiae*. Chapter 3 describes the life span analysis on mutants that have high stress resistances as a result of lowered Hsp90 chaperone activity (Duina et al., 1998). Strains deleted for the *Cpr7* cochaperone and the *hsp82* E381K point mutation extended the chronological life span of glucose-grown cells (though not the longer lived glycerol-grown cells). This demonstrates that cells which are more stress resistant can survive better in G_0. This has also been shown for C.*elegans* where the age-1 mutation causes not only 65% longer life expectancy but also an increased intrinsic thermotolerance (Lithgow *et al.*, 1995) and in *Drosophila*, which when selected for increased longevity is more stress tolerant (Service et al., 1985). Elevated stress resistances do not however, increase the replicative potential of yeast cells, where ERC accumulation may be the major factor limiting life span.

A prolonged stationary phase survival compared to wild type was not observed in the *Δcpr7* and *hsc82*-E381K mutants when they were optimised for G_0 survival on non-fermentable carbon sources. Respiratory adapted cells have an increased chronological life span compared to cells grown by fermentation. Other work in the laboratory which has identified physiological conditions that optimise yeast chronological life span has shown that respiratory adapted cells survive longer periods in G_0 (MacLean et al., 2001). Cells grown by respiration have a higher tolerance for stress (Martinez-Pastor et al., 1996). The survival of respiratory cells might therefore be optimal, because further increases in stress resistance as a result of low Hsp90 chaperone activity, did not further extend this life span (Chapter 3)

In Chapter 4 increases in oxidant scavenging enzymes were shown to slow the chronological ageing of cells adapted to respiratory growth. Studies of the factors that determine ageing are on firmer ground when it can be shown that these can allow long

life spans, close to the maximum for the organism under study, to be extended. This is because a shortened life span might merely represent reduced "fitness" rather than any effect upon the natural processes of ageing. Since this increased free radical scavenging can generate up to 2-fold increases in the life span of yeast optimised for G_0 survival we can propose that ageing of these cells has indeed been slowed; also that levels of antioxidant enzymes yeast are not optimised for longevity. Thus just as increases in free radical scavenging slow chronological ageing in the nondividing cells and tissues of adult *Drosophila* and *C. elegans*, they also extend the life span of nondividing yeast cells. Yeast optimised for G_0 survival show a dramatic increase in protein oxidation at the same time that it starts to show appreciable losses of viability (Fig. 4.20). Cells are known to steadily become more prooxidant as they age (Sohal and Weindruch, 1996), which compromises those antioxidant defenses that rely on the reduced forms of glutathione and thioredoxins. In such prooxidant cells, superoxide and H_2O_2 scavenging enzymes will become even more critical in the prevention of oxidative damage. This is the most plausible explanation for the delays to the acquisition of substantial protein oxidation and the loss of viability when the activity of Cu,Zn-Sod is increased (Fig. 4.20).

Even though the overexpression of oxidant-scavenging activities was associated with increases to the chronological life span in yeast it resulted in variable degrees of shortening of the replicative life span (Fig. 4.21). Increases in oxidant scavenging enzymes are therefore not universally beneficial. The extension to chronological life span is most striking with the *SOD1+CCS1* overexpressing cells. However these cells, despite an almost normal replicative life-span, display a marked shortening of this replicative life span in response to a period in G_0 arrest (Fig. 4.27). Mn-Sod overexpression also causes small increases in chronological life span, resistance to agents that enhance endogenous oxidative stress and the maximum temperature of growth (Fig. 4.29b). However it also dramatically shortens the replicative life span (Fig. 4.21a), due apparently to a defective mitochondrial segregation process in old mother cells (Fig. 4.26). There is therefore a trade-off between the beneficial and detrimental effects of overexpressing these activities. Overexpressions of both Cu,Zn-Sod and Mn-

Sod are clearly beneficial for some processes, but detrimental for others. Adverse effects of the overexpression of protective enzymes are also apparent in other situations. For example, both the total loss and the overexpression of certain DNA repair enzymes generates mutator phenotypes in *E. coli,* the lack of enzyme activity causing a repair defect and an *excess* leading to the excision of undamaged bases from DNA (Berdal et al., 1998).

Studies in other systems have already provided strong indications that the constitutive overexpression of Cu,Zn-Sod can be detrimental to dividing cells and tissues. It exerts toxic effects during *Drosophila* development (Reveillaud et al., 1991). It also causes cell type-specific developmental and functional abnormalities in transgenic mice (Avraham et al., 1988; Bar-Peled et al., 1996), these being associated with an increased endogenous oxidative stress (Peter et al., 2001). In contrast it would appear that the overexpression of Cu,Zn-Sod in nondividing cells and tissues also has protective effects, as it extends the life spans of adult *Drosophila* (Parkes et al., 1998; Sun and Tower, 1999). In yeast also overexpressing active Cu,Zn-Sod appears to have beneficial effects for survival maintenance of nondividing cells but detrimental effects in the capacity of these cells to undergo subsequent division. At the current time there is considerable interest in the life span extending effects of low molecular weight Sod mimetics (Melov et al., 2000). It will be important though to establish if these have different effects in development and in dividing cells as compared to their apparent protective effects in adult, differentiated tissues and nondividing cells. Such Sod mimetics may not have effects identical to those seen with Sod overexpression. For example, the effects of Mn-Sod overexpression on mitochondrial morphology may relate more to the accumulation of large amounts of this protein in the mitochondrial matrix rather than any specific effects on superoxide radical scavenging.

In considering the basis of the beneficial and detrimental effects of *SOD1* and *CCS1* gene overexpression, it is important to differentiate between those effects that are due to an overexpression of the Cu,Zn-Sod *apo*protein and those due to overexpression of Cu,Zn-Sod activity. Increasing levels of Cu,Zn-Sod activity will lower $O_2^{\bullet-}$ levels but at the same time increase the superoxide reductase activity of this enzyme, in which an

electron donor other than $O_2^{\bullet-}$ reduces the active site Cu(II) to Cu(I). It has been suggested that the reports of deleterious effects with overexpression of Cu,Zn-Sod could be explained if this reductant were to be an essential molecule, or toxic in its oxidised form (Liochev and Fridovich, 2000).The potential for Cu,Zn-Sod to be a superoxide reductase and a superoxide oxidase involve either conversion of Cu(II) to Cu(I), or Cu(1) to Cu(II), respectively (Liochev and Fridovich, 2000),

The detrimental effects of overexpressing the Cu,Zn-Sod *apo*protein, in the absence of simultaneous Ccs1p overexpression appear to relate to an increase in oxidative stress. This study provides the first demonstration that that they are largely reversed with the simultaneous overexpression of the Ccs1p chaperone, therefore Cu^{2+} loading of the Sod1p protein. These detrimental effects of Cu,Zn-Sod *apo*protein overexpression cannot be attributed to the reductase and oxidase activities of Cu,Zn-Sod, as these require the copper-loaded form of the enzyme (interconversion of Cu(II) to Cu(I) or Cu(1) to Cu(2) respectively (Liochev and Fridovich, 2000). They appear to be associated with increased oxidative stress, which in turn is the probable cause of the increased mutation rate. Similar increases in both oxidative stress and mutation of nuclear genes are seen in the *sod1*Δ mutant (Gralla and Valentine, 1991). In such cells elevated $O_2^{\bullet-}$ is thought to inactivate enzymes containing labile [4Fe-4S] clusters. The oxidation of these [4Fe-4S] clusters in turn liberates iron that is then free to catalyse Fenton chemistry, leading to production of highly toxic hydroxyl radicals (Srinivasan et al., 2000).

How does accumulation of the Sod1p *apo*protein enhance oxidative stress *in vivo*? Again this oxidative stress may represent an elevated $O_2^{\bullet-}$ causing increases in the cytosolic levels of ions that engage in Fenton chemistry. One possibility arises from the ability of the Cu,Zn-Sod apoprotein dimer and the Ccs1p dimer to form a very stable complex under conditions when Cu^{2+} is limiting (Schmidt et al., 2000). When Cu^{2+} levels are low, *such in vivo* complex formation may abrogate Ccs1p function by sequestering the limiting levels of Ccs1p into nonproductive complexes. Even though our data indicates no reduction in Cu,Zn-Sod activity when the *SOD1* gene is overexpressed in

the absence of *CCS1*, this and other possible mechanisms of the damaging effects of Cu,Zn-Sod apoprotein accumulation *in vivo* merit further investigation.

Finally this study developed a method of robotically screening the yeast deletant collection for mutants that have increased optimised G_0 survival. Unfortunately due to the time constraints this screen was not applied to the complete collection of the predicted yeast ORF deletes held in the Euroscarf collection (http://www.uni-frankfurt.de/fb15/mikro/ euroscarf/) (Winzeler et al., 1999). The screen enables the life span determination of each mutant. Any long lived mutant (one which out survives the wild type) will identify a gene whose presence is detrimental to G_0 survival, a prosenescence gene. Such a screen of mutants for increased longevity might be expected to uncover mutants with elevated stress resistance resistances which inturn generates increases in longevity. It might identify mutations that lead to overactivation of the regulons of oxidative stress protection, therefore leading to increased ROS scavenging. Alternatively, it might select strains with reduced levels of endogenous ROS production. The latter could arise with mutations that reduce the overall rates of oxidative metabolism (as with *clk1*, a life span-extending mutation of *C. elegans* that lowers respiration activity (therefore endogenous ROS production) by lowering ubiquinone levels (Raha and Robinson, 2000).

Overall this study has extended the use of *S.cerevisiae* as a valuable model organism for ageing research, so that it can take its place alongside the more widely accepted invertebrate models (*C.elegans* and *Drosophila*) . The chronological survival of stationary phase (G_0) yeast is probably limited by the same processes that limit the survival of post-mitotic cells in these invertebrate models. The use of genomics in the study of yeast biology is further advanced than in other model organisms, therefore yeast is a very powerful tool with which to investigate ageing processes. Future work should screen the yeast deletant collection for prosenescence functions using the methods developed in this study. Completion of this obvious goal for the future will represent the first genome wide screen in any organism for genes involved in ageing.

7 References

Abraham, J., Kelly, J., Thibault, P., and Benchimol, S. (2000). Post-translational modification of p53 protein in response to ionizing radiation analyzed by mass spectrometry. J Mol Biol *295*, 853-64.

Adams, A., Gottschling, D. E., Kaiser, C. A., and Stearns, T. (1997). Methods in Yeast Genetics. (Cold Spring Harbor, New York: Cold Spring Harbor Laboratory Press).

Aebi, H. (1984). Catalase in vitro. Methods Enzymol *105*, 121-6.

Afshar, G., and Murnane, J. P. (1999). Characterization of a human gene with sequence homology to *Saccharomyces cerevisiae* RAD52. Gene *234*, 161-8.

Appella, E., and Anderson, C. W. (2000). Signaling to p53: breaking the posttranslational modification code. Pathol Biol (Paris) *48*, 227-45.

Arking, R. (1998). Biology of aging : observations and principles, 2nd Edition (Sunderland, Mass.: Sinauer Associates).

Ashrafi, K., Lin, S. S., Manchester, J. K., and Gordon, J. I. (2000). Sip2p and its partner Snf1p kinase affect aging in *S. cerevisiae*. Genes Dev. *14*, 1872-1885.

Ashrafi, K., Sinclair, D., Gordon, J. I., and Guarente, L. (1999). Passage through stationary phase advances replicative aging in *Saccharomyces cerevisiae*. Proc. Natl. Acad. Sci. USA *96*, 9100-9105.

Avraham, K. B., Schickler, M., Sapoznikov, D., Yarom, R., and Groner, Y. (1988). Down's syndrome: abnormal neuromuscular junction in tongue of transgenic mice with elevated levels of human Cu/Zn-superoxide dismutase. Cell *54*, 823-829.

Bandara, P. D., Flattery-O'Brien, J. A., Grant, C. M., and Dawes, I. W. (1998). Involvement of the *Saccharomyces cerevisiae UTH1* gene in the oxidative stress response. Curr. Genet. *34*, 259-268.

Bar-Peled, O., Korkotian, E., Segal, M., and Groner, Y. (1996). Constitutive overexpression of Cu/Zn superoxide dismutase exacerbates kainic acid-induced apoptosis of transgenic Cu/Zn superoxide dismutase neurons. Proc. Natl. Acad. Sci. USA *93*, 8530-8535.

Barker, M. G., Brimage, L. J. E., and Smart, K. A. (1999). Effect of Cu,Zn superoxide dismutase disruption mutation on replicative senescence in *Saccharomyces cerevisiae*. FEMS Microbiol. Lett. *177*, 199-204.

Berdal, K. G., Johansen, R. F., and Seeberg, E. (1998). Release of normal bases from intact DNA by a native DNA repair enzyme. EMBO J. *17*, 363-367.

Bereiter-Hahn, J., and Voth, M. (1994). Dynamics of mitochondria in living cells: shape changes, dislocations, fusion, and fission of mitochondria. Microsc Res Tech *27*, 198-219.

Borkovich, K. A., Farrely, F. W., Finkelstein, D. B., Taulein, J., and Lindquist, S. (1989). Hsp82 is an essential protein that is required in higher concentrations for growth of cells at higher temperature. Mol. Cell. Biol. *9*, 3919-3930.

Brachmann, C. B., Sherman, J. M., Devine, S. E., Cameron, E. E., Pillus, L., and Boeke, J. D. (1995). The SIR2 gene family, conserved from bacteria to humans, functions in silencing, cell cycle progression, and chromosome stability. Genes Dev *9*, 2888-902.

Braunstein, M., Rose, A. B., Holmes, S. G., Allis, C. D., and Broach, J. R. (1993). Transcriptional silencing in yeast is associated with reduced nucleosome acetylation. Genes Dev *7*, 592-604.

Braunstein, M., Sobel, R. E., Allis, C. D., Turner, B. M., and Broach, J. R. (1996). Efficient transcriptional silencing in | *Saccharomyces cerevisiae* requires a heterochromatin histone acetylation pattern. Mol Cell Biol *16*, 4349-56.

Brewer, B. J., and Fangman, W. L. (1988). A replication fork barrier at the 3' end of yeast ribosomal RNA genes. Cell *55*, 637-43.

Brown-Borg, H. M., Melinska, C. J., and Bartke, A. (1996). Dwarf mice and the ageing process. Nature *384*, 33.

Canman, C. E., Lim, D. S., Cimprich, K. A., Taya, Y., Tamai, K., Sakaguchi, K., Appella, E., Kastan, M. B., and Siliciano, J. D. (1998). Activation of the ATM kinase by ionizing radiation and phosphorylation of p53. Science *281*, 1677-9.

Charizanis, C., Juhnke, H., Krems, B., and Entian, K.-D. (1999). The mitochondrial cytochome c peroxidase Ccp1 of *Saccharomyces cerevisiae* is involved in conveying an oxidative stress signal to the transcription factor Pos9 (Skn7). Mol. Gen. Genet. *262*, 437-447.

Costa, V., Amorim, M. A., Reis, E., Quintanilha, A., and Moradas-Ferreira, P. (1997). Mitochondrial superoxide dismutase is essential for ethanol tolerance of *Saccharomyces cerevisiae* in the post-diauxic phase. Microbiology *143*, 1649-1656.

Cowen, T. (2002). Selective vulnerability in adult and ageing mammalian neurons. Auton Neurosci *96*, 20-4.

Culotta, V. C., Klomp, L. W., Strain, J., Casareno, R. L., Krems, B., and Gitlin, J. D. (1997). The copper chaperone for superoxide dismutase. J Biol Chem *272*, 23469-72.

Defossez, P.-A., Prusty, R., Kaeberlein, M., Lin, S.-J., Ferrigno, P., Silver, P. A., Keil, R. L., and Guarente, L. (1999). Elimination of replication block protein Fob1 extends the life span of yeast mother cells. Molecular Cell *3*, 447-455.

Denis, C. L., and Audino, D. C. (1991). The CCR1 (SNF1) and SCH9 protein kinases act independently of cAMP-dependent protein kinase and the transcriptional activator ADR1 in controlling yeast ADH2 expression. Mol Gen Genet *229*, 395-9.

Drubin, D. G., Jones, H. D., and Wertman, K. F. (1993). Actin structure and function: roles in mitochondrial organization and morphogenesis in budding yeast and identification of the phalloidin-binding site. Mol Biol Cell *4*, 1277-94.

Duina, A. A., Kalton, H. M., and Gaber, R. F. (1998). Requirement for Hsp90 and a Cyp40-type cyclophilin in negative regulation of the heat shock response. J. Biol. Chem. *273*, 18974-18978.

el-Deiry, W. S., Tokino, T., Velculescu, V. E., Levy, D. B., Parsons, R., Trent, J. M., Lin, D., Mercer, W. E., Kinzler, K. W., and Vogelstein, B. (1993). WAF1, a potential mediator of p53 tumor suppression. Cell *75*, 817-25.

Evans, M. V., H.E., T., Grant, C. M., and Dawes, I. W. (1997). Toxicity of linoleic acid hydroperoxide to *Saccharomyces cerevisiae*: Involvement of a respiration-related process for maximal sensitivity and adaptive response. J. Bacteriol. *180*, 483-490.

Ewbank, J. J., Barnes, T. M., Lakowski, B., Lussier, M., Bussey, H., and Hekimi, S. (1997). Structural and functional conservation of the *Caenorhabditis elegans* timing gene *clk-1*. Science *275*, 980-983.

Fabrizio, P., Pozza, F., Pletcher, S. D., Gendron, C. M., and Longo, V. D. (2001). Regulation of longevity and stress resistance by Sch9 in yeast. Science *292*, 288-290.

Feinberg, A. P., and Vogelstein, B. (1983). A technique for radiolabelling DNA restriction endonuclease fragments to high specific activity. Anal Biochem *132*, 6-13.

Flattery-O'Brien, J. A., Grant, C. M., and Dawes, I. W. (1997). Stationary phase regulation of the *Saccharomyces cerevisiae SOD2* gene is dependent on additive effects of HAP2/3/4/5 and STRE-binding elements. Mol. Microbiol. *23*, 303-312.

Flohe, L., and Otting, F. (1984). Superoxide dismutase assays. Methods Enzymol *105*, 93-104.

Frye, R. A. (1999). Characterization of five human cDNAs with homology to the yeast SIR2 gene: Sir2-like proteins (sirtuins) metabolize NAD and may have protein ADP-ribosyltransferase activity. Biochem Biophys Res Commun *260*, 273-9.

Galiazzo, F., and Labbe-Bois, R. (1993). Regulation of CuZn and Mn-superoxide dismutase transcription in *Saccharomyces cerevisiae*. FEBS Lett. *315*, 197-200.

Gamonet, F., and Lauquin, G. J. (1998). The*Saccharomyces cerevisiae* : LYS7 gene is involved in oxidative stress protection. Eur J Biochem *251*, 716-23.

Gangloff, S., Zou, H., and Rothstein, R. (1996). Gene conversion plays the major role in controlling the stability of large tandem repeats in yeast. Embo J *15*, 1715-25.

Gietz, R. D., Schiestl, R. H., Willems, A. R., and Woods, R. A. (1995). Studies on the transformation of intact yeast cells by the LiAc/SS-DNA/PEG procedure. Yeast *11*, 355-60.

Glerum, D. M., Shtanko, A., and Tzagoloff, A. (1996). Characterization of COX17, a yeast gene involved in copper metabolism and assembly of cytochrome oxidase. J Biol Chem *271*, 14504-9.

Gottlieb, S., and Esposito, R. E. (1989). A new role for a yeast transcriptional silencer gene, SIR2, in regulation of recombination in ribosomal DNA. Cell *56*, 771-6.

Gottschling, D. E. (2000). Gene silencing: two faces of SIR2. Curr Biol *10*, R708-11.

Gottschling, D. E., Aparicio, O. M., Billington, B. L., and Zakian, V. A. (1990). Position effect at S. cerevisiae telomeres: reversible repression of Pol II transcription. Cell *63*, 751-62.

Gralla, E. B., and Kosman, D. J. (1992). Molecular genetics of superoxide dismutases in yeasts and related fungi. Adv. Genet. *30*, 251-319.

Gralla, E. B., and Valentine, J. S. (1991). Null mutants of *Saccharomyces cerevisiae* Cu,Zn superoxide dismutase: Characterisation and spontaneous mutation rates. J. Bacteriol. *173*, 5918-5920.

Grubmeyer, C. T., Gross, J. W., and Rajavel, M. (1999). Energy coupling through molecular discrimination: nicotinate phosphoribosyltransferase. Methods Enzymol *308*, 28-48.

Guarente, L. (2001). SIR2 and aging--the exception that proves the rule. Trends Genet *17*, 391-2.

Guarente, L., and Kenyon, C. (2000). Genetic pathways that regulate ageing in model organisms. Nature *408*, 255-62.

Halliwell, B., and Gutteridge, J. M. C. (1998). Free Radicals in Biology and Medicine, 3rd. Edn. (Oxford: Oxford University Press).

Harris, N., MacLean, M., Hatzianthis, K., Panaretou, B., and Piper, P. W. (2001). Increasing *Saccharomyces cerevisiae* stress resistance, through the overactivation of the heat shock response resulting from defects in the Hsp90 chaperone, does not extend replicative life span but can be associated with slower chronological ageing of nondividing cells. Mol Genet Genomics *265*, 258-63.

Heim, R., Cubitt, A. B., and Tsien, R. Y. (1995). Improved green fluorescence. Nature *373*, 663-4.

Hermanns, J., Asseburg, A., and Osiewacz, H. D. (1994). Evidence for a life span-prolonging effect of a linear plasmid in a longevity mutant of *Podospora anserina*. Mol. Gen. Genet. *243*, 297-307.

Hershko, A., and Ciechanover, A. (1998). The ubiquitin system. Annu. Rev. Biochem. *67*, 425-479.

Heydari, A. R., You, S., Takahashi, R., Gutsmann, A., Sarge, K. D., and Richardson, A. (1996). Effect of caloric restriction on the expression of heat shock protein 70 and the activation of heat shock transcription factor 1. Dev. Genet. *18*, 114-124.

Hockenbery, D. M., Oltvai, Z. N., Yin, X. M., Milliman, C. L., and Korsenmeyer, S. J. (1993). Bcl-2 functions in an antioxidant pathway to prevent apoptosis. Cell *75*, 241-5.

Hoffmann, H. P., and Avers, C. J. (1973). Mitochondrion of yeast: ultrastructural evidence for one giant, branched organelle per cell. Science *181*, 749-51.

Horecka, J., Kinsey, P. T., and Sprague, G. F., Jr. (1995). Cloning and characterization of the *Saccharomyces cerevisiae* YS7 gene: evidence for function outside of lysine biosynthesis. Gene *162*, 87-92.

Imai, S.-I., Armstrong, C. M., Kaeberlein, M., and Guarente, L. (2000). Transcriptional silencing and longevity protein Sir2 is a NAD-dependent histone deacetylase. Nature *403*, 795-800.

Jamet-Vierny, C., Begel, O., and Belcour, L. (1980). Senescence in *Podospora anserina:* amplification of a mitochondrial sequence. Cell *21*, 189-194.

Johnson, F. B., Sinclair, D. A., and Guarente, L. (1999). Molecular biology of aging. Cell *96*, 291-302.

Johnston, J. R. (1994). Molecular Genetics of Yeast: A Practical Approach (Oxford: I.R.L. Press).

Kaeberlein, M., McVey, M., and Guarente, L. (1999). The SIR2/3/4 complex and SIR2 alone promote longevity in *Saccharomyces cerevisiae* by two different mechanisms. Genes Dev *13*, 2570-80.

Kennedy, B. K., Austriaco, N. R., J., Z., and Guarente, L. (1995). Mutation in the silencing gene *SIR4* can delay ageing in *Saccharomyces cerevisiae*. Cell *80*, 485-496.

Kenyon, C., Chang, J., Gensch, E., Rudner, A., and Tabtiang, R. (1993). A *Caenorhabditis elegans* mutant that lives twice as long as wild type. Nature *366*, 461-464.

Kimura, K. D., Tissenbaum, H. A., Liu, Y., and Ruvkun, G. (1997). daf-2, an insulin receptor-like gene that regulates longevity and diapause in *Caernorhabtidis elegans* Science *277*, 942-6.

Kirchman, P. A., Kim, S., Lai, C.-Y., and Jazwinski, S. M. (1999). Interorganelle signalling is a determinant of longevity in *Saccharomyces cerevisiae*. Genetics *152*, 179-190.

Kirkwood, T. B. (2002). Evolution of ageing. Mech Ageing Dev *123*, 737-45.

Kobayashi, T., and Horiuchi, T. (1996). A yeast gene product, Fob1 protein, required for both replication fork blocking and recombinational hotspot activities. Genes Cells *1*, 465-74.

Laemmli, U. K. (1970). Cleavage of structural proteins during the assembly of the head of bacteriophage T4. Nature *227*, 680-685.

Lambert, P. F., Kashanchi, F., Radonovich, M. F., Shiekhattar, R., and Brady, J. N. (1998). Phosphorylation of p53 serine 15 increases interaction with CBP. J Biol Chem *273*, 33048-53.

Larionov, V., Kouprina, N., and Karpova, T. (1984). Stability of recombinant plasmids containing the ars sequence of yeast extrachromosomal rDNA in several strains of Saccharomyces cerevisiae. Gene *28*, 229-35.

Larson, P., Albert, P., and Riddle, D. (1995). Genes that regulate both development and longevity in *Caenorhabditis elegans*. Genetics *139*, 1567-1583.

Levine, A. J. (1997). p53, the cellular gatekeeper for growth and division. Cell *88*, 323-31.

Levine, R. L., Wehr, N., Williams, J. A., Stadtman, E. R., and Shacter, E. (2000). Determination of carbonyl groups in oxidized proteins. Methods Mol Biol *99*, 15-24.

Levine, R. L., Williams, J. A., Stadtman, E. R., and Shacter, E. (1995). Carbonyl assays for the determination of oxidatively modified proteins. Meth. Enzymol. *233*, 346-357.

Lin, K., Dorman, J. B., Rodan, A., and Kenyon, C. (1997). daf-16: An HNF-3/forkhead family member that can function to double the life-span of *Caernorhabtidis elegans* Science *278*, 1319-22.

Lin, S.-J., Defossez, P.-A., and Guarente, L. (2000). Requirement of NAD and *SIR2* for life-span extension by calorie restriction in *Saccharomyces cerevisiae.* Science *289*, 2126-2128.

Lin, S. J., Pufahl, R. A., Dancis, A., O'Halloran, T. V., and Culotta, V. C. (1997). A role for the Saccharomyces cerevisiae ATX1 gene in copper trafficking and iron transport. J Biol Chem *272*, 9215-20.

Lin, Y., Ma, W., and Benchimol, S. (2000). Pidd, a new death-domain-containing protein, is induced by p53 and promotes apoptosis. Nat Genet *26*, 122-7.

Liochev, S. I., and Fridovich, I. (2000). Copper- and zinc-containing superoxide dismutase can act as a superoxide reductase and a superoxide oxidase. J Biol Chem *275*, 38482-5.

Lithgow, G. J. (1996). Invertebrate gerontology: the age mutations of *Caenorhabditis elegans*. BioEssays *18*, 809-815.

Longo, V. D., Ellerby, L. M., Bredesen, D. E., Valentine, J. S., and Gralla, E. B. (1997). Human Bcl-2 reverses survival defects in yeast lacking superoxide dismutase and delays death of wild-type yeast. J Cell Biol *137*, 1581-8.

Longo, V. D., Gralla, E. B., and Valentine, J. S. (1996). Superoxide dismutase is essential for stationary phase survival in *S. cerevisiae*: Mitochondrial production of toxic oxygen species *in vivo*. J. Biol. Chem. *271*, 12275-12280.

Longo, V. D., Liou, L. L., Valentine, J. S., and Gralla, E. B. (1999). Mitochondrial superoxide decreases yeast survival in stationary phase. Arch Biochem Biophys *365*, 131-42.

Luger, K., and Richmond, T. J. (1998). The histone tails of the nucleosome. Curr Opin Genet Dev *8*, 140-6.

Luo, J., Nikolaev, A. Y., Imai, S., Chen, D., Su, F., Shiloh, A., Guarente, L., and Gu, W. (2001). Negative control of p53 by Sir2alpha promotes cell survival under stress. Cell *107*, 137-48.

MacLean, M., Harris, N., and Piper, P. W. (2001). Chronological life span of stationary phase yeast cells; a model for investigating the factors that might influence the ageing of postmitotic tissues in higher organisms. Yeast *18*, 499-509.

Maniatis, T., Fritsch, E. F., and Sambrook, J. (1989). Molecular Cloning, A laboratory Manual (Cold Spring Harbor, New York: Cold Spring Harbor Laboratory Press).

Martin, G. M., Austad, S. N., and Johnson, T. E. (1996). Genetic analysis of aging: role of oxidative damage and environmental stresses. Nature Genet. *13*, 25-34.

Martin, S. G., Laroche, T., Suka, N., Grunstein, M., and Gasser, S. M. (1999). Relocalization of telomeric Ku and SIR proteins in response to DNA strand breaks in yeast. Cell *97*, 621-33.

Martinez-Pastor, M. T., Marchler, G., Schüller, C., Marchler-Bauer, A., Ruis, H., and Estruch, F. (1996). The *Saccharomyces cerevisiae* zinc finger proteins Msn2p and Msn4p are required for transcriptional induction through the stress response element (STRE). EMBO J. *15*, 2227-2235.

McAinsh, A. D., Scott-Drew, S., Murray, J. A., and Jackson, S. P. (1999). DNA damage triggers disruption of telomeric silencing and Mec1p-dependent relocation of Sir3p. Curr Biol *9*, 963-6.

McConnell, S. J., Stewart, L. C., Talin, A., and Yaffe, M. P. (1990). Temperature-sensitive yeast mutants defective in mitochondrial inheritance. J Cell Biol *111*, 967-76.

Meinkoth, J., and Wahl, G. (1984). Hybridization of nucleic acids immobilized on solid supports. Anal Biochem *138*, 267-84.

Melov, S., Ravenscroft, J., Malik, S., Gill, M. S., Walker, D. W., Clayton, P. E., Wallace, D. C., Malfroy, B., Doctrow, S. R., and Lithgow, G. J. (2000). Extension of life-span with superoxide dismutase/catalase mimetics. Science *289*, 1567-1569.

Mills, K. D., Sinclair, D. A., and Guarente, L. (1999). *MEC1*-dependent redistribution of the Sir3 silencing protein from telomeres to DNA double strand breaks. Cell *97*, 609-620.

Moradas-Ferreira, P., and Costa, V. (2000). Adaptive response of the yeast Saccharomyces cerevisiae to reactive oxygen species: defences, damage and death. Redox Rep *5*, 277-85.

Morris, J. Z., Tissenbaum, H. A., and Ruvkin, G. (1996). A phosphatidylinositol-3-OH kinase family member regulating longevity and diapause in *Caenorhabditis elegans*. Nature *382*, 536-539.

Mortimer, R. K., and Johnston, J. (1959). Life span of individual yeast cells. Nature *183*, 1751-1752.

Muller, I., Zimmermann, M., Becker, D., and Flomer, M. (1980). Calendar life span versus budding life span of *Saccharomyces cerevisiae* Mech Ageing Dev *12*, 47-52.

Nathan, D. F., and Lindquist, S. (1995). Mutational analysis of Hsp90 function: interactions with a steroid receptor and a protein kinase. Mol Cell Biol *15*, 3917-25.

Nathan, D. F., and Lindquist, S. (1995). Mutational analysis of Hsp90 function: interactions with a steroid receptor and a protein kinase. Molecular and Cellular Biology *15*, 3917-3925.

Nestelbacher, R., Laun, P., Vondrakonva, D., Pichova, D., Schuller, C., and Breitenbach, M. (2000). The influence of oxygen toxicity on yeast mother cell-speciic aging. Exp. Gerontol. *35*, 63-70.

O'Halloran, T. V., and Culotta, V. C. (2000). Metallochaperones, an intracellular shuttle service for metal ions. J Biol Chem *275*, 25057-60.

Ogg, S., Paradis, S., Gottlieb, S., Patterson, G. I., Lee, L., Tissenbaum, H. A., and Ruvkun, G. (1997). The Fork head transcription factor DAF-16 transduces insulin-like metabolic and longevity signals in *C. elegans*. Nature *389*, 994-9.

Oren, M. (1999). Regulation of the p53 tumor suppressor protein. J Biol Chem *274*, 36031-4.

Ozcan, S., and Johnston, M. (1999). Function and regulation of yeast hexose transporters. Microbiol Mol Biol Rev *63*, 554-69.

Panaretou, B., Prodromou, C., Roe, S. M., O'Brien, R., Ladbury, J. E., Piper, P. W., and Pearl, L. H. (1998). ATP binding and hydrolysis are essential to the function of the Hsp90 molecular chaperone *in vivo*. EMBO J. *17*, 4829-4836.

Paradis, S., Ailion, M., Toker, A., Thomas, J. H., and Ruvkun, G. (1999). A PDK1 homolog is necessary and sufficient to transduce AGE-1 PI3 kinase signals that regulate diapause in Caenorhabditis elegans. Genes Dev *13*, 1438-52.

Parkes, T. L., Elia, A. J., Dickinson, D., Hilliker, A. J., Phillips, J. P., and Boulianne, G. L. (1998). Extension of *Drosophila* lifespan by overexpression of human *SOD1* in motorneurons. Nature Genetics *19*, 171-174.

Pedruzzi, I., Burckert, N., Egger, P., and De Virgilio, C. (2000). Saccharomyces cerevisiae Ras/cAMP pathway controls post-diauxic shift element-dependent transcription through the zinc finger protein Gis1. Embo J *19*, 2569-79.

Peter, Y., Rotman, G., Lotem, J., Elson, A., Shiloh, Y., and Groner, Y. (2001). Elevated Cu/Zn-SOD exacerbates radiation sensitivity and hematopoietic abnormalities in Atm-deficient mice. EMBO J. *20*, 1538-1546.

Piper, P. W. (1999). Yeast superoxide dismutase mutants reveal a prooxidant action of weak organic acid food preservatives. Free Radic. Biol. Med. *27*, 1219-1227.

Prives, C., and Hall, P. A. (1999). The p53 pathway. J Pathol *187*, 112-26.

Pufahl, R. A., Singer, C. P., Peariso, K. L., Lin, S. J., Schmidt, P. J., Fahrni, C. J., Culotta, V. C., Penner-Hahn, J. E., and O'Halloran, T. V. (1997). Metal ion chaperone function of the soluble Cu(I) receptor Atx1 [see comments]. Science *278*, 853-6.

Rae, T. D., Schmidt, P. J., Pufahl, R. A., Culotta, V. C., and O'Halloran, T. V. (1999). Undetectable intracellular free copper: the requirement of a copper chaperone for superoxide dismutase [see comments]. Science *284*, 805-8.

Raha, S., and Robinson, B. H. (2000). Mitochondria, oxygen free radicals and disease. Trends Biochem. Sci. *25*, 502-508.

Rajavel, M., Lalo, D., Gross, J. W., and Grubmeyer, C. (1998). Conversion of a cosubstrate to an inhibitor: phosphorylation mutants of nicotinic acid phosphoribosyltransferase. Biochemistry *37*, 4181-8.

Reveillaud, I., Niedzwiecki, A., Bensch, K. G., and Fleming, J. E. (1991). Expression of bovine superoxide dismutase in *Drosophila melanogaster* augments resistance to oxidative stress. Mol. Cell. Biol. *11*, 632-640.

Riddle, D. L., Swanson, M. M., and Albert, P. S. (1981). Interacting genes in nematode dauer larva formation. Nature *290*, 668-71.

Rine, J., and Herskowitz, I. (1987). Four genes responsible for a position effect on expression from HML and HMR in *Saccharomyces cerevisiae* Genetics *116*, 9-22.

Ross-Macdonald, P., and et.al. (1999). Large-scale analysis of the yeast genome by transposon tagging and gene disruption. Nature *402*, 413-418.

Rutherford, S. L., and Lindquist, S. (1998). Hsp90 as a capacitor for morphological evolution. Nature *396*, 336-342.

Scandalios, J. G. (1992). Molecular Biology of Free Radical Scavenging Systems., J. G. Scandalios, ed. (New York: Cold Spring Harbor Laboratory Press).

Schmidt, P. J., Kunst, C., and Culotta, V. C. (2000). Copper activation of superoxide dismutase 1 (SOD1) in vivo. ROLE FOR PROTEIN-PROTEIN INTERACTIONS WITH THE COPPER CHAPERONE FOR SOD1 [In Process Citation]. J Biol Chem *275*, 33771-6.

Service, P. M., Hutchinson, E. W., MacKinley, M. D., and Rose, M. R. (1985). Resistance to environmental stress in *Drosophila melanogaster* selected for postponed senescence. Physiol. Zool. *58*, 380-389.

Shama, S., Lai, C.-Y., Antoniazzi, J. M., Jiang, J. C., and Jazwinski, S. M. (1998). Heat stress-induced life span extension in yeast. Exptl. Cell Res. *245*, 379-388.

Shieh, S. Y., Ahn, J., Tamai, K., Taya, Y., and Prives, C. (2000). The human homologs of checkpoint kinases Chk1 and Cds1 (Chk2) phosphorylate p53 at multiple DNA damage-inducible sites. Genes Dev *14*, 289-300.

Shoemaker, D. D., Lashkari, D. A., Morris, D., Mittmann, M., and Davis, R. W. (1996). Quantitative phenotypic analysis of yeast deletion mutants using a highly parallel molecular bar-coding strategy. Nat Genet *14*, 450-6.

Sikorski, R. S., and Hieter, P. (1989). A system of shuttle vectors and yeast host strains designed for efficient manipulation of DNA in *Saccharomyces cerevisiae*. Genetics *122*, 19-27.

Siliciano, J. D., Canman, C. E., Taya, Y., Sakaguchi, K., Appella, E., and Kastan, M. B. (1997). DNA damage induces phosphorylation of the amino terminus of p53. Genes Dev *11*, 3471-81.

Sinclair, D. A., and Guarente, L. (1997). Extrachromosomal rDNA circles - a cause of aging in yeast. Cell *91*, 1033-1042.

Sinclair, D. A., Mills, K., and Guarente, L. (1997). Accelerated aging and nucleolar fragmentation in the yeast *sgs1* mutant. Science *277*, 1313-1316.

Sinclair, D. A., Mills, K., and Guarente, L. (1998). Molecular mechanisms of yeast aging. Trends Biochem Sci *23*, 131-4.

Smeal, T., Claus, J., Kennedy, B. K., Cole, F., and Guarente, L. (1996). Loss of transcriptional silencing causes sterility in old mother cells of *Saccharomyces cerevisiae*. Cell *84*, 633-642.

Smith, A., Ward, M. P., and Garrett, S. (1998). Yeast PKA represses Msn2p/Msn4p-dependent gene expression to regulate growth, stress response and glycogen accumulation. EMBO J. *17*, 3556-3564.

Sohal, R. S., and Weindruch, R. (1996). Oxidative stress, caloric restriction and ageing. Science *273*, 59-63.

Srinivasan, C., Liba, A., Imlay, J. A., Valentine, J. S., and Gralla, E. B. (2000). Yeast lacking superoxide dismutase(s) show elevated levels of "free iron" as measured by whole cell electron paramagnetic resonance. J. Biol. Chem. *275*, 29187-29192.

Stenlund, P., and Tibell, L. A. (1999). Chimeras of human extracellular and intracellular superoxide dismutase. Analysis of structure and function of the individual domains. Protein Eng. *12*, 319-325.

Sturtz, L. A., Diekert, K., Jensen, L. T., Lill, R., and Culotta, V. C. (2001). A fraction of the yeast Cu/Zn superoxide dismutase and its metallochaperone, CCS, localise to the intermembrane space of mitochondria: a physiological role for SOD1 in guarding against mitochondrial oxidative damage. J. Biol. Chem. *276, 38084-38089*

Sun, J., Childress, A. M., Pinswasdl, C., and Jaswinski, S. (1994). Divergent roles of *RAS1* and *RAS2* in yeast longevity. J. Biol. Chem. *269*, 18638-18645.

Sun, J., and Tower, J. (1999). FLP recombinase-mediated induction of Cu/Zn-superoxide dismutase transgene expression can extend the lifespan of adult *Drosophila melanogaster* flies. Mol. Cell. Biol. *19*, 216-228.

Tarpey, M. M., and Fridovich, I. (2001). Methods of detection of vascular reactive species: nitric oxide, superoxide, hydrogen peroxide, and peroxynitrite. Circ Res *89*, 224-36.

Taub, J., Lau, J. F., Ma, C., Yang, H. H., Hoque, R., Rothblatt, J., and Chalfie, M. (1999). A cytosolic catalase is needed to extend adult lifespan in *C. elegans daf-C* and *clk-1* mutants. Nature *399*, 162-166.

Thevelein, J. M., and de Winde, J. H. (1999). Novel sensing mechanisms and targets for the cAMP-protein kinase A pathway in the yeas *Saccharomyces cerevisiae* . Mol Microbiol *33*, 904-18.

Thompson, J. R., Register, E., Curotto, J., Kurtz, M., and Kelly, R. (1998). An improved protocol for the preparation of yeast cells for transformation by electroporation. Yeast *14*, 565-71.

Tissenbaum, H. A., and Guarente, L. (2001). Increased dosage of a sir-2 gene extends lifespan in *Caernorhabtidis elegan*. Nature *410*, 227-30.

Tower, J. (2000). Transgenic methods for increasing *Drosophila* life span. Mech. Ageing Dev. *118*, 1-14.

Turton, H. E., Dawes, I. W., and Grant, C. M. (1997). *Saccharomyces cerevisiae* exhibits a yAP-1-mediated adaptive response to malondialdehyde. J. Bacteriol. *179*, 1096-1101.

Valentine, J. S., and Gralla, E. B. (1997). Delivering copper inside yeast and human cells [comment]. Science *278*, 817-8.

Vaziri, H., Dessain, S. K., Ng Eaton, E., Imai, S. I., Frye, R. A., Pandita, T. K., Guarente, L., and Weinberg, R. A. (2001). hSIR2(SIRT1) functions as an NAD-dependent p53 deacetylase. Cell *107*, 149-59.

Venema, J., and Tollervey, D. (1999). Ribosome synthesis in *Saccharomyces cerevisiae* Annu Rev Genet *33*, 261-311.

Vogelstein, B., Lane, D., and Levine, A. J. (2000). Surfing the p53 network. Nature *408*, 307-10.

Walsh, R. B., Kawasaki, G., and Fraenkel, D. G. (1983). Cloning of genes that complement yeast hexokinase and glucokinase mutants. J Bacteriol *154*, 1002-4.

Wawryn, J., Krzepilko, A., Mytszka, A., and Bilinski, T. (1999). Deficiency in superoxide dismutases shortens life span of yeast cells. Acta. Biochim. Pol. *46*, 249-253.

Werner-Washburne, M., Braun, E., Johnston, G. C., and Singer, R. A. (1993). Stationary phase in the yeast *Saccharomyces cerevisiae*. Microbiol. Rev. *57*, 383-401.

Westerbeek-Marres, C. A., Moore, M. M., and Autor, A. (1988). Regulation of manganese superoxide dismutase in *Saccharomyces cerevisiae*. The role of respiratory chain activity. Eur. J. Biochem. *174*, 611-620.

Westermann, B., and Neupert, W. (2000). Mitochondria-targeted green fluorescent proteins: convenient tools for the study of organelle biogenesis in *Saccharomyces cerevisiae*. Yeast *16*, 1421-1427.

Winzeler, E. A., Shoemaker, D. D., Astromoff, A., Liang, H., Anderson, K., Andre, B., Bangham, R., Benito, R., Boeke, J. D., Bussey, H., Chu, A. M., Connelly, C., Davis, K., Dietrich, F., Dow, S. W., El Bakkoury, M., Foury, F., Friend, S. H., Gentalen, E., Giaever, G., Hegemann, J. H., Jones, T., Laub, M., Liao, H., Davis, R. W., (1999). Functional characterization of the S. cerevisiae genome by gene deletion and parallel analysis. Science *285*, 901-6.

Wood, W. B. (1998). Aging of *C. elegans*: mosaics and mechanisms. Cell *95*, 147-150.

Yu, C. E., Oshima, J., Fu, Y. H., Wijsman, E. M., Hisama, F., Alisch, R., Matthews, S., Nakura, J., Miki, T., Ouais, S., Martin, G. M., Mulligan, J., and Schellenberg, G. D. (1996). Positional cloning of the Werner's syndrome gene. Science *272*, 258-62.

Zabarovsky, E. R., and Winberg, G. (1990). High efficiency electroporation of ligated DNA into bacteria. Nucleic Acids Res *18*, 5912.

Zou, J., Guo, Y., Guettouche, T., Smith, D. F., and Voellmy, R. (1998). Repression of heat shock transcription factor HSF1 activation by HSP90 (HSP90 complex) that forms a stress-sensitive complex with HSF1. Cell *94*, 471-480.

Zwaan, B. J., Bijlsma, R., and Hoekstra, R. F. (1991). On the developmental theory of ageing. I, starvation resistance and longevity in *Drosopila melanogaster* in relation to pre-adult breeding conditions. Heredity *66*, 29-39.